

Analysis of the role of Rad5 for the regulation of repair of DSB, small deletions and oxidative damage

Dissertation der Fakultät für Biologie
der Ludwig-Maximilian-Universität München



Submitted by
Idoia Gómez Paramio
March 27, 2007

1. Examiner: Prof. Dr. Eckardt-Schupp
 2. Examiner: Prof. Dr. Leonhardt
- Oral examination: 28.11.2007

ACKNOWLEDGMENTS

Firstly, I would like to thank my “Doktormutter” Prof. Dr. Friederike Eckardt-Schupp for giving me the opportunity to carry out this work as a member of her research group.

I wish to express my sincere gratitude to my scientific supervisor Dr. Simone Mörtl for her patient guidance, advice and the stimulating discussions, which were decisive for the achievement of this work. Her endless optimism and enthusiastic attitude have never ceased to encourage me in difficult times during my thesis.

I owe my gratitude to the group for creating such a friendly atmosphere. Especially I would like to express my gratitude to Klaudia Winkler for her extraordinary technical assistance, but above all, for her invaluable human understanding. I also wish to thank warmly Daniel Sagan for his help but especially for his friendship, filling my PhD with enjoyable moments.

My special thanks to Dr. Herbert Brasselmann for teaching me the basics of Delphi and for all the knowledge and dedication necessary to develop Geltool. I also would like to thank Dr. Anna Friedl for guiding me through the world of PFGE.

Finally, my deepest thanks to my family and friends for bringing happiness into my life and in particular to Wolfgang Behr for being at my side, listening to me and giving me support.

This work was carried out at the Institute for Radiobiology (ISB) at the GSF-Forschungszentrum für Umwelt und Gesundheit and the Faculty of Biology at the Ludwig-Maximilians University (LMU) in Munich, Germany during the time 31.05.2002 - 31.12.1005.

This study has been supported by the by EU grant FIGH-CT-2002-00207.

1. INTRODUCTION	1
1.1. DNA damage and its repair	1
1.2. Radiation and its effects	1
1.3. DNA Repair	3
1.4. Direct repair	4
1.5. Excision repair	4
1.5.1. Base Excision Repair	5
1.6. DNA Double Strand Break Repair	8
1.6.1. Homologous Recombination (HR)	8
1.6.2. Nonhomologous End Joining (NHEJ)	15
1.6.3. Balance between HR and NHEJ	18
1.7. Post-replication repair (PRR)	20
1.7.1. Rad5	23
1.8. Goals	25
2. MATERIALS	27
2.1. Equipment	27
2.2. Chemicals, Enzyme and other Materials	28
2.2.1. Chemicals	28
2.2.2. Enzymes	30
2.2.3. Lengths standards	30
2.2.4. Kits	30
2.3. Computer programs and web sites	30
2.4. Oligonucleotides	31
2.5. Plasmids	33
2.5.1. pJD1	33
2.5.2. pFA6-KANMX6	34
2.5.3. pUC 19 (Fermentas)	35
2.5.4. pGEM-T (Promega)	36
2.6. Solutions and buffers	37
2.7. Growth medium	37
2.7.1. Growth medium for bacteria	37
2.7.2. Growth medium for yeast strains	37
2.7.3. Liquid Holding Recovery Buffer for yeast	38
2.8. Freezing medium for yeast	38
2.9. Strains	39
2.9.1. Bacterial strain	39
2.9.2. Yeast strains	39
3. METHODS	41
3.1. Microbiology methods	41
3.1.1. Working with bacteria	41
3.1.2. Working with yeast	42
3.2. Biomolecular methods	44
3.2.1. Isolation of DNA	44
3.2.2. Cleavage of DNA by restriction endonucleases	48
3.2.3. Separation of DNA fragments by gel electrophoresis	49
3.2.4. Amplification of DNA by PCR	49
3.2.5. Purification of DNA	50
3.2.6. Photometric determination of DNA concentration	51

3.2.7.	Sequence analysis of DNA	51
3.2.8.	Cleavage of the 5'-phosphate groups	52
3.2.9.	Ligation of DNA restriction fragments into plasmids	53
3.2.10.	Use of X-GAL for identification of <i>LacZ</i> expression	53
3.3.	Determination of the survival capacity after irradiation	54
3.3.1.	Drop test of yeast cells	54
3.3.2.	Survival capacity of yeast after irradiation	54
3.4.	Repair assay with the plasmid pJD1	55
3.5.	DSB Quantification by Pulsed Field Gel Electrophoresis	57
3.5.1.	Streaking, irradiation and cultivation of yeast cells	57
3.5.2.	DNA preparation	58
3.5.3.	Pulsed Field Gel Electrophoresis	60
3.5.4.	Gel staining and densitometry evaluation	61
3.5.5.	Quantification of DSB	61
3.6.	Determination of the mutation capacity	62
4.	RESULTS	63
4.1.	Role of Rad5 in the HR and NHEJ repair pathways	63
4.1.1.	Generation of <i>rad52</i> mutants using the cassette <i>KANMX6</i>	63
4.1.2.	Survival capacity after gamma and UV radiation	64
4.1.3.	Role of Rad5 for the repair of chromosomal DSB	69
4.1.4.	Repair of DSB in HR and NHEJ deficient mutants	78
4.1.5.	Repair of plasmidial gaps	80
4.2.	Role of Rad5 in base excision repair	88
4.2.1.	Generation of knockout mutants	88
4.2.2.	Survival capacity after gamma irradiation	92
4.2.3.	Repair at chromosomal level	94
4.2.4.	Survival capacity after UV irradiation	95
4.2.5.	UV-mutagenicity in BER mutants	96
5.	DISCUSSION	99
5.1.	Role of Rad5 in the HR and NHEJ repair pathways	100
5.1.1.	Synergism between Rad5 and Rad52	100
5.1.2.	<i>rad5</i> phenotype suppression in NHEJ deficient mutants	104
5.1.3.	Gamma-induced repair depends on the growth phase	106
5.2.	Role of yKu70 for DSB repair in a HR deficient background	108
5.3.	Haploid strains can repair DSB in high stationary phase	110
5.4.	Role of Rad5 in the BER repair	113
5.4.1.	Suppression of <i>rad5</i> phenotype in BER deficient mutants for repair of gamma-induced ...	114
5.4.2.	Suppression of the <i>rad5</i> phenotype in BER deficient mutants after UV irradiation	115
5.4.3.	Mutagenic effect of the deletion of <i>RAD5</i> in a BER deficient background	116
6.	SUMMARY	118
7.	APPENDIX	120
7.1.	Abbreviations	120
7.2.	References	122
7.3.	Talks and poster presentations	136
7.4.	Curriculum Vitae	137

1. INTRODUCTION

1.1. DNA damage and its repair

The DNA, as carrier of the inherited information of each organism, must remain conserved to guarantee the preservation of organisms in the course of time. DNA damages can arise spontaneously during metabolism or exogenously after exposition to agents like chemicals or radiation. If they remain unrepaired or are incorrectly repaired, these damages can lead to cell death or, in higher organisms, to genetic changes and finally to malignant transformations. This shows the crucial role of DNA repair systems for cell survival.

1.2. Radiation and its effects

According to its energy, radiation is categorized into ionizing and non-ionizing radiation. Ionizing radiation is subdivided into electromagnetic radiation (gamma radiation and X-rays) and particle radiation, as for instance α and β particles, protons, neutrons and accelerated ions. Ionizing radiation ionizes cell components such as nucleic acids, proteins and membrane components, when it penetrates matter with high energy. These modifications can be the result of the direct absorption of radiation energy or the result of the interaction of the biomolecules with reactive primary products such as water radicals.

In DNA, ionizing radiation can cause different lesions. Base damage can arise by pyrimidine and purine oxidation generating for example cytosine or thymine glycols, 8-hydroxyguanine and formamidopyridine. These products are responsible for the destabilization of the N-glycosidic bond leading to the loss of bases causing apurinic and apyrimidinic (AP) sites. Single strand breaks (SSB), double strand breaks (DSB) and multiply damaged sites (MDS), in which different lesions concentrate at a DNA site, can arise after irradiation. DSB are very toxic for cells, since they give rise to deletions or chromosomal rearrangements, leading to loss of genetic information.

In non ionizing electromagnetic radiation, the energy of the photons is lower than the binding energy between the nucleus and its electrons and therefore absorption of a photon can not ionize molecules. This is the case for UV radiation, which however can still damage DNA by exciting pyrimidine rings. Its spectrum has been subdivided by wavelength into UV-A (320-400nm), UV-B (295-320nm), and UV-C (100-295nm). UV-A and UV-B constitute the main solar UV radiation. However, UV-C is commonly used in laboratory studies because it produces mostly the same damages as UV-A and UV-B, but it is more efficient (Friedberg 2006).

The most frequent damages induced by UV-C radiation are cyclobutane pyrimidine dimers (CPD) such as thymine dimers. CPD arise after covalent bonds between adjacent pyrimidines by saturation of the C5 and C6 double bonds of the pyrimidine, resulting in the formation of a four-member ring structure. Other damages are the pyrimidine-pyrimidone (6-4) adduct (also called (6-4) photoproduct) originated by the linkage between the C6 position of the 5' pyrimidine and the C4 position of the 3' pyrimidine, the 5-thyminy1-5,6-dihydrothymine, the 5,6-dihydro-6-hydroxy-cytosine (also called cytosine hydrate), and the 5,6-dihydroxy-5,6- dihydrothymine (thymine glycol). Moreover, deamination and oxidative damages such as 2,6-diamino-4-hydroxy-5-formamidopyrimidine (FapyG) (Crespo-Hernandez and Arce 2004) or 8-oxo-guanin (Le Page, Guy et al. 1998) can be caused by UV irradiation. These damages impede the correct base pairing and recognition by sequence-specific proteins, or even lead to the distortion of the DNA helix. Therefore their repair is important to avoid mutations, regulatory disturbances, or the arresting of replication (Friedberg 2006).

1.3. DNA Repair

Organisms have developed various systems to repair spontaneous and induced DNA damages to guarantee the structural and functional integrity of the genome. These mechanisms and the corresponding proteins are highly conserved, which allows the understanding of the processes in humans from studies in model organisms (Putnam, Pennaneach et al. 2005). The model organism *Saccharomyces cerevisiae* offers many advantages for studies of DNA repair. First, *S. cerevisiae* is easy to manipulate, to grow and to store, reducing time, place and cost. Second, sequence information of the complete yeast genome was available early on (Mewes, Albermann et al. 1997) and today the functions of more than half of the yeast genes are known.

Moreover, there are large numbers of mutants in different metabolic pathways and many cellular components are characterized. And last but not least, yeast allows easy testing for various phenotypes (Aylon and Kupiec 2004). DNA repair mechanisms active in yeast cells can be classified into direct repair (also known as direct reversal), excision repair, double strand break repair and post-replication repair.

1.4. Direct repair

Cyclobutane pyrimidine dimers and (6-4) photoproducts can be directly repaired by photoreversal under the action of two different photolyases, which possess a similar structure (a monomeric protein with two chromophore cofactors) and similar repair mechanisms (Sancar A. 2004). Yeast and many other species present these photolyases, while they are absent in mammalian cells, in which only proteins with similar sequence and structure but without the repair function (cryptochromes) can be found. DNA photolyase uses blue light photons as energy source for the photoreversal of UV-induced pyrimidine dimers and (6-4)-photoproducts. In the repair of pyrimidine dimers, the absorption of a photon and its transfer between the cofactors of the photolyase allows the splitting of the pyrimidine dimer into two ordinary pyrimidines.

In addition to this photoreversal of UV-lesions, there are other direct repair mechanisms with different phylogenetic distributions, substrates and mechanisms. The most important one, which is present in nearly all organisms, is the removal of O⁶-methylgroups from O⁶ methylguanine (O⁶ MeGua) by methylguanine DNA methyltransferase (Sancar A. 2004).

1.5. Excision repair

Excision repair is active when only one strand of the DNA double helix is damaged. In this process a damaged nucleotide (with or without the neighbouring nucleotides) is cut out, leaving a gap in one of the strands of the DNA, that is further processed by a polymerase and ligase. There are three different types of excision repair systems: Mismatch repair (MMR), nucleotide excision repair (NER) and base excision repair (BER). These three systems use different proteins and they are controlled by different genetic pathways. However, they work in a similar way and they can process the same substrate. MMR acts on mispaired bases, small deletions and insertions, which can arise during replication and recombination. NER is carried out by the *RAD3* epistasis group and repairs base damages that would otherwise produce disturbances in the DNA conformation, such as cyclobutane pyrimidine dimers or pyrimidine (6–4) pyrimidone photoproducts.

1.5.1. Base Excision Repair

Base excision repair is the most important DNA repair pathway in yeast and mammals for the removal of base damages. Substrates include oxidative damage (8-oxo-7,8-dihydroguanine (8-oxoG) and 5,6-dihydroxy-5,6-dihydrothymine (Tg)), deamination damage (2,6-diamino-4-hydroxy-5-formamidopyrimidine (FapyG) and 4,6-diamino-5-formamidopyrimidine (FapyA)), methylation damage (N^7 -methylguanine, (N^7 -meG)), AP sites formed by spontaneous loss of bases and uracil residues in DNA. These damages are detected and removed from the DNA by specific N-glycosylases causing apurinic/aprimidinic (AP) sites (Scharer and Jiricny 2001). AP sites are among the most frequent DNA lesions and can also arise by spontaneous hydrolysis of the N-glycosidic bond. Replication past unrepaired AP sites by translesion synthesis can be mutagenic (see 1.7). If AP sites are neither repaired nor tolerated, they can block DNA replication and transcription (Friedberg 2003). However, BER repair of AP sites can sometimes generate mutations by insertion of incorrect bases, as has been seen in *E. coli* and yeast (Otterlei, Kavli et al. 2000; Prakash and Prakash 2002), single strand breaks (SSB) with 3' or 5' blocked ends that are not processable by DNA polymerases and ligases (Krokan, Standal et al. 1997) or double strand breaks (DSB), if DNA with SSB is replicated (Figure 1, Figure 2).

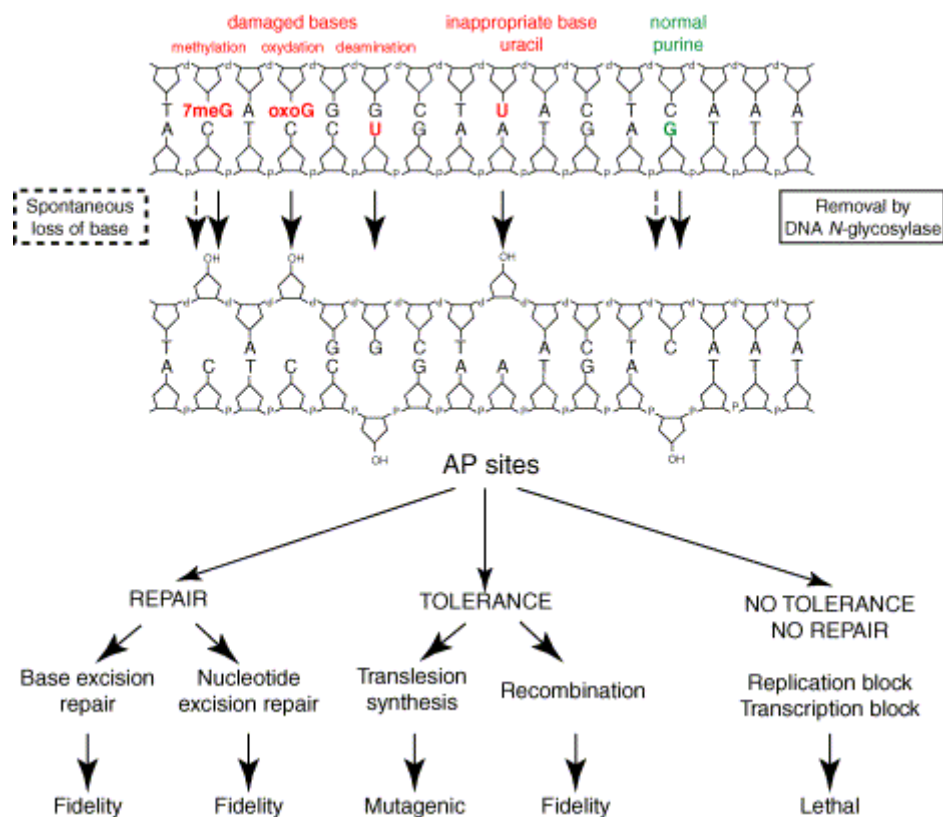


Figure 1: Origin, repair and consequences of AP sites in *S. cerevisiae* (Boiteux and Guillet 2004). AP sites arise spontaneously or during repair of damaged or incorrectly paired bases. AP sites can be repaired error free or tolerated. If neither repair nor toleration occurs, the AP sites block replication and transcription.

In mammals, BER can be subdivided in a long and a short pathway (Sancar A. 2004) and in yeast in a major and minor pathway (Boiteux and Guillet 2004). In *S. cerevisiae*, BER is initiated by the N-glycosylases/AP lyases Ntg1 and Ntg2 that remove damaged or mispaired bases from DNA leaving an AP site. Ogg1, another N-glycosylase, removes exclusively 8-oxoG and FapyG lesions. Then, the generated AP site is recognised and can be processed by AP endonucleases or by N-Glycosylases. In the major pathway AP endonucleases (mainly the Apn1) yield a 5' deoxyribosephosphate (5'-dRP) that after polymerisation of the 3'-end is removed by the action of the Rad27 endonuclease. In the minor pathway, the N-Glycosylases Ntg1 and Ntg2 through their AP lyase activity produce 3' unsaturated aldehydic ends that are then excised by the 3'-phosphodiesterase activity of Apn1 and Apn2. Alternatively, a 3'-flap structure with a 3' unsaturated aldehydic end can be formed and cut out by the Rad1-Rad10 endonuclease. The subsequent DNA polymerisation (Figure 2) seems to be mediated through the C-terminal domain of polymerase ϵ (Pol ϵ), known as polymerase 2 (Pol2), and the ligation by Cdc9 (Boiteux and Guillet 2004).

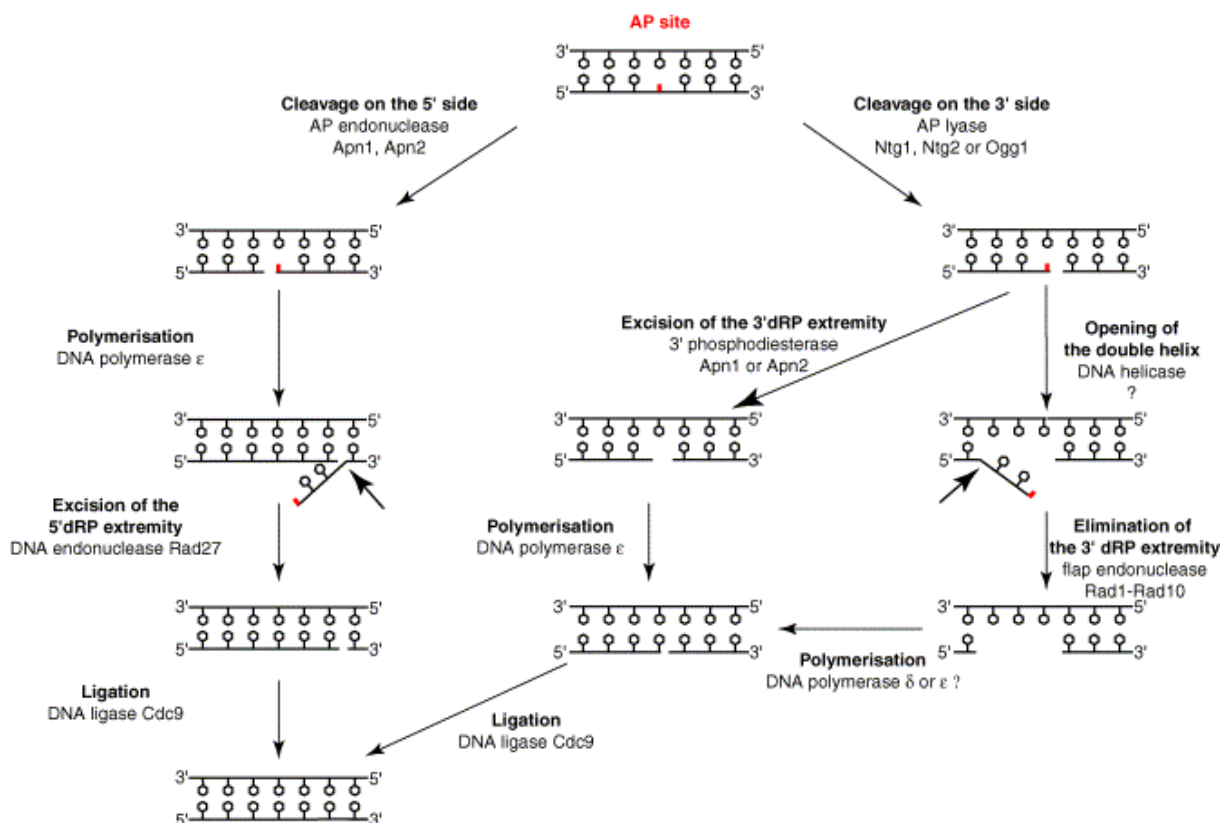


Figure 2: Base excision repair in *S. cerevisiae* (Boiteux and Guillet 2004). *Left:* Major BER pathway in wild-type cells. An AP-endonuclease recognises AP-sites and cleaves them generating 5' deoxyribosephosphate (5'-dRP) ends. Then, the 3'-end is elongated by the DNA polymerase Pol ϵ (Pol2) and the 5' dRP end is released by the 5'-flap endonuclease Rad27. Finally, the ligase Cdc9 seals the nick. *Right:* Minor BER pathway in wild-type cells. Sometimes AP sites are cleaved by an AP-lyase (Ntg1, Ntg2 and Ogg1) that generates 3'-unsaturated aldehydic ends (3'-dRP). These ends are excised by Apn1 and Apn2 endonucleases. Alternatively, 3'-unsaturated aldehydic ends generate 3'-flap structures that are then cleaved by the Rad1-Rad10 endonuclease. Repair of the AP site finishes with polymerization and ligation.

1.5.1.1. Apn1

APN1 is localized downstream of *RAD27* on chromosome XI and expresses a 367 aa, and 41.4 kDa monomeric protein homologous to NfoI of *E. coli*. It is the main AP-endonuclease (cleaves DNA on the 5' side of oxidatively damaged bases (Ischenko and Saparbaev 2002)) and 3' phosphodiesterase in yeast, presenting 97% of the activity in a cell free extract (Popoff, Spira et al. 1990; Ramotar, Popoff et al. 1991; Guillet and Boiteux 2002). Apn1, which binds three zinc atoms, exhibits other catalytic activities such as 3' tyrosyl DNA topoisomerase (Liu, Pouliot et al. 2002) and 3'-5' exonuclease (Vance and Wilson 2001). Although Apn1 is a nuclear protein, it has also been localized in mitochondria (Vongsamphanh, Fortier et al. 2001). Apn1 protects nuclear and mitochondrial DNA from exogenous (oxidation and alkylation) and endogenous DNA lesions.

1.5.1.2. Ntg1 and Ntg2

NTG1 and *NTG2* are localized on the chromosomes I and XV and express proteins of about 40 kDa. Ntg1 and Ntg2 are DNA glycosylases with an additional AP lyase activity. They recognise and excise a vast spectrum of base damage products such as oxidized pyrimidines and formamidopyrimidines by cleaving the N-glycosidic bond. Furthermore, it has been recently proposed that the glycosylase activities of Ntg1 and Ntg2 can protect cells from DNA methylation damage (Hanna, Chow et al. 2004). It has been generally accepted that the generated AP sites are then processed by AP-endonucleases. However, recent studies (Meadows, Song et al. 2003) have proposed Ntg1 and Ntg2 as major contributors (together with Apn1) for the initial processing of AP sites by means of their AP lyase activity. Ntg1 and Ntg2 cleave the phosphodiester backbone at the 3' side of the AP site – that can be opposite to each of the four DNA bases (Senturker, Auffret van der Kemp et al. 1998)- via a β -elimination reaction generating SSB with 3' unsaturated aldehydic ends (Boiteux and Guillet 2004).

Ntg1 and Ntg2 present similarities and differences. Both proteins present a helix-hairpin-helix motif, but only Ntg2 presents an iron-sulphur cluster. Both proteins are localized in mitochondria but only Ntg1 is also nuclear (You, Swanson et al. 1999). Ntg1 is damage inducible, whereas Ntg2 is constitutively expressed (Alseth, Eide et al. 1999).

1.6. DNA Double Strand Break Repair

DNA double strand break repair is necessary to restore the chromosomal integrity when both DNA strands are interrupted. DSB arise during the cell metabolism or as a consequence of exogenous agents such as ionizing radiation (Jeggo 1998; Olive 1998; Wallace 1998), mechanical stress, chemicals like MMS or bleomycin (Povirk 1996). In dividing cells, DSB can also arise from the replication of a SSB or UV-damaged DNA (Galli and Schiestl 1998). The repair of these breaks is of essential importance to avoid chromosomal fragmentation that can lead to cell death (Dudas and Chovanec 2004). There are two major groups of repair pathways, which differ regarding their mechanisms and proteins as well as in their importance in different organisms. These mechanisms are Homologous Recombination (HR) and Nonhomologous End Joining (NHEJ).

1.6.1. Homologous Recombination (HR)

Homologous recombination (HR) can be defined as the exchange of DNA between homologous sequences. It guarantees the correct segregation of chromosomes and the increase of the genomic diversity in meiotic cells, whereas in mitotic cells it is responsible for the repair of DSB. In yeast, HR is the major DSB repair pathway and it is catalyzed by the *RAD52* epistasis group (*RAD52*, *RAD50*, *RAD51*, *RAD54*, *RDH54/TID1*, *RAD55*, *RAD57*, *MRE11* and *XRS2*) (Paques and Haber 1999). Due to the high conservation of the responsible proteins the mechanistic insights obtained in *S. cerevisiae* can be inferred to higher eukaryotes.

HR requires the search and extensive pairing of homologous sequences (Aylon and Kupiec 2004). In meiotic cells, homologous chromosomes are in close proximity to each other, which promotes interactions between homologous sequences. However, in mitotic cells, the search for homology involves the whole genome (Inbar, Liefshitz et al. 2000). Thus, broken chromosomes can be repaired by use of homologous sequences located in the sister chromatid (Gonzalez-Barrera, Cortes-Ledesma et al. 2003), in the homologous chromosome (allelic recombination, Palmer, Schildkraut et al. 2003) or anywhere in the genome (ectopic recombination, Inbar and Kupiec 1999; Aylon, Liefshitz et al. 2003).

Table 1: HR proteins in *S. cerevisiae*, human homologs and interacting partners in yeast (Dudas and Chovanec 2004)

<i>S. cerevisiae</i>	Humans	Biochemical activity/function	Interacting partners (in yeast)
Rad50	Rad50	ATP-dependent DNA-binding and ATPase activities	Mre11
Mre11	Mre11	3'-5' dsDNA exonuclease, ssDNA endonuclease DNA-binding, ssDNA annealing, DNA duplex unwinding and hairpin cleavage activities	Itself, Rad50, Xrs2, Zip2, Zip3
Xrs2	Nbs1	Human: regulates DNA duplex unwinding and nuclease activities of the MRN complex; recruits the MRN complex to vicinity of DNA damage	Mre11
Rad51	Rad51	ATP-dependent DNA-binding protein, ATP-dependent homologous pairing and DNA strand exchange activities	Rad52, Rad54, Rad55, Rdh54/Tid1, Sgs1, Rsi1/Apc2, Zip3, Mlh1, Dmc1*, Sap1, Ubc9, YMR233W, YPLC238C, YPR011C
Rad52	Rad52	DNA-binding, ssDNA annealing, weak DNA strand exchange and weak homologous pairing activities	RPA, Rad51, Rad52, Rad59
Rad54	Rad54	DNA-binding, dsDNA-dependent ATPase, dsDNA unwinding and dsDNA topology-modifying activities	Rad51, Mus81
Rdh54/Tid1	Rad54B	DNA-binding and dsDNA-dependent ATPase activity	Rad51, Dmc1
Rad55	Xrcc2	ATPase	Rad51, Rad57
Rad57	Xrcc3	ATPase	Rad55, Zip3
Rad59	-	DNA-binding and ssDNA annealing activities	Rad52, Rad51*

*Indirect interaction or interaction that was detected by one method but not confirmed by other methods.

1.6.1.1. The Rad52 protein

Rad52 is the most important protein within the *RAD52* epistasis group for DSB repair in yeast, as it is required in spontaneous and DSB induced mitotic recombination events such as mating-type switching (White and Haber 1990), synthesis dependent strand annealing (SDSA), double-strand break repair (DSBR), single strand annealing (SSA, Sugawara and Haber 1992) and break-induced replication (BIR, Bosco and Haber 1998), as well as in meiotic recombination. *rad52* mutants are highly sensitive to IR, MMS, actinomycin D, hexavalent chromium (O'Brien, Fornasaglio et al. 2002), bleomycin, MNNG (N-methyl-N'-nitro-N-nitrosoguanine, Brozmanova, Vlckova et al. 1994), cisplatin, MMC (mitomycin C), 8-MOP (8-methoxypsoralen, de Morais, Vicente et al. 1996) and alkylating agents (Dolling, Boreham et al. 1999; Simon, Szankasi et al. 2000).

This 52.4 kDa and 471 aa protein (Mortensen, Erdeniz et al. 2002) binds to ssDNA and forms ring-like structures of approx. 10 nm distributed along the DNA, resembling necklaces (Shinohara, Shinohara et al. 1998). Microscopy studies have also shown the colocalization of the Rad52 DNA repair foci with DSB, where Rad52 can recruit more than one DSB (Lisby, Mortensen et al. 2003).

Rad52 interacts with Rad51 through its non-conserved C-terminus (Milne and Weaver 1993), facilitating the loading of Rad51 to the recombination site in strand exchange processes dependent on Rad51 (Benson, Baumann et al. 1998; New, Sugiyama et al. 1998; Shinohara and Ogawa 1998) by two ways: either by facilitating Rad51 the access to ssDNA through displacing the RPA or by forming a complex with RPA-ssDNA, which at the same time recruits Rad51. Moreover, the interaction of Rad52 with Rad51 leads to additional stability in the formation of single nucleofilaments and is necessary to form D-loops through the binding of the protein-ssDNA complex and the dsDNA (Arai, Ito et al. 2005).

The N-terminus of Rad52 is conserved and homologous to the N-terminus of Rad59. This terminus mediates the promotion of the Rad51-independent single strand annealing process (Tsukamoto, Yamashita et al. 2003) and it has ssDNA and dsDNA binding activity (Mortensen, Bendixen et al. 1996; Mortensen, Erdeniz et al. 2002). It also appears to be responsible for a weak pairing activity (Kagawa, Kurumizaka et al. 2001) as well as for the homodimerization of Rad52 (Hays, Firmenich et al. 1998).

The middle region seems to play a role in the post-transcriptional regulation of Rad52. Studies of the regulation of the Rad52 level in the cell have shown that mutations within the middle region increase the level and half-life of Rad52 (Asleson and Livingston 2003).

1.6.1.2. Models for homologous recombination

Several subpathways of homologous recombination -all depending on Rad52- have been proposed: the classical DSB repair model (DSBR), the Synthesis Dependent Strand Annealing model (SDSA), the Break-induced Replication model (BIR) and the Single Strand Annealing model (SSA, Paques and Haber 1999).

Since the **Synthesis Dependent Strand Annealing model (SDSA)** explains most of the mitotic recombination events (Aylon and Kupiec 2004), it will be described in more detail (see Figure 3). After DSB formation DNA ends are processed yielding 3' ssDNA tails (Fishman-Lobell, Rudin et al. 1992; Aylon, Liefshitz et al. 2003). This processing appears to require at least the Rad50-Mre11-Xrs2 complex (MRX) (Bressan, Baxter et al. 1999; Symington 2002; Krogh and Symington 2004) and the checkpoint protein Rad24 (Aylon and Kupiec 2003). The new 3' ssDNA tails are then covered by the RPA protein till the incorporation of Rad51 (Sung 1997; Wang and Haber 2004). Rad51 accumulates on ssDNA targeted by Rad52 (Song and Sung 2000) and generates a nucleofilament. Subsequently, a sequence homologous to the 3' ssDNA tail is searched in the genome. This homologous donor sequence is invaded by the ssDNA, which forms a D-loop and displaces the Rad51 (Sugawara, Wang et al. 2003). At this stage degradation is inactivated. The invading ssDNA, used as a primer, is elongated by a DNA polymerase. Then, the newly synthesised strand is displaced from the D-loop and reanneals with the opposite broken arm. Rad52, which has remained at the interacting strands (Miyazaki, Bressan et al. 2004), may possibly have a role in the reannealing of the synthesized DNA with the broken arm (Aylon and Kupiec 2004), as in vitro experiments have already shown (Mortensen, Bendixen et al. 1996). Finally, ligation of the DNA ends finalizes the process (see Figure 3).

There are other proteins and complexes involved in SDSA (and other homology-dependent pathways), the most important being Rad59, Rad55, Rad57 and Rad54. Rad59, is homolog to Rad52 at the N-terminal region and can reanneal complementary ends (Bai, Davis

et al. 1999; Davis and Symington 2001). The Rad55/Rad57 complex binds sequences flanking the DSB and possibly has a function for the invasion of the strands, in the completion of gene conversion and in the stabilization of the Rad51 filament. Rad54, a member of the Swi2/Snf2 family, can remodel chromatin in vivo (Wolner and Peterson 2005). It has a function as mediator of Rad51 binding to ssDNA (Wolner, van Komen et al. 2003) and in the disassembly of Rad51 and Rad52 foci (Miyazaki, Bressan et al. 2004). See Figure 3 and Table 1 for more information.

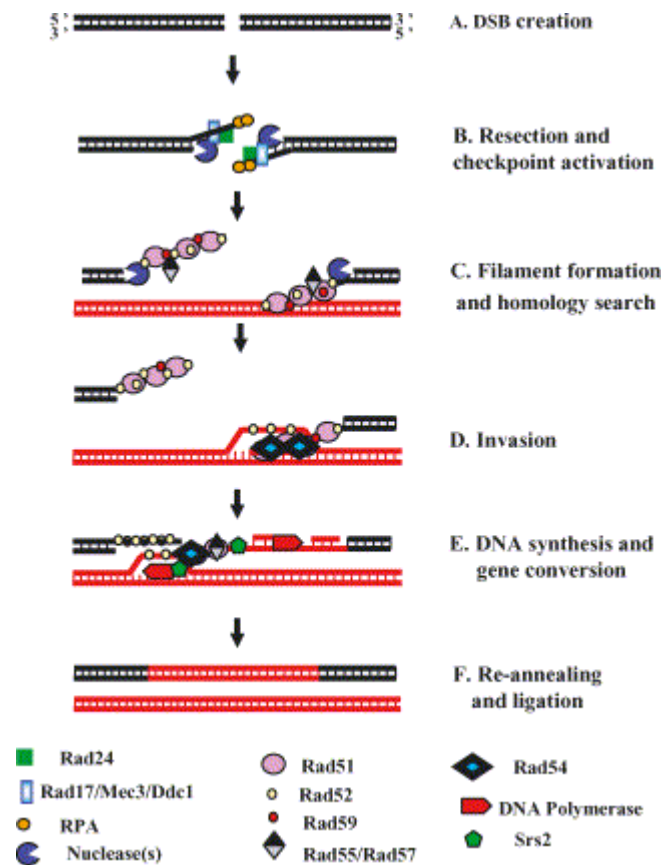


Figure 3: The SDSA model (Aylon and Kupiec 2004). (A) After DSB formation, (B) one or both DNA ends are degraded by nucleases producing 3' tails and checkpoint proteins are activated. The Rad17/Mec3/Ddc1 complex is loaded by Rad24. (C) The exposed 3'-tails are covered by RPA till Rad52 and the Rad55/Rad57 complex mediate the formation of the Rad51 nucleofilament, that also includes Rad59, displacing RPA. Homologous sequences are searched in the genome. (D) Once homology is found, degradation stops and the single strands invade the homologous sequence. (E) Next, Srs2 disassembles the Rad51 nucleofilament and DNA is synthesized. (F) This newly synthesized DNA is then reannealed and sealed with the opposite broken arm. Rad52 and Rad55/Rad57 complex are required at this step.

Another important model for DSB repair is known as the **Double-strand break repair model (DSBR)** and it was proposed in 1983 by Szostak (Szostak, Orr-Weaver et al. 1983). In this model (see Figure 4), there is also a processing of the broken ends for the generation of ssDNA 3'OH tails. However, both of these ssDNA tails invade the homologous duplex. The displaced ssDNA forms a D-loop and pairs with the non-invading strand, starting the synthesis of the 3'-ends of this strand. This pairing generates double-Holliday-junctions (dHj) (for a review, see Symington 2002), which can be resolved in crossover or non-crossover events (Orr-Weaver and Szostak 1983).

Break-induced replication (BIR) (Malkova, Ivanov et al. 1996) can arise with or without the action of the Rad51 (Davis and Symington 2004), leading to different kinetics and checkpoint responses (Malkova, Naylor et al. 2005). BIR is a process very similar to SDSA, but in this process the invading ssDNA is replicated till the end of the donor chromosome (Haber 2000). Probably this process is important for the maintenance of telomeres in the absence of telomerase (Le, Moore et al. 1999; Teng, Chang et al. 2000).

Single-strand annealing (SSA) (Pastink, Eeken et al. 2001) is the major HR pathway for repairing DSB arisen between repeated sequences longer than 30bp (Sugawara, Ira et al. 2000). SSA is an error prone repair pathway independent of Rad51 (Ivanov, Sugawara et al. 1996). Once a DSB arises, 5'tails are resected up to a homology region, leading to the formation of a heteroduplex. Next, the nonhomologous tails are removed and the process ends with DNA synthesis and ligation. Recent studies have shown that the heteroduplex formation is impaired by moderate differences between the homologous regions in a process known as heteroduplex rejection (Sugawara, Goldfarb et al. 2004). In this process, the mismatch repair proteins Msh2 and Msh6 appear to recognize the mismatches during the heteroduplex DNA formation and recruit the Sgs1 helicase to unwind the annealed DNA. The importance of SSA differs with the ploidy, the cell cycle phase and among organisms (Heidenreich, Novotny et al. 2003).

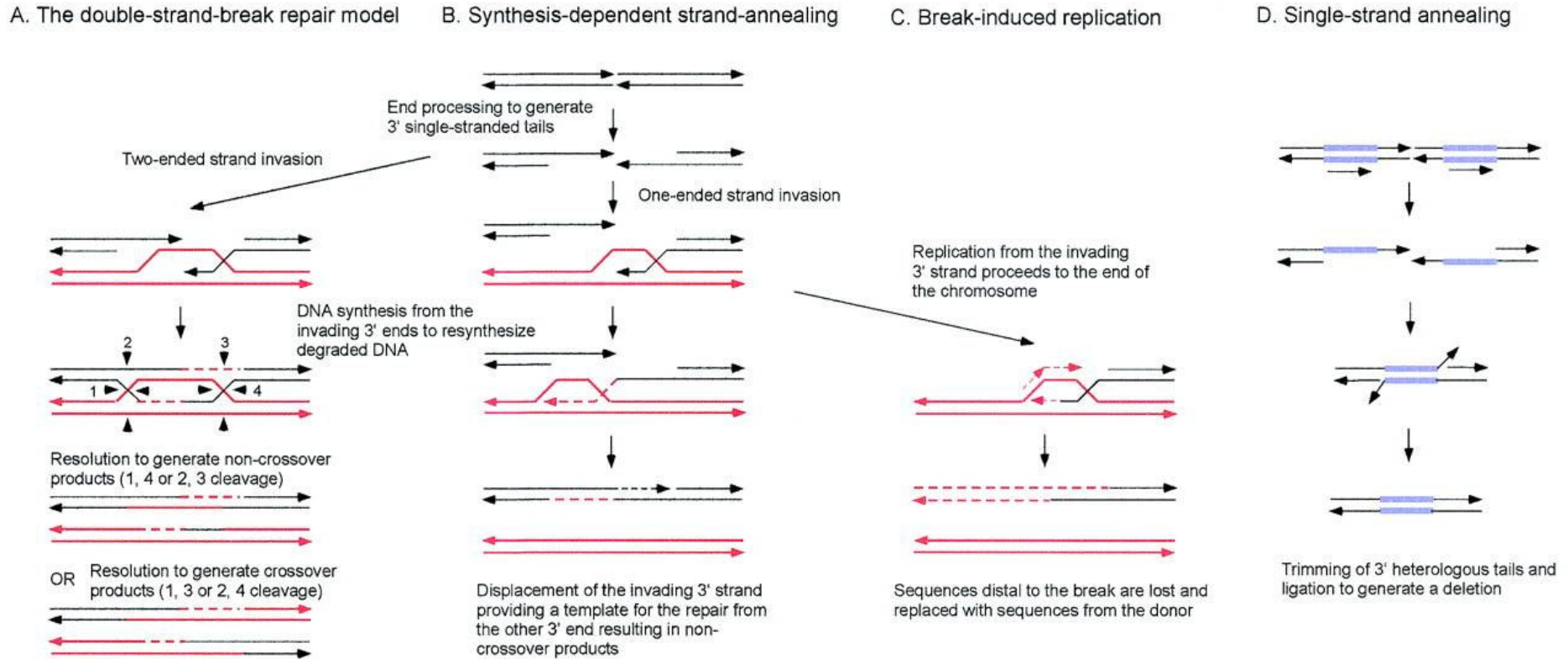


Figure 4: DSB repair models (Symington 2002). (A) DSBR model: End degradation yields 3' ends, which invade the homologous donor, triggering DNA synthesis. After ligation, the dHJ can be resolved with or without crossover. (B) SDSA model: End degradation yields 3' ends. One end invades the homologous donor triggering DNA synthesis. The D-loop can be elongated by DNA synthesis or can migrate with the newly synthesized DNA. Then, the synthesized DNA strand is displaced and paired with the other 3' end. DNA synthesis finalizes the process. (C) BIR model: In this process after invasion of the donor strand, DNA synthesis is carried out up to the end of the DNA molecule. (D) SSA model: After DSB formation between homologous sequences, 5' ends are degraded till the homologous sequences are exposed. Then, homologous sequences anneal and the 3' tails are removed. Ligation of the nicks finalizes the process. Arrow heads indicate 3' ends.

1.6.2. Nonhomologous End Joining (NHEJ)

NHEJ or illegitimate recombination is the most important DSB repair pathway in mammals but it has only a minor role in yeast (Milne, Jin et al. 1996; Siede, Friedl et al. 1996), where it is only apparent when HR is inactive (Siede, Friedl et al. 1996; Critchlow and Jackson 1998; Sonoda, Hohegger et al. 2006). Therefore, most of the proteins and mechanisms were initially identified in mammals.

NHEJ starts when the yKu70/yKu80 complex (Figure 5 and Figure 2) binds to the DNA ends of a DSB (Lewis and Resnick 2000), possibly protecting them from degradation (Lee, Moore et al. 1998). Then, the Mre11/Rad50/Xrs2 complex (MRX) associates with the Ku complex, probably acting as end bridging factor (Paull and Gellert 2000). Subsequently, the Dnl4/Lif1 complex is recruited to the DSB ends. It has been shown that the interaction between Xrs2 and Lif1 is decisive for the stimulation of intermolecular ligation (Chen, Trujillo et al. 2001). The Dnl4/Lif1 complex recruits the Rad27 endonuclease and the NHEJ polymerase Pol4 to the repair site, promoting the processing and gap filling of the DNA ends. Finally, Dnl4 seals the break (Pastwa and Blasiak 2003; Hefferin and Tomkinson 2005).

Table 2: NHEJ repair proteins in yeast and human homologs (Hefferin and Tomkinson 2005)

<i>S. cerevisiae</i>	<i>H. sapiens</i>	Properties/functions
yKu70/yKu80	Ku70/Ku80	Non-specific dsDNA end binding
-	DNA-PKcs/Artemis	Protein kinase/Protein nuclease
		Endonuclease activity, DNA end bringing activity
Dnl4/Lif1	DNA ligase IV/XRCC4	ATP-dependent DNA ligase
Rad50/Mre11/Xrs2	Rad50/Mre11/Nbs1	Mre11: 3'-5' exonuclease, structure specific endonuclease; Rad50: ATP binding; Xrs2 and Nbs: end binding activity
Pol4	Pol μ and Pol λ	DNA polymerases
Rad27	FEN1	5' Flap endonuclease
Nej1	Cernunnos	Cell type-specific regulator of NHEJ

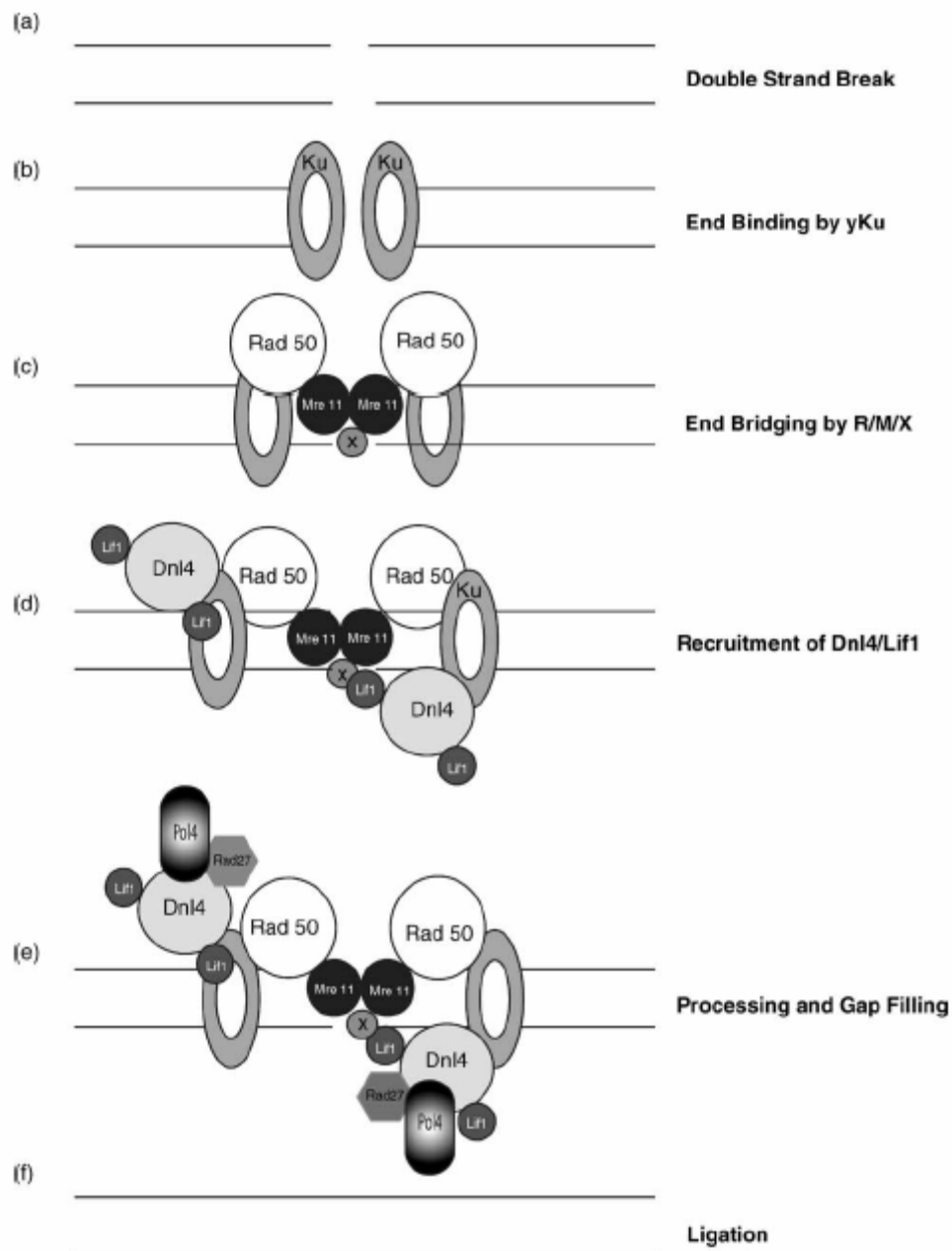


Figure 5: NHEJ in *S. cerevisiae* (Hefferin and Tomkinson 2005). After DSB (a) the yKu complex binds to the DSB ends (b). The MRX complex associates with the Ku complex (c). The Dnl4/Lif1 complex is recruited to the DSB ends (d) and it recruits the Rad27 endonuclease and the NHEJ polymerase Pol4 (e). After processing and filling of the DNA ends Dnl4 seals the break (f).

NHEJ allows the simple and direct rejoining of DNA ends (Critchlow and Jackson 1998) and it is commonly considered an error-prone DSB repair pathway, due to the possible addition or deletion of nucleotides at the free DNA ends and the generation of gross chromosomal rearrangements by rejoining of false ends. Although NHEJ does not require homology between sequences in trans, several studies have revealed that many NHEJ events involve the alignment of short complementary sequences (1-4 nucleotides in cis), also known as microhomologies, by a mechanism called microhomology mediated end joining (Kramer, Brock et al. 1994; Boulton and Jackson 1996; Moore and Haber 1996; Wilson and Lieber 1999; Yu, Marshall et al. 2004).

Thus, DSB can be repaired with different accuracy, generating different types of errors such as mispairing of overhangs, joining by microhomologies, chromosome rearrangements and synthesis errors (Daley, Palmbo et al. 2005). Overhangs and therefore DNA end structure play a decisive role in the accuracy of NHEJ by joining both DNA ends of a DSB by bp-pairing and serving as a template for the resynthesis of damage sequences. In yeast, blunt ends are poorly rejoined (Boulton and Jackson 1996), whereas pairing between 4-bp overhangs is very accurate (Moore and Haber 1996; Wilson and Lieber 1999). Sometimes the bases of an overhang can pair with the bases of the other overhang in different ways depending on the thermodynamic stability of the possible pairing (Wilson and Lieber 1999; Daley and Wilson 2005). Since NHEJ does not reject incorrect pairings, mispairing of overhangs can arise. Overhangs can also be degraded up to a microhomology in order to allow the rejoining, which generates a shortening of the repaired sequence. This rejoining by microhomologies arises especially in DSB presenting incompatible overhangs (Ma, Kim et al. 2003). When two or more DSB occur simultaneously, chromosome rearrangements can occur. Although the frequency of this process is not known, it seems to be low (Daley, Palmbo et al. 2005), possibly due to the action of MRX, which maintains the DNA ends of a DSB in proximity (Lobachev, Vitriol et al. 2004). And finally, synthesis errors can occur during the replacing of damaged nucleotides by the Pol4, which operates with a marked error rate.

1.6.2.1. yKu70

yKu70, a 70.6 kDa protein and the yeast homolog of the mammalian Ku70, was initially called Hdf1 (high affinity DNA-binding factor) due to its high DNA binding capacity (Feldmann and Winnacker 1993). *yku70* mutants show increased sensitivity to bleomycin, MMS (Milne, Jin et al. 1996) and to ionizing radiation in a HR deficient background (Siede, Friedl et al. 1996). These mutants also present a temperature-sensitive phenotype for growth at 37°C (Feldmann and Winnacker 1993; Boulton and Jackson 1996), are involved in mating-type switching and spontaneous mitotic recombination (Mages, Feldmann et al. 1996) and show exchange-type aberrations (Friedl, Kiechle et al. 1998).

yKu70 forms a complex with yKu80, a 80 kDa protein homolog to the mammalian Ku80 (Boulton and Jackson 1996; Feldmann, Driller et al. 1996). The Ku heterodimer binds to DNA ends in a sequence-independent way and promotes repair through NHEJ (Milne, Jin et al. 1996). Another important function of yKu70 is the maintenance of the telomere region (Porter, Greenwell et al. 1996; Boulton and Jackson 1998). It has been revealed that yKu70 binds directly to telomeres (Gravel, Larrivee et al. 1998; Driller, Wellinger et al. 2000), where yKu70 either can protect telomeres against nucleases and recombinases (Polotnianka, Li et al. 1998) or has a role in telomere organization in the yeast nucleus (Laroche, Martin et al. 1998). Further studies have shown a defective TPE function (telomere position effect) in *yku70* mutants, which leads to the loss of the condensed chromatin structure and the expression of genes which are normally silenced due to their proximity to the telomere (Nugent, Bosco et al. 1998). The different roles yKu70 plays for DSB and telomeres, where it presents antagonist functions (promoting and avoiding end joining), can only be explained by the performance of different activities at these different DNA termini (Bertuch and Lundblad 2003).

1.6.3. Balance between HR and NHEJ

The importance of HR and NHEJ differs between mammals and yeast. HR pathways are predominant in yeast. They are more complex and ensure accuracy by using homologous sequences, but may also cause rearrangement of the genome. In yeast, where the genome compaction simplifies the homology search, accuracy is essential to avoid cell death due to incorrect repair.

In mammals, DSB are repaired mainly by NHEJ, although recent studies have also revealed an important contribution of HR (Morrison and Takeda 2000; Johnson and Jasin 2001; Thompson and Schild 2001; van den Bosch, Lohman et al. 2002). The potentially inaccurate repair by NHEJ can be tolerated in somatic mammalian cells, where large genome fractions are not functional (Kanaar, Hoeijmakers et al. 1998) and NHEJ can avoid replication stops of the HR repair machinery.

In yeast, it was suggested that NHEJ regulation depends on the ploidy, on the growth phase and on proteins such as Rad5. The ploidy of a cell can control NHEJ due to the action of *NEJ1*. *NEJ1* is an haploid-specific gene that facilitates the transport of Lif1 (ligase interfacing factor 1) into the nucleus, controlling the formation of the Dnl4/Lif1 complex necessary for NHEJ (Kegel, Sjostrand et al. 2001; Valencia, Bentele et al. 2001; Jazayeri and Jackson 2002; Wilson 2002). Thus, the missing activity of Nej1 would explain the downregulation of NHEJ in diploid cells, which present homologous chromosomes and therefore can repair accurately by HR. In contrast, haploid yeast cells use both, HR and NHEJ (Astrom, Okamura et al. 1999; Valencia, Bentele et al. 2001).

The growth phase also influences this balance by promoting NHEJ in G1 cells, since in G1 DSB 5'-ends are not resected and this is necessary for HR (Karathanasis and Wilson 2002; Daley, Palmboos et al. 2005). It has recently been suggested that yeast cells repair the broken chromosomes during the G1 stage by NHEJ and during the rest of the cell cycle by HR (Aylon and Kupiec 2005). This could be due to the inactivity of the cyclin-dependent kinase Cdk1 (Cdc28) during G1. Cdk1 is involved in the efficient 5'-3' resection of DSB ends and in the recruitment of RPA and Rad51, therefore being responsible for the cell checkpoint activation and for the DSB-induced HR at any stage (Ira, Pellicioli et al. 2004). The inactivation of Cdk1 also explains in part the increase in NHEJ also observed in G0 cells, which are deprived of nutrient during long periods and under high oxidative stress (Karathanasis and Wilson 2002). NHEJ seems to precede HR temporally and can therefore also arise in S/G2 stage if it can be completed rapidly before end resection takes over (Frank-Vaillant and Marcand 2002).

A different active regulation was previously proposed by Ahne, F. *et al.*, (Ahne, Jha *et al.* 1997), in which Rad5, a member of the *RAD6* epistasis group performing so called post-replication repair (PRR), was supposed to have a regulatory role in the balance between HR and NHEJ. The further study of this regulation is a goal of this work.

1.7. Post-replication repair (PRR)

When blocking lesions are not repaired before S phase through the BER or NER pathways, replication can stop and cells can die. Since cells have developed mechanisms to tolerate these damages, replication can continue independently of the lesion removal. These “tolerance mechanisms” generate gaps in the newly synthesized strand that have to be filled by post-replication repair (PRR), whereas in the template strand the damage remains unrepaired. Because of the fact that the initial damage is not repaired but tolerated, this mechanism is more a damage avoidance way than a true repair pathway. The repair of the gaps can be carried out either by HR or template switching with the sister chromatid, which is relatively error-free, or by translesion synthesis (TLS), which however can be error-prone (Xiao, Chow *et al.* 1999; Xiao, Chow *et al.* 2000). Initially, it was thought that the gaps left after replication were repaired by HR, and the term post-replication repair was used for this special repair pathway.

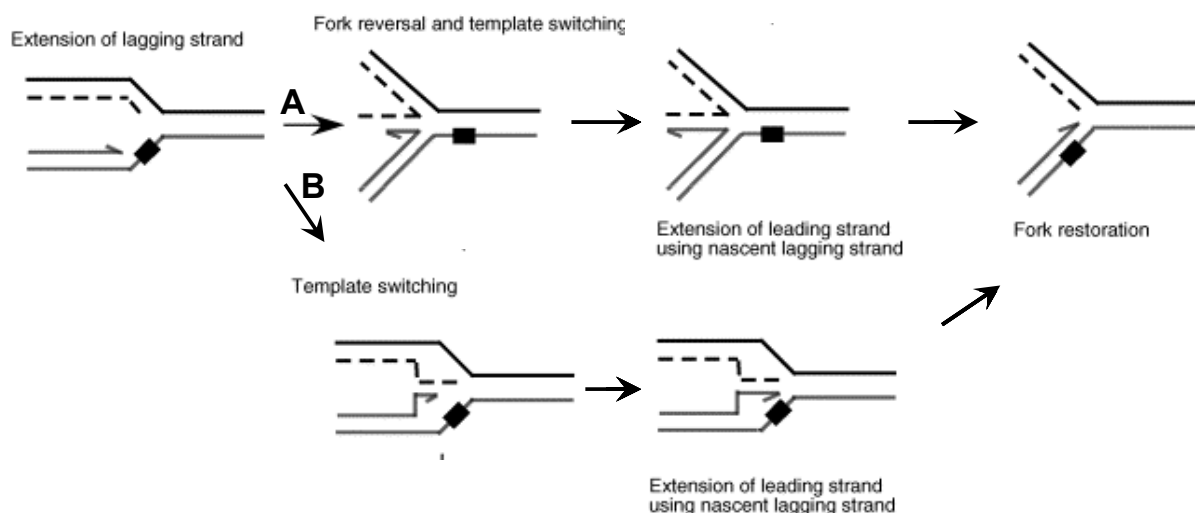


Figure 6: Model of template switching in error-free PRR (Smirnova and Klein 2003). When a lesion on the leading strand (rectangle) blocks the replication fork, the synthesis on the lagging strand can continue producing an overshoot nascent DNA. Then, there are two ways to repair the lesion correctly. (A) The replication fork can revert, allowing the annealing of strands and the synthesis of the leading strand beyond the stalling lesion. (B) The leading and lagging strand pair with each other allowing the synthesis beyond the lesion. Finally, the lesion is bypassed through pairing of nascent and template strands and the restoration of the fork.

Later on, translesion synthesis (TLS) was found to be predominant. The term PRR is now used to describe the mechanism managing the different pathways and favouring TLS over HR. In template switching, when a lesion on the leading strand template blocks the replication, the synthesis on the lagging strand continues, generating an overshoot of nascent strand. Two pathways have been proposed (Figure 6). In one of them (Figure 6 - B), the nascent strand can anneal with the leading strand and act as template, allowing the synthesis of the blocked leading strand. After the extension of the leading strand beyond the blocking lesion, the fork can be restored and the synthesis of the leading and lagging strands continues (Lawrence 1994). A different model (Figure 6 – A) proposes the reversion of the replication fork previous to annealing between leading and lagging DNA strands (Smirnova and Klein 2003). The error prone pathways lead to mutagenesis due to the bypass of DNA replication blocks and the incorporation of incorrect nucleotides by the DNA polymerase ζ . Recent studies (Minesinger and Jinks-Robertson 2005) have proposed two different error-prone pathways promoted either by Rad5 or Rad18 (Figure 7).

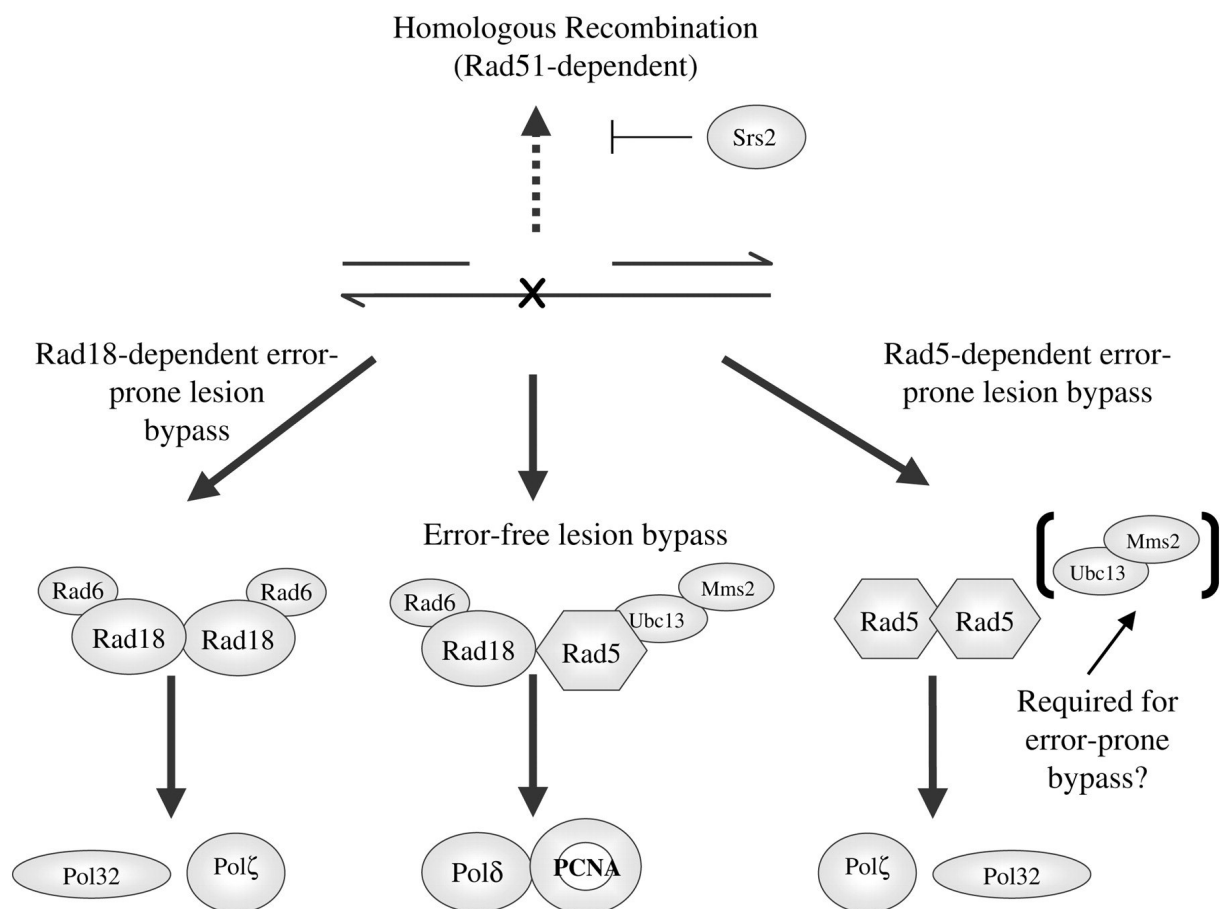


Figure 7: Current model for spontaneous lesion bypass through the *RAD6* epistasis group. This model proposes the activity of Rad18 and Rad5 in different error-prone repair pathways, which are Pol ζ dependent. In the error-free pathway proteins involved in DNA replication act together with Rad5 and Rad18 (Minesinger and Jinks-Robertson 2005).

These DNA damage tolerance pathways are controlled by two systems of protein modification exclusive of eukaryotes: the ubiquitination and sumoylation. Ubiquitin and SUMO (small ubiquitin-related modifier) are small and highly conserved proteins which can be attached covalently to different cellular proteins, affecting their stability, localization and activity. The attachment of multiple ubiquitin (multiubiquitination) marks short-lived proteins for degradation, and the attachment of a single ubiquitin (monoubiquitination) can also regulate the chromatin structure of histones. Although sumoylation is less well understood, it has been probed to affect the localization of the target proteins, their enzymatic properties and their protein-protein interactions (Ulrich 2005).

PRR is mediated by the *RAD6* epistasis group, which is conserved throughout evolution and is composed of *RAD6* (*UBC2*), *RAD18*, *REV1*, *REV3*, *REV7*, *RAD30* and *RAD5* (*REV2*). However, the necessity of *SRS2* (Friedl, Liefshitz et al. 2001; Ulrich 2001) and a partial role of *RAD52* (Broomfield, Hryciw et al. 2001) have also been proposed. The main proteins in PRR involved in all sub-pathways are Rad6 and Rad18. Rad6 and Rad18 form a heterodimer and present ubiquitin-conjugating activity, ATPase activity and ssDNA binding activity (Bailly, Lauder et al. 1997). In *S. cerevisiae*, Rad6 is also necessary for functions like sporulation, protein degradation and telomere silencing (Huang, Kahana et al. 1997). Rad18, which possesses a ring finger domain, acts together with Rad5 for the repair of spontaneous lesions, but it also plays an alternative role to Rad5 in mutagenic repair (Liefshitz, Steinlauf et al. 1998). *RAD5* and *POL30* are involved in two different error-free pathways, promoted by the action of *MMS2* and *UBC13* (Broomfield, Hryciw et al. 2001). *POL30* encodes for the proliferating cell nuclear antigen (PCNA), which is required for Pol δ and Pol ϵ mediated DNA synthesis (Ayyagari, Impellizzeri et al. 1995). *REV1* encodes a deoxycytidyl transferase and *REV3* encodes for the catalytic subunit of the non-essential DNA polymerase ζ (Nelson, Lawrence et al. 1996; Nelson, Lawrence et al. 1996) that also contains *REV7*. *REV1*, *REV3* and *REV7* are involved in the *REV3* pathway, responsible for the error-prone repair of lesions caused by mutagenic substances such as aflatoxin B₁ (Guo, Breeden et al. 2005).

1.7.1. Rad5

Rad5 (Rev2), a protein of 134 kDa and 1169 aa, is a member of the SNF2/SWI2 superfamily and seems to be posttranscriptionally regulated by Dun1 kinase and Pan2-Pan3 (poly(A)-nuclease) (Hammet, Pike et al. 2002). It presents weak homologies with the SMARCA3 protein in humans and with different proteins of other organisms (see Figure 8), a functional homology not having been detected so far. Rad5 possesses a leucine zipper motif preceded by a basic region, which is probably involved in homodimer binding (Johnson, Henderson et al. 1992). It also presents a conserved DNA-dependent ATPase domain composed by seven helicase consensus motifs (Johnson, Henderson et al. 1992; Johnson, Prakash et al. 1994). However, there is currently no evidence for any helicase activity. The helicase-like domain situated in the C-terminal half of the sequence is disrupted by a (central) ring finger domain with zinc-binding capacity which is responsible for the interaction to Ubc13 and for ubiquitin ligase activity (Ulrich and Jentsch 2000). By its interaction with the ubiquitin-conjugating complex Ubc13-Mms2, Rad5 catalyzes the polyubiquitination of PCNA (Hoegge, Pfander et al. 2002; Haracska, Torres-Ramos et al. 2004; Pfander, Moldovan et al. 2005). An additional role of Rad5 in DNA repair independent of the ring finger domain is being discussed (Ulrich 2003). Studies of Martini have suggested a further interaction of Rad5 with the histone H2B in the Rad5 - dependent subpathway of PRR (Martini, Keeney et al. 2002).

Deletion of *RAD5* leads to a very pleiotropic phenotype. Besides a high sensitivity towards UV radiation, the *rad5* mutant is also sensitive towards gamma radiation (Friedl, Liefshitz et al. 2001). Moreover, the *rad5* mutant displays elevated rates of spontaneous mitotic recombination (Liefshitz, Steinlauf et al. 1998) and gross chromosomal rearrangements (Smith, Hwang et al. 2004). Based on these observations, it has been suggested that Rad5 contributes to DSB repair. Hence, a regulatory role of Rad5 has been proposed for the balance between HR and NHEJ due to the channelling of DSB repair to NHEJ in *rad5* mutants (75% of the events) in contrast to the WT (less than 1%) (Ahne, Jha et al. 1997). About the role of Rad5 in other repair pathways very little is known. Rad5 could target repair factors to minor groove adducts that distort the double helix and are usually repaired by NER (Kiakos, Howard et al. 2002). However, the relations of Rad5 to BER remain unknown.

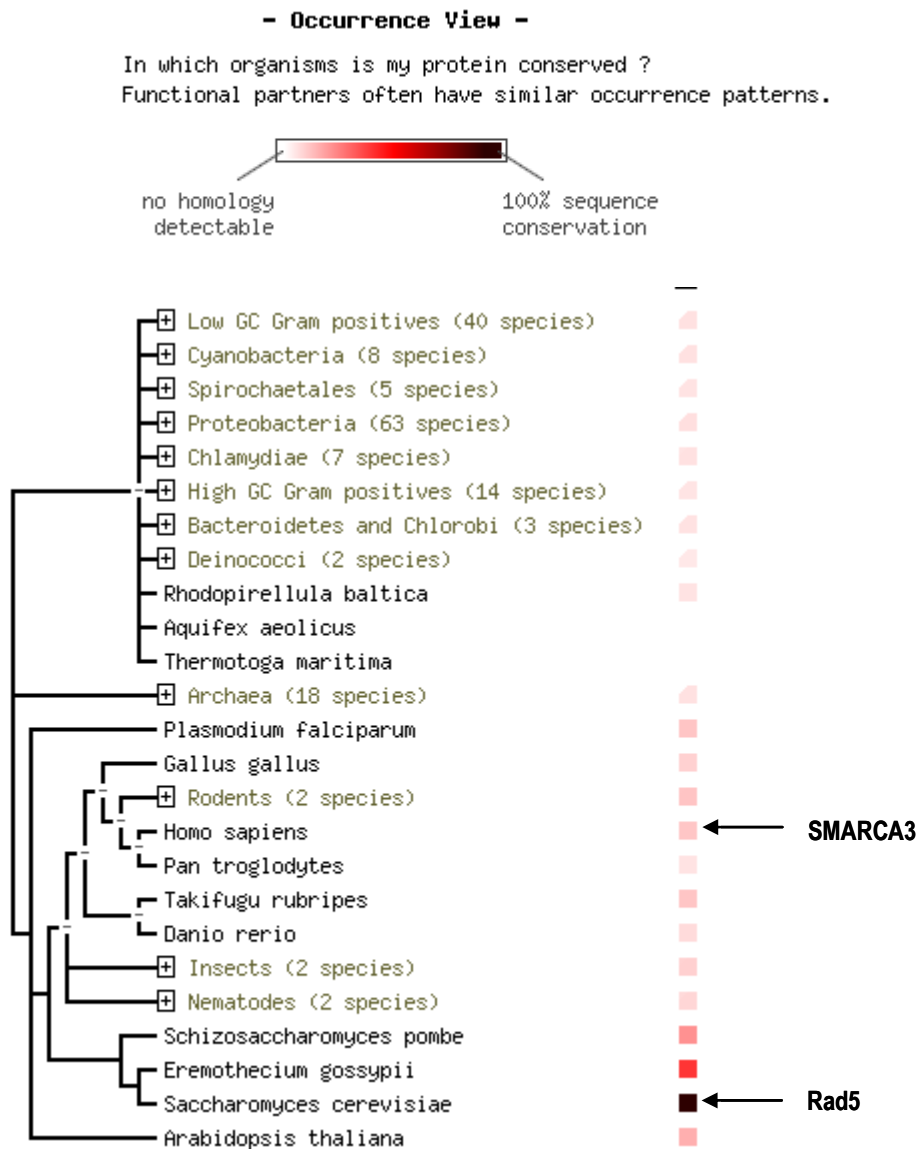


Figure 8: Rad5 homology in different organisms according to data of STRING (<http://string.embl.de/>). The colour intensity of the squares indicates the percentage of homology with respect to Rad5, e.g. black refers to 100% homology, whereas white refers to a complete lack of homology. In humans, the SMARCA3 protein, also a member of the SNF2/SWI2 family, could be a Rad5 homolog.

1.8. Goals

The main goal of this thesis is the further analysis of the role of Rad5 in DNA repair, and in particular its possible regulatory role for the balance between HR and NHEJ.

For this purpose, HR- and NHEJ-deficient *yku70*, *rad5*, *rad52*, *rad52rad5* and *yku70rad52* mutants are generated. Their phenotypes are checked by measuring their survival capacity after UV and ⁶⁰Co gamma irradiation. The repair of gamma-induced lesions at chromosomal level is evaluated, giving special attention to the influence of the cell cycle, since NHEJ is best studied in stationary and HR in logarithmic growth phase. To quantify DSB at chromosomal level by pulsed field gel electrophoresis (PFGE), a new evaluation technique together with specific software for densitometry analysis is developed. This allows the direct determination of the DSB repair efficiency of the mutants.

The role of Rad5 for the repair of DSB and its interplay with Rad52 and yKu70 is studied in more detail at plasmidial level and compared with the results at the chromosomal level. Therefore, the efficiency and accuracy of the repair of a gap induced by restriction enzymes in a plasmid is analyzed. Additionally, PCR and sequence analysis of incorrectly repaired plasmids provides further information on the repair pathways used.

Since the sensitivity of the *rad5* mutant towards gamma irradiation cannot be explained by DSB repair data alone, gamma-induced base damage might also play a role. As BER is the most important repair pathway for this kind of damage, the interplay between Rad5 and BER proteins is studied.

2. MATERIALS

2.1. Equipment

Agarose gel electrophoresis device	BioRad, Munich, Germany
Balance	- 1264 MP, Sartorius, Göttingen, Germany - ABS, Kern & Sohn, Balingen, Germany
Camera	Polaroid MP4-Land Camera, Cambridge, England
Centrifuge	-Multifuge 3SR, Minifuge RF and Biofuge pico, Heraeus, Hanau, Germany -Sigma: 1K15, 2K15 and 201 m, Sigma Laborzentrifugen GmbH, Osterode am Harz, Germany -Eppendorf centrifuge 5415c, Eppendorf, Hamburg, Germany
Clean Bench	Fröbel Labortechnik GmbH, Lindau, Germany
Cooling unit	Liebherr GmbH, Lienz, Austria
Cryo tubes	Nunc GmbH & Co KG, Wiesbaden, Germany
Cuvette	Cuvette 220-1600nm, Eppendorf, Hamburg, Germany
Dry block bath	TR 0287, Bachhofer, Reutlingen, Germany
FACS Device	LRS II, BD Biosciences, Heidelberg, Germany
Freezing unit	- 20°C
	- 86°C
Films	Polaroid 667 Positiv, Sigma, Deisenhofen, Germany
Gamma source	⁶⁰ Co source, Atomic Energy of Canada, Ltd., Kanata, Ontario, Canada
Glass beads	0.25-0.5 mm diameter, Carl-Roth, Karlsruhe, Germany
Gel documentation Geldoc 2000	BioRad, München, Germany
Glass ware	- Schott, Mainz, Germany - Braun, Melsungen, Germany
Incubator	- Memmert, Schwabach, Germany - Heraeus, Hanau, Germany - Sanyo, Japan
Magnetic stirrer	-Ikamag RCT, REO and RCH; IKA-Labortechnik, Staufen i.Br., Germany - Heidolph MR 3000, Schwabach, Germany
Microscope	Olympus C, Olympus Optikal Co., Hamburg, Germany
Microwave	Samsung, Schwalbach, Germany
PCR-Device	- Primus, MWG, Biolab - Cyclone gradient, Peqlab Biotechnologie GmbH, Erlangen
Pulsed Field Gel Electrophoresis device	CHEF MAPPER XA, Bio Rad, München, Germany - 1000 Mini Chiller, Bio Rad, München, Germany - Variable Speed Pump, Bio Rad, München, Germany
Photometer	- BioPhotometer, Eppendorf, Hamburg, Germany

		- Epson MX-82 F/T, Epson GmbH, Düsseldorf, Germany
pH meter		- InoLab pH Level 1, UK - Inolab, WTW, Weilheim, Germany
Pipettes		Eppendorf, Hamburg, Germany
Power supply unit		- Electrophoresis Power Supply-EPS600 Amersham Pharmacia Biotech, Freiburg, Germany - Consort electrophoresis power supply, Fröbel Labortechnik GmbH, Lindau, Germany
Reaction tubes		- 0,5 ml, 1,5 ml, 2,0 ml Eppendorf Hamburg - 15 ml, 50 ml Falcon USA and Greiner Labortechnik, Frickenhausen, Germany - PCR-tubes, Biozym Diagnostik, Hess-Oldendorf, Germany
Scanner		Umax, PowerLook 1000, Willich, Germany
Shaker	Incubators	- HT, INFORS GmbH, Einsbach, Germany - Minitrons HT, INFORS GmbH, Einsbach, Germany
	Mixer	- Mixer 5432, Eppendorf, Hamburg
	Rotational	- Roto-Shake Genie, Scientific Industries Inc., USA
	Thermo mixer	- Thermomixer compact, Eppendorf, Hamburg, Germany - Thermomixer comfort, Eppendorf, Hamburg, Germany
Sequencing device		CEQ 3100, Beckman Coulter, Fullerton, USA
Sterile filter		Sartorius, Göttingen, Germany
UV source		Typ 3.260.002 $\lambda = 254$ nm, Schütt Labortechnik, Göttingen, Germany
UV-Transilluminator		Vilber lourmat, AGS, Heidelberg, Germany
Vacuum pump		VacUubrad RS-4, F.Schultheiss, München, Germany
Vacuum dryer		Speed Vac Concentrator, Eppendorf, Hamburg, Germany
Vortex		- VF2, IKA-Labortechnik, Staufen, Germany - Combi spin, FVL-2400, Peqlab, Erlangen, Germany
Water bath		- Frigomix U1, Braun, Melsungen, Germany - Julabo C, Bachhofer, Reutlingen, Germany - Fisons, Haake, Karlsruhe, Germany

2.2. Chemicals, Enzyme and other Materials

2.2.1. Chemicals

Agarose	standard	Biozym, Hess, Oldendorf, Germany
	SeaKem LE	
	Low Melting Point	Invitrogen, Paisley, Scotland, U.K.
	Low EE0	SIGMA-ALDRICH, Taufkirchen, Germany
Ammoniumacetate		Merk KG, Darmstadt, Germany
Ammoniumpersulfate		Serva, Heidelberg, Germany
Ampicillin		
Amino acids		SIGMA-ALDRICH, Taufkirchen, Germany

ATP	Pharmacia Biotech GmbH, Freiburg, Germany
Bacto Agar	Difco, Hamburg, Germany
Bacto Peptone	
Bacto Tryptone	
Bacto Yeast Extract	
Bacto Yeast Nitrogen Base	
Boric acid	Merck KG aA, Darmstadt, Germany
Bromophenol blue	Roche Molecular Diagnostics, Mannheim, Germany
Calcium chloride	Merck KG aA, Darmstadt, Germany
dATP, dCTP, dGTP, dTTP	Pharmacia Biotech GmbH, Freiburg, Germany
di-Potassium hydrogen phosphate	Merck KG aA, Darmstadt, Germany
Dithiothreitol	Serva, Heidelberg, Germany
DMSO	SIGMA-ALDRICH, Taufkirchen, Germany
EDTA	
Ethanol absolute	Merck KG aA, Darmstadt, Germany
Ethidium bromide	Serva, Heidelberg, Germany
Formaldehyde	SIGMA-ALDRICH, Taufkirchen, Germany
Glucose	Merck KG aA, Darmstadt, Germany
Glutaraldehyde	SIGMA-ALDRICH, Taufkirchen, Germany
Glycerin	
Heavy white oil	
Hydrochloric acid	
Hydrogen peroxide	
Isopropanol	Merck KG aA, Darmstadt, Germany
Magnesium chloride	
Magnesium sulfate	
2- β -Mercaptoethanol	
PBS	SIGMA-ALDRICH, Taufkirchen, Germany
PEG3350	
Phenol/Chloroform/Isoamylalcohol (25:24:1)	
Potassium dihydrogen phosphate	Merck KG aA, Darmstadt, Germany
Potassium chloride	
Salmon sperm	SIGMA-ALDRICH, Taufkirchen, Germany
SDS	Serva, Heidelberg, Germany
Sodium acetate	Merck KG aA, Darmstadt, Germany
Sodium chloride	
Sodium carbonate	
Sodium hydroxide	
Sodium thiosulfate	SIGMA-ALDRICH, Taufkirchen, Germany
Sodium lauroylsarcosine	Merck KG aA, Darmstadt, Germany
Sodium lauryl sulfate	
Trichloroacetic acid	
Tris(hydroxymethyl)aminomethane (Tris)	
Triton X-100	
Tween-20	
YNB	DIFCO, Hamburg, Germany
X-Gal	MBI Fermentas, Vilnius, Litauen

2.2.2. Enzymes

Alkaline phosphatase, Calf intestinal	New England Biolabs, Frankfurt, Germany
Lyticase (#L2524)	SIGMA-ALDRICH, Taufkirchen, Germany
<i>PfuI</i> DNA-Polymerase	Stratagene GmbH, Heidelberg, Germany
Proteinase K (#2308)	SIGMA-ALDRICH, Taufkirchen, Germany
Restriction endonucleases and associated buffers	Roche Molecular Diagnostics, Mannheim MBI Fermentas, Vilnius, Litauen New England Biolabs, Frankfurt, Germany
<i>Taq</i> DNA-Polymerase	Gibco BRL, Eggenstein, Germany
T4 DNA Ligase	Invitrogen, Karlsruhe, Germany

2.2.3. Lengths standards

1 kb DNA-Molecular weight standard	MBI Fermentas, Vilnius, Litauen
2-Log DNA Ladder	New England Biolabs, Frankfurt, Germany

2.2.4. Kits

CEQ Dye Terminator Cycle Sequencing Kit	Beckman Coulter, Fullerton, USA
QIAquick Gel Extraction Kit	QIAGEN GmbH, Hilden, Germany
QIAquick PCR Purification Kit	
QIAprep Maxiprep Kit	
QIAprep Midiprep Kit	
QIAprep 8 Miniprep Kit	

2.3. Computer programs and web sites

For figures processing	Adobe Photoshop 7.0
For text processing	Microsoft Word 2000
For oral presentations	Microsoft Powerpoint 2000
For calculations	Microsoft Excel 2002
For poster presentations	Adobe Illustrator 10 Microsoft Powerpoint 2000

For literature enquiries	http://www.ncbi.nlm.nih.gov/ http://www.ebi.ac.uk/embl/ http://mips.gsf.de/genre/proj/yeast/ http://www.yeastgenome.org/ http://www.genome.jp/kegg/kegg2.html http://string.embl.de/
For sequence processing	Bioedit 5.0.9 http://prodes.toulouse.inra.fr/multalin/multalin.html http://bioinformatics.org/sms/rev_comp.html
Dictionaries and translators	http://dict.leo.org/?lang=de http://babel.altavista.com/tr http://www.chemie.fu-berlin.de/cgi-bin/acronym http://cancerweb.ncl.ac.uk/omd/
For gel evaluation	QuantityOne 4.4.1, Bio Rad
For DSB quantification	PULSE, Anna Friedl et al., 1995 Geltool, Idoia Gomez Paramio and Herbert Brasselman

2.4. Oligonucleotides

Calculation of the annealing temperature T_A according to the Wallace rule:

$$T_A (^{\circ}\text{C}) = [m \times 2 + n \times 4] - 5$$

T_A = Annealing temperature

m = Number of A and T

n = Number of C and G

The melting temperature T_M is 5°C higher than the calculated annealing temperature. Primers working together should have a similar T_A .

The nucleotides used as primers have the following sequences:

Name	Sequence
rad52 knockout rev	5' GAG TAA CTA GAG GAT TTT GG 3'
rad52 knockout fw	5' TTC CCG TTA GTG ATT CTC 3'
KANMXrad52 rew	5' CAA GTA GGC TTG CGT GCA TGC AGG GGA TTG ATC TTT GGT CGA TGG CGG CGT 3'
KANMXrad52 fw	5' GGT TAC GCG ACC GGT ATC GAA TGG CGT TTT TAA GCT ATT TGG GTC ACC CGG 3'
26-62-2/5 rad5C(anti)	5' CCC CGG ATC CTT CAA ACA GCA TCT GGA T 3'
10-4090-8/8 rad5-2217	5' AAC AGG AAC ACC AAT TAT TAA CAG G 3'
URA3-1	5' GCA GCC GCA CGC GGC GCA TC 3'
URA3-3	5' GAG AAC TGT GAA TGC GCA AAC CAA 3'
URA3-4	5' CTC GCG TAT CGG TGA TTC ATT CT 3'
P2	5' CTG CTA ACA TCA AAA GGC CC 3'
INV5	5' ATA GAT CAG TTC GAG TTT TCT T 3'
sonde rev	5' TTA GTT TTG CTG GCC GCA TCT TCT 3'
RAD5-2352anti	5' AAC GAC CTC CTT TGG TGG 3'
hdf1 N	5' CCC CGG ATC CAT GCG GCC AGT CAC TAA TG 3'
hdf1 C	5' CCC CAG ATC TTA TAT TGA ATT TCG GCT TTT T 3'
rad5-2117	5' AAC AGG AAC ACC AAT TAT TAA CAG G 3'
fw apn1 -667 upstr.	5' GGT GTT GGT CCA GTG ACA GC 3'
rev apn1 EcoR1	5' GGT ATG GAT GAA TTC GAA GCG 3'
fw -225 NTG1	5' GGT TCA AGG ATA ACG GCA ACT GC 3'
rev +254 NTG1	5' GGA CGA CGC TGT GTC AAG ACG 3'
fw -474 NTG2	5' GCA GTC TGT GCC TAT AAC TCC 3'
rev +237 NTG2	5' AAC GGA CTT CTG CTC ACA GG 3'

All synthetic oligonucleotides were synthesised by Metabion GmbH, Martinsried, Germany. Storage was at -20°C.

2.5. Plasmids

2.5.1. pJD1

The plasmid pJD1 (courtesy of S. Moertl) is a derivative of the *E. coli* yeast shuttle Plasmid YCp50 (Rose M. 1987). An approx. 300 bp EcoRI/BamHI fragment of the tetracycline resistance gene was removed from the plasmid YCp50 and replaced by a functional *TRP1* gene (800bp). The *TRP1* gene was isolated from the plasmid pSM21 (courtesy of David Schild, Berkeley) by digestion with EcoRI/ BglII. pJD1 includes the ARS sequence that allows an autosomal replication and the sequence CEN4, which promotes a chromosomal-like segregation of the plasmid in yeast. The integration of the plasmid in the chromosome is lethal, due to the presence of a CEN4 sequence. Selection in bacteria was possible by means of an *AMP* resistance gene and in yeast by means of *URA3* and *TRP1* genes.

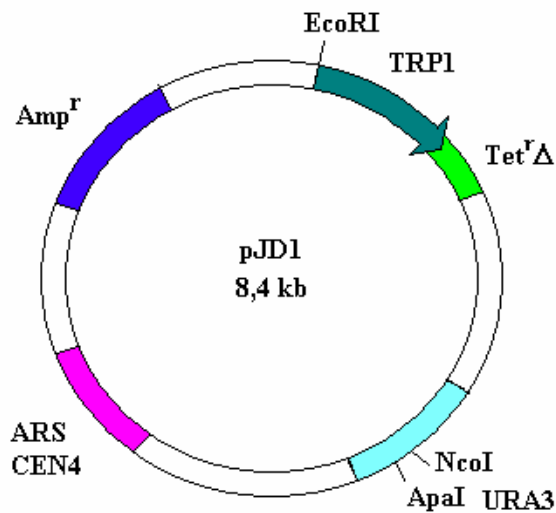


Figure 9: *E. coli* plasmid pJD1.

Amp^r is a selection marker for *E. coli*. *TRP1* and *URA3* are selection markers for yeast. The unique cut sites *NcoI* and *ApaI* in *URA3* gene are shown. ARS is the autosomal replication sequence and CEN4 the centromere sequence.

2.5.2. pFA6-KANMX6

pFA6-KANMX6 (courtesy of W.D.Heyer) was used for the generation of the PCR disruption cassette *KANMX6*. Plasmid pFA6-KANMX6 contains an ampicillin resistant gene (2523-3380 bp), a replication origin (1897 - 2096) and the *KANMX6* module. This module includes the TEF promoter (115 - 457) and the TEF terminator (1277- 1470) flanking the kanamycin resistance gene (459 -1267). *KANMX6*-module and the previously described *KANMX4*-module (Wach, et al., 1994) are identical except for a restriction site (*PmeI* instead of *SalI*).

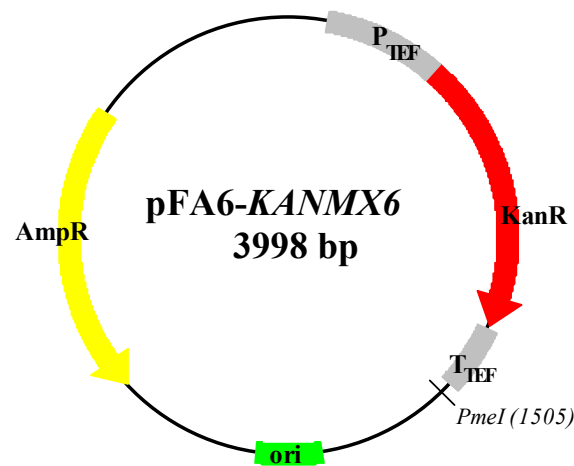


Figure 10: pFA6 - *KANMX6*.

Amp^r is a selection marker for *E. coli*. *Kan^R* (*KANMX6*) is a selection marker for yeast. P_{TEF} and T_{TEF} are the promoter and terminator regions of the *Kan^R* gene.

2.5.4. pGEM-T (Promega)

The plasmid pGEM-T was used for the direct cloning of PCR products. The plasmid is linearised at the EcoRV cut site, where thymidine residues are attached to the 3'-ends. These overhangs improve the efficiency of ligation of PCR product into the plasmids by preventing recircularization. Moreover, the plasmid provides compatible overhangs for PCR products generated by Taq-polymerase, which frequently adds a single deoxyadenosine to the 3' ends of the amplified fragments. pGEM contains the T7 and SP6 RNA polymerase promoters flanking a multiple cloning site within the α -peptide coding region of the enzyme β -galactosidase. The inactivation of the α -peptide by insertion of a PCR fragment allows the direct identification of recombinant clones by their white colour on indicator plates. pGEM can also replicate autonomously in *E. coli* and presents the Amp^R marker for bacterial selection.

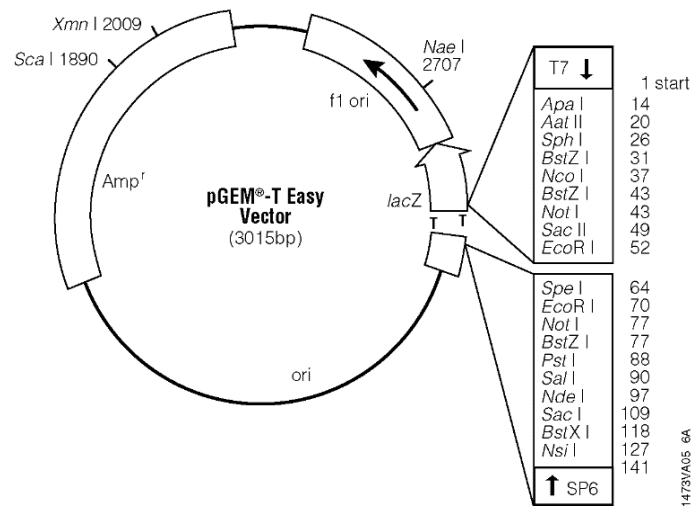


Figure 12: Plasmid pGEM-T (Promega). See text above for information

2.6. Solutions and buffers¹

<u>TBE</u> (10x running buffer for agarose gels)	1 M Tris 2 mM EDTA pH 8,3 adjusted with boric acid
<u>TE</u>	10 mM Tris 1 mM EDTA pH 8,0
<u>Potassium phosphate buffer</u>	25 mM KH ₂ PO ₄ 25 mM K ₂ HPO ₄ pH 7,0 adjusted with KOH

2.7. Growth medium^{1,2}

2.7.1. Growth medium for bacteria

<u>LB-Medium</u>	1 % (w/v) Bacto tryptone 1 % (w/v) NaCl 0,5 % (w/v) Bacto yeast extract pH 7,0 adjusted with NaOH
------------------	--

-Ampicillin (100 µg/ml) was added for breeding of transformed bacteria.

2.7.2. Growth medium for yeast strains

<u>YPD</u> (rich medium)	2 % (w/v) Glucose 2 % (w/v) Bacto peptone 1 % (w/v) Bacto yeast extract
-----------------------------	---

- for the G418-Petri-dishes add extra 250µg/ml geneticin.

<u>YPAD</u>	2 % Glucose 2 % Bacto peptone 1 % Bacto yeast extract 0.008 % Adenin sulfate
-------------	---

¹ Prepared with Milli Q water and autoclaved after preparation.

² Addition of 2% (w/v) bacto agar of for petri dishes before autoclaving.

SC-Medium 2 % (w/v) Glucose
(according to Kupiec/Fiedl) 2 % (w/v) Bacto-agar, autoclave

- Cool down to 50-55°C before adding a solution containing:

25g	Bacto Yeast Nitrogen Base w/o
75g	NH ₄ ⁺ (NH ₄) ₂ SO ₄
1.0 g	Adenine
1.0 g	Arginine
1.0 g	Histidine
4.0 g	L-Isoleucine
20.0 g	L-Leucine
3.0 g	Lysine
10.0 g	Threonine
2.5 g	Phenylalanine
1.0 g	Methionine
1.0 g	L-Tryptophan
1.0 g	Uracil
7.5 g	L-Valine
5.0 g	Aspartic acid
5.0	Glutamic acid
3.0 g	Tyrosine
20.0 g	Serine

- Selective medium lack of the corresponding aa.

- Plates for mutation experiments (3.8) lack of lysine and contain 0.5 g adenine.

2.7.3. Liquid Holding Recovery Buffer for yeast

LHR 100 mM Glucose
0.067 mM potassium dihydrophosphate
pH 5.0 adjusted with 67 mM dipotassium
hydrophosphate

2.8. Freezing medium for yeast

Yeast freezing medium 2 % Peptone
1 % Yeast extract
15 % Glycerin

2.9. Strains

2.9.1. Bacterial strain

DH5 α F⁻ ϕ 80 δ lacZ Δ M15 Δ (lacZYA-argF) U169 *deoR recA1 endA1 hsdR17*(r_K⁻,m_K⁺) *phoA supE44 λ thi-1 gyrA96 relA1*

2.9.2. Yeast strains

MKP0 *RAD; MAT α ; can1-100; ade2-1; lys2-1; ura3-52; leu2-3, 112; his 3- Δ 200; trp1- Δ 901* (B. Kunz, Geelong, Australia)

MKP0 *rad52 Δ ::LEU2* *rad52 Δ ::LEU2, MAT α ; can1-100; ade2-1; lys2-1; ura3-52; leu2-3, 112; trp1- Δ 901* (F. Ahne, 1997)

MKP0 *rad52 Δ ::kanMX* *rad52 Δ ::kanMX, MAT α ; can1-100; ade2-1; lys2-1; ura3-52; leu2-3, 112; trp1- Δ 901* (This work)

MKP0 *rad5 Δ (2000)* *rad5 Δ ::HIS3MX; MAT α ; can1-100; ade2-1; lys2-1; ura3-52; leu2-3, 112; trp1- Δ 901* (Simone Mörthl, 2000)

MKP0 *yku70 Δ ::LEU2* *yku70 Δ ::LEU2; RAD; MAT α ; can1-100; ade2-1; lys2-1; ura3-52; leu2-3, 112; trp1- Δ 901* (F. Ahne, 1997)

MKP0 *rad52::LEU2 rad5 Δ ::HIS3* *rad52 Δ ::LEU; rad5 Δ ::HIS3; MAT α ; can1-100; ade2-1; lys2-1; ura3-52; leu2-3, 112; trp1- Δ 901* (F. Ahne, 1997)

MKP0 *rad52Δ::kanMX*

rad5Δ::HIS3MX

rad5Δ::HIS3MX; rad52Δ::kanMX; MAT α; can1-100; ade2-1; lys2-1; ura3-52 ; leu2-3, 112 ; trp1-Δ901 (This work)

MKP0 *rad5Δ::HIS3*

yku70Δ::LEU2

rad5Δ::HIS3; yku70Δ::LEU2; MAT α; can1-100; e2-1; lys2-1 ; ura3-52 ; leu2-3, 112; trp1-Δ901
(F. Ahne, 1997)

MKP0 *rad52Δ::kanMX*

yku70Δ::LEU2

rad52Δ::kanMX; yku70Δ::LEU2; MATα; can1-100; ade2-1; lys2-1; ura3-52, leu2-3, 112; trp1-Δ901
(This work)

MKP0 *apn1Δ::LEU2*

ntg1Δ::URA3 ntg2Δ::TRP1

apn1Δ::LEU2; ntg1Δ::URA3; ntg2Δ::TRP1; MATα; can1-100; ade2-1; lys2-1; ura3-52, leu2-3, 112; trp1-Δ901 (This work)

MKP0 *apn1Δ::LEU2*

ntg1Δ::URA3 ntg2Δ::TRP1

rad5Δ::HIS3MX

apn1Δ::LEU2; ntg1Δ::URA3; ntg2Δ::TRP1; rad5Δ::HIS3MX; MATα; can1-100; ade2-1; lys2-1; ura3-52, leu2-3, 112; trp1-Δ901
(This work).

3. METHODS^{3,4}

3.1. Microbiology methods

3.1.1. Working with bacteria

3.1.1.1. Cultivation of bacteria in liquid medium

A single bacterial colony was removed from a LB plate with a toothpick and inoculated in LB medium containing 100 µg/ml ampicillin. The bacteria culture was shaken at 160 rpm at 37°C for 12-16 h. Other selective medium were used depending on the existence and kind of plasmids inside the bacteria.

3.1.1.2. Streaking of bacteria plates⁵

Bacteria were picked from a frozen culture by immersing a loop or a toothpick in the cryo tube containing the culture. Alternatively bacteria were picked from a liquid culture by immersing a loop in it. The loop used for inoculation was flamed and briefly cooled before it contacted the colony. Then the loop was used to streak out the cells on the surface of LB plates. After an incubation of 12 -16 h at 37°C colonies were visible.

3.1.1.3. Freezing of bacteria cultures

0.8 ml of an over night culture in selective medium was transferred into cryo tubes, mixed with 0.2 ml glycerine and stored at -80°C.

³ Every laboratory glass, plastic and metal ware used was sterile.

⁴ Water refers to distilled water.

⁵ Plates should be inverted in the incubator to prevent condensation from dripping on the colonies.

3.1.1.4. Transformation of *E.coli*

Bacterial transformation is used to amplify plasmid DNA in a short time. 200 µl of *E.coli* DH5α were thawed slowly on ice. Then, 20 µl of a ligation mixture (or 100 ng plasmid DNA) was added and the sample was incubated on ice for 20 min. After a heat shock for 2 min at 42°C the sample was placed into ice again. Subsequently 500 µl LB medium was added and cells were shaken for 1h at 37°C. After this time appropriate amounts were plated on LB medium containing ampicillin (2.7.1). Only cells containing the gene for resistance against ampicillin were able to grow up after incubation for 24 h at 37°C.

3.1.2. Working with yeast^{6,7}

3.1.2.1. Culture of yeast cells in liquid medium

Two or three yeast colonies were inoculated in different media depending on the experiment. The cells were shaken at 200 rpm in plastic tubes or Erlenmeyer flasks at 30°C. All media and objects used for the culture were previously sterilized.

3.1.2.2. Freezing of yeast cells

Yeast cells were taken from a rich medium plate using an inoculating loop. Then cells were transferred to a cryo tube and mixed with 1 ml of freezing medium (2.8). Finally cells were stored at -80°C.

3.1.2.3. Determination of the yeast cell number

A Neubauer counting chamber and the suitable cover glass were cleaned with 70 % ethanol. The cover glass was set on the counting chamber, so that Newton rings were formed at the bearing surfaces. This indicates that the distance between glass and counting chamber is exactly 0.1 mm. A drop of the cell suspension was pipetted on the lower fissure between the cover glass and chamber.

⁶ Yeast cells were harvested at 4°C at 4000 rpm during 5 min or at 3000 rpm during 10 min.

⁷ Yeast cells were shaken at 30°C at 200 rpm.

Then the cells of 25 small squares were counted under the microscope and the cell density of the suspension was determined according to the following equation:

$$\text{Cell number in 25 small square} \times 10^4 \times \text{Dilution factor} = \text{Cells / ml cell suspension}$$

$$10^4 = \text{Volume of 25 small squares} = 1\text{mm}^2 \text{ surface} \times 0.1 \text{ mm depth} = 0.1 \text{ mm}^3 = 10^{-4}\text{ml}$$

3.1.2.4. Transformation of *S. cerevisiae*

Two or three single colonies of the yeast strains were inoculated in 10 ml YPAD and incubated ON under agitation at 30°C. Then 3×10^6 c/ml were inoculated in 100 ml of YPAD and shaken at 30°C till a cell concentration of at least 10^7 c/ml was reached (3 - 3.5 h). Cells were harvested by centrifugation, the supernatant was removed and the pellet was washed with 20 ml water. Subsequently cells were resuspended in 20 ml 0.1M LiOAc and shaken for 15 min. After centrifugation cells were resuspended in 0.1 M lithium acetate with a concentration of 10^9 c/ml. Per transformation 95 μl of the cell suspension were mixed (briefly vortexed) with 20 μl plasmid DNA, 240 μl PEG 50%, 31 μl 1M LiOAc and 15 μl ss salmon sperm, which previously was denatured at 95°C for 10 min. Cells were shaken for 30 min at 30°C before a heat shock at 42°C for 20 min. After centrifugation (5000 rpm, 1 min), control cells were resuspended in 1000 μl deionized water, thereof 50 μl were plated on selective medium. For transformation cells were resuspended in 500 μl and thereof 100 μl were plated on selective medium. Finally plates were incubated at 30°C for 72 h. Transformation rate was determined according to the following equation:

$$\text{Transformation rate} = \text{colony number} / \mu\text{g DNA}$$

For the creation of new mutants the method differs as follow: After the heat shock and centrifugation cells are shaken 2 h in 1 ml rich medium at 30°C, then cells are harvested (5000 rpm, 1 min) and the pellet is resuspended in 400 μl milli-Q water. Finally 100 μl cells were plated on selective medium.

3.1.2.5. Generation of knockout mutants by homologous recombination

Knockout mutants were produced by the complete substitution of chromosomal genes through selectable marker genes presented in plasmids or cassettes. These plasmids and cassettes include regions of homology with the target gene that allows their correct substitution by means of homologous recombination. The transformed cells were plated on selective medium and after three days cells replica were plated on fresh selective medium. Only the strains presenting the selective gene could grow on this medium. Finally the healthiest colonies of these plates were examined.

3.2. Biomolecular methods

3.2.1. Isolation of DNA

3.2.1.1. Isolation of Plasmid-DNA from *E. coli*

This procedure has been adapted from the QIAGEN Plasmid Purification Handbook (March 2001). The method was used for purification of 100 µg -500 µg of bacterial plasmid using gravity-flow anion exchange resins under appropriate low-salt and pH conditions. RNA, proteins and other impurities are removed by medium-salt wash. Plasmid DNA is eluted in a high salt buffer and then concentrated and desalted by isopropanol precipitation.

A single bacteria colony from a freshly streaked selective plate was picked and inoculated in 500 ml of LB medium containing ampicillin. After ON incubation at 37°C and 300 rpm shaking, cells were harvested by centrifugation at 6000 g for 15 min at 4°C. The bacterial pellet was then resuspended in 10 ml buffer P1 and mixed gently and thoroughly with 10 ml buffer P2 by inverting 4 - 6 times and then incubated for 5 min at room temperature. After this time, 10 ml of chilled buffer P3 were added and mixed immediately but gently by inverting 4 - 6 times and then incubated on ice for 20 min. Lysated cells were then harvested at 13000 rpm for 30 min and the supernatant containing the plasmid DNA was removed promptly. The supernatant was allowed to enter a resin column previously equilibrated with 10 ml buffer QBT. The column was washed twice with 30 ml buffer QC before the elution of DNA with 15 ml buffer QF.

The pellet was resuspended in 500 µl water, mixed with 50 µl 3M NaAc and 1400 µl ethanol 100 % and centrifuged at 15000 rpm for 10 min at 4°C. Then the supernatant was carefully decanted, mixed with 1ml of 80 % ethanol and centrifuged at 15000 rpm for 10min at 4°C. Afterwards the supernatant was decanted and dried for 10 min in a speed vacuum. Finally the pellet was resuspended in 100 - 200⁸ µl deionized water.

<u>Buffer P1</u> Resuspension buffer	50 mM Tris/HCl, pH 8.0 10 mM EDTA, pH 8.0 100 µg/ml RNase A
<u>Buffer P2</u> Lysis_buffer	200 mM NaOH 1 % SDS (w/v)
<u>Buffer P3</u> Neutralization buffer	3 M Potassium acetate, pH 5.5
<u>Buffer QTB</u> Equilibration buffer	750 mM NaCl 50 mM MOPS, pH 7.0 15 % Isopropanol (v/v) 0.15 % Triton X-100 (v/v)
<u>Buffer QC</u> Wash buffer	1,0 M NaCl 50 mM MOPS, pH 7.0 15 % (v/v) Isopropanol
<u>Buffer QF</u> Elution buffer	1.25 M NaCl 50 mM Tris/HCl, pH 8.5 15 % (v/v) Isopropanol

3.2.1.2. Isolation of plasmid-DNA from yeast

This procedure has been adapted from the QIAprep Spin Miniprep Kit Protocol. This method was used for purification of plasmid DNA from yeast after lysis of cells followed by adsorption of DNA onto silica in the presence of high salt.

A single colony was inoculated into 10 ml of the appropriate selective media and incubated for 48 h at 30°C. Cells were harvested by centrifugation at 4°C and 4000 rpm for 5 min and resuspended in 250 µl Buffer P1 containing 0.1 mg/ml RNase A. Cells were then transferred to a 1.5 ml microfuge tube. Then 50 - 100 µl of acid-washed glass beads (Sigma G-8772)

⁸Modification of the standard QIAGEN method.

were added and tubes were vortexed for 2 min. The supernatant was then transferred to a fresh 1.5 ml microfuge tube. 250 µl of lysis buffer P2 was added to the tube and inverted immediately but gently 4 - 6 times. After an incubation of 5 min at room temperature 350 µl of neutralisation buffer N3 was added to the tube and mixed by inversion 4 - 6 times. Afterwards the lysate was centrifuged at 13000 rpm for 10 min and then transferred to a QIAprep spin column, which was placed in a 2 ml collection tube. After centrifugation of the column for 60 sec, the flow-through was discarded. Column was then washed with buffer PE and centrifuged 60 s at 13000 rpm. Subsequently the flow-through was discarded and the column was centrifuged again to remove residual buffer. For isolation of the plasmid, the column was placed in a 1.5 ml collection tube, incubated for 1 min with 75 µl EB buffer at RT and centrifuged 60 s at 13000 rpm. The column was discarded and 10% sodium acetate 3M (pH 5.2) and 2.5 volumes of 95% ethanol were added to the DNA sample, which was inverted to mix and incubated at -20°C for at least 20 min. The sample was centrifuged at 13000 rpm in a microcentrifuge for 15 min at 4°C and the supernatant was decanted. 70% ethanol (corresponding to about two times the volume of the original sample) was added, the sample was incubated at room temperature for 5-10 min, centrifuged again for 5 min, the supernatant was decanted and the sample was drained inverted on a paper towel. The pellet was dried in vacuum for 1 min and the dried DNA dissolved in TE- buffer or dist. water.

<u>Buffer P1</u> Resuspension buffer	50 mM Tris/HCl, pH 8.0 10 mM EDTA, pH 8.0 100 µg/ml RNase A
<u>Buffer P2</u> Lysis buffer	200 mM NaOH 1 % SDS (w/v)
<u>Buffer N3</u> Neutralization buffer	3 M Potassium acetate, pH 5.5
<u>Buffer EB</u> Elution buffer	10mM Tris/HCl, pH 8.5

3.2.1.3. Isolation of genomic DNA from yeast

The isolation of genomic DNA from yeast cells was according to a protocol by Hoffmann and Winston (Hoffmann et al., 1987).

Yeast cells were inoculated in 6 ml rich medium and incubated up to the stationary growth phase (36 - 48 h). After cell harvesting⁹ the supernatant was completely discarded. The cell pellet was resuspended in 0.2 ml lysis buffer and transferred in a clean 1.5 ml microfuge tube. Then 0.3 g glass beads and 0.2 ml PCI were added and cells were vortexed for 5 min. After centrifugation¹⁰ the upper aqueous phase was transferred in a fresh microfuge tube. Subsequently 0.15 ml of TE buffer and 1 ml of 100 % ethanol were added and mixed prior centrifugation. Subsequently the supernatant was discarded and the pellet was briefly dried. 0.3 ml TER solution (TE with 50 µg/ml RNase A) were then added and warmed up twice for 5 min at 65°C. Between the incubation steps tubes were briefly vortexed. Then the pellet was resuspended in 0.1 ml 10 N ammonium prior addition of 1 ml 100 % ethanol. After centrifugation⁸ and discarding of the supernatant the pellet was washed with 1 ml 70 % ethanol. Finally the pellet was air dried and resuspended in 50 µl TE buffer or deionized water. Chromosomal DNA was stored at 4°C.

<u>Lysis buffer II</u>	2 % (v/v) Triton X 100
Freshly prepared each time	1 % (v/v) SDS
	0.1 M sodium chloride
	10 mM Tris/HCl, pH 8.0
	1 mM EDTA, pH 8.0

⁹ 5 min, 4000 rpm, 4°C.

¹⁰ 5 min, 15000 rpm, 4°C.

3.2.2. Cleavage of DNA by restriction endonucleases

Endonucleases were used for creation of DSB in specific localizations due to their property of breaking phosphodiester bonds by a hydrolytic cleavage. One unit of restriction endonuclease is the amount required to hydrolyze 1 µg of DNA in 60 min in a total reaction volume of 50 µl. For preparative digestion 2.5 U enzyme/ µg of DNA and an incubation of 12 h were necessary for the complete cleavage of DNA. On the contrary, for analytical experiments (where complete cleavage of DNA was not necessary) 1 U of enzyme/µg and 1-2 hours incubation was enough. The incubation temperature for an optimal restriction activity depends on the enzyme. In case of multiple digestions it was tried to select a buffer, in which the different enzymes presented as optimal activity as possible. The completeness of the digestion was checked in a 0.8% agarose gel.

3.2.2.1. Cleavage of plasmid pJD1 with the RE *ApaI* and *NcoI*

Different buffer requirements for *ApaI* and *NcoI* necessitate two steps for cleavage. For complete cutting of 50 µg of the plasmid pJD1 was used firstly 12.5 U of *ApaI* and 15 µl *ApaI* buffer in a total volume of 150 µl. After 16 h at 37°C incubation, 12.5 U of *NcoI* and 10 µl *NcoI*-buffer were added to the mix. The enzyme *NcoI* was used in the second step due to its capacity to have an activity in *ApaI* buffer. Then, the final volume was increased up to 250 µl with milli-Q water. The second incubation took place at 37°C for 8 h. Finally the cut plasmid was isolated by agarose gel electrophoresis (3.2.5).

ApaI (37°C)
1 x ApaI Buffer

10³ U/ml
66 mM Potassium acetate
33 mM Tris-acetate
10 mM Magnesium acetate
0.5 mM dithiothreitol, pH 7.9

NcoI (25°C)
1 x NcoI Buffer

10³ U/ml
50 mM Potassium acetate
20 mM Tris-acetate
10 mM Magnesium acetate
1 mM dithiothreitol, pH 7.9

3.2.3. Separation of DNA fragments by gel electrophoresis

Gel electrophoresis is used for analysis, isolation and purification of DNA fragments depending on their size. For isolation of plasmids a 0.8 % agarose gel was used. Agarose gels were stained with ethidium bromide (150 µg /l) prior or after electrophoresis. The agar solution (0.8 % agar in 1 x TBE) was boiled in a microwave till the agar was dissolved. The solution was cooled till 60°C and then 150 µg /l ethidium bromide was added. If needed, tape was placed across the ends of the gel form and a comb was also placed into the form. The cooled agar was poured into the form so that 1/3 -1/2 of the bottom of the comb is immersed. The comb was removed when the agar had solidified. Samples were mixed with 1/6 volume of “gel running buffer” and then loaded in the wells of the gel. 1x TBE was used as running buffer. The voltage for electrophoresis was 12V/cm. DNA size and quantity was estimated using a 1kb DNA-Ladder.

<u>Gel loading buffer (6 x)</u>	60 mM EDTA
	60 % Glycerin 15 % (w/v) Ficoll 400
	0.09 % Bromophenol blue
	0.09 % Xylencyanol FF

3.2.4. Amplification of DNA by PCR

This protocol is according to Innis, M. A. (Innis 1990). The composition for four samples is the following:

Composition for 4 samples	Volume
10 x Buffer minus Mg ²⁺	10 µl
10 x mM dNTP mixture	2 µl
50 mM MgCl ₂	3 µl
Primer-Mix (each 10µM)	5 µl
Genomic DNA	min 0.1 µl
Plasmid DNA or PCR-Product	min 2 µl
Taq-DNA-Polymerase (5U/µl)	0.5 µl
Deionized water	till 100 µl

The contents were mixed and collected by centrifugation. The PCR follows the next program:

1 st Denaturation	95°C	2 min	
30x {	Denaturation	95°C	30 sec
	Annealing	T _A	45 sec
	Extension	72°C	Depending on the fragment length
Final denaturation	72°C	4 min	
Final holding	4°C		

Finally 2-5 µl of the amplification product was analyzed by agarose gel electrophoresis and visualized by ethidium bromide staining.

<u>10 x PCR buffer</u>	500 mM KCl
	100 mM Tris/ HCl pH 8.4
	0.05 % (v/v) detergent W-1

3.2.5. Purification of DNA

3.2.5.1. From agarose gels

This protocol is according to QIAEX Gel Extraction Protocol of the QIAEX II Handbook (February 1999). This method was used for extraction and purification of DNA from any agarose gel in either TAE or TBE buffer without phenol extraction or ethanol precipitation.

3.2.5.2. After PCR amplification

This protocol is according to QIAquick PCR Purification Kit Protocol of the QIAquick Spin Handbook (March 2001). This method was used for direct purification of double stranded PCR products (100 bp – 10 kb) from amplification reactions and other enzymatic reactions.

3.2.6. Photometric determination of DNA concentration

For the photometric determination of nucleic acids a wave length of 260 nm was used. An aliquot of the DNA solution was placed into a photometric cuvette and analysed. Only values between 0.1 and 1 were considered, because a linear relation between extinction and nucleic acids concentration exists only in this range. The concentration of nucleic acids was determined according to the following formula:

$$\text{OD}_{260} \times \text{dilution factor} \times 50 \text{ ng}/\mu\text{l}$$

$$\text{OD}_{260} \Rightarrow 1 = 50 \text{ ng}/\mu\text{l} C_{\text{DNA}}$$

3.2.7. Sequence analysis of DNA

The DNA sequencing protocol is according to the dideoxy chain termination method by Sanger et al. (1977). The sequencing reaction was prepared with the CEQ Dye Terminator Cycle Sequencing Kit of Beckman Coulter (Handbook, August 2000).

The DNA sequencing reaction was prepared as follow:

Components	Volume
DNA Template	0.5 – 3.0 μl (50-100 fmol)
Primer	1 μl (1.6 pmol/ μl)
DTCS Premix	6 μl
Water	ad 10 μl

The components were mixed thoroughly and then the contents were collected to the bottom of the tube by brief centrifugation. Amplification of DNA follows the next program.

1 st denaturation	96°C	1 min
30x	{ Denaturation Annealing Extension	96° C 20 sec
		50° C 20 sec
		60° C 4 min
Final holding	4° C	

After successful PCR amplification the DNA was purified by ethanol precipitation. First 2 µl of stop solution and 1 µl of glycogen (20 mg/ml) were added to each PCR reaction. Then 60 µl of 95 % ethanol (-20°C cold) was added and mixed thoroughly. The reaction was immediately centrifuged at 14000 rpm (4°C) for 15 min. Then the supernatant was carefully removed. The sample was rinsed twice with 200 µl of 70 % ethanol (-20°C). After each rinsing step the sample was centrifuged immediately at 14.000 rpm (4°C) for a minimum of 2 min. Then supernatant was carefully removed. Subsequently the sample was vacuum dried for 15 min. The sample was resuspended in 40 µl of the Sample Loading Solution and transferred to the wells of a polypropylene sample plate. Finally the sample was overlaid with one drop of light mineral oil and loaded into the CEQ2000.

<u>Stop Solution</u> fresh prepared	NaOAc 1.5 M EDTA 50mM	
<u>DTCS Premix</u> (Dye Terminator Cycle Sequencing)	10 x Sequencing Reaction Buffer	200 µl
	dNTP Mix	100 µl
	ddUTP Dye Terminator	200 µl
	ddGTP Dye Terminator	200 µl
	ddCTP Dye Terminator	200 µl
	ddATP Dye Terminator	200 µl
<hr/>		
Total Volume		1200 µl

3.2.8. Cleavage of the 5'- phosphate groups

Removal of 5' phosphate groups from DNA triphosphates was carried out by means of the alkaline phosphatase. Since dephosphorylated ends cannot self-ligate, this method was used to reduce the vector background in ligation experiments.

For dephosphorylation reactions the reaction mixture contains 10 % of 10x alkaline phosphatase buffer, 1U of enzyme per 30 µg of linearised plasmid and deionized water till a volume of 40 µl. The incubation was carried out at 37°C for 50 min. Finally DNA was purified using the QIAquick PCR purification kit (3.2.5.2).

3.2.9. Ligation of DNA restriction fragments into plasmids

This protocol is according to GibcoBRL. The ligation of restriction fragments with linearised plasmids was done by using the T4 DNA ligase, which forms a phosphodiester bond with a 5'-phosphate and a 3'-hydroxyl group. 100 ng dephosphorylated linear plasmid was supplemented with 1/5 volume of ligation buffer, and insert and plasmid were added in a molar ratio of 3:1, respectively. It was also added 1 µl of T4 DNA ligase (1 U/1 µl) and milli-Q water up to an end volume of 20 µl. Subsequently the mixture was incubated at 16°C ON.

3.2.10. Use of X-GAL for identification of *LacZ* expression

X-Gal is a chromogenic substrate for beta-galactosidase, which hydrolyzes X-Gal forming an intense blue precipitate. X-Gal is most frequently used in conjunction with IPTG, which induces activity of beta-galactosidase by binding and inhibiting the *lac* repressor in blue/white colony screening to distinguish recombinants (white) from non-recombinants (blue).

For the detection of *LacZ* expression ampicillin plates were overlaid with a solution containing 40 µl of X-Gal (200 mg/ml in dist.water), 4 µl of IPTG (20 mg/ml in DMSO) and 56 µl of deionized water.

3.3. Determination of the survival capacity after irradiation

3.3.1. Drop test of yeast cells

A drop test is a very simple and quick procedure to test the survival capacity of yeast cells after UV and gamma irradiation. In this method, the cell number of a culture was determined (3.1.2.3) and then adjusted to 2×10^8 c/ml. Samples were diluted with potassium phosphate up to a concentration of 2×10^3 c/ml. Each cell concentration was pipetted five times in a row, for respectively five different irradiation doses (see Figure 13). In UV experiments 5 μ l of each dilution were pipetted in the corresponding row and then each column was irradiated with 2 J/m²s for 0s (0J/m²), 5s (10 J/m²), 10s (20J/m²), 20s (40J/m²) and 40s (80J/m²). In gamma experiments cells were irradiated with 0 Gy, 100 Gy, 200 Gy and 500 Gy prior to their transferring to the plate. Finally plates were incubated for 72 h at 30°C.

2x	0	1	2	3	4
10 ⁷					
10 ⁶					
10 ⁵					
10 ⁴					
10 ³					

Figure 13: Labelling for drop test. First row shows different irradiation doses. First column: shows different cell concentrations.

3.3.2. Survival capacity of yeast after irradiation

2 or 3 colonies were inoculated in 100 ml rich medium and grown by shaking till the stationary phase was achieved. Then cells were harvested and the pellet was washed twice with potassium phosphate buffer. After resuspension of the cells in 5-10 ml potassium phosphate buffer the cell number was determined (see 3.1.2.3). Finally cells were adjusted with potassium phosphate buffer up to a concentration of 2×10^8 c/ml.

3.3.2.1. UV irradiation

Starting with a concentration of 2×10^8 c/ml a dilution row was prepared up to 2×10^3 c/ml. According to the results of the drop test 100 μ l of the adequate cell concentrations were plated three times, so that 50 - 200 colonies per plate were expected after incubation. Cells were irradiated over a dose range from 5 to 80 J/m² with UV light. ($\lambda = 254$ nm, 2 J/sec). Control cells were not irradiated. Finally, plates were incubated for 72 h at 30°C.

3.3.2.2. Gamma irradiation

A cell suspension (2×10^8 c/ml) was gamma irradiated with 0 Gy, 100 Gy, 200 Gy and 500 Gy respectively. Samples were kept on ice during the irradiation. Subsequently a dilution serie was made for each dose according to the result of the drop test. Finally three plates were plated for each doses and incubated for 72 h at 30°C.

3.3.2.3. Evaluation

For evaluation it has been considered that unirradiated cells (control) have a 100% survival capacity. The survival rate for a dose is the relation between irradiated and unirradiated cells considering the dilution factor of the plates.

3.4. Repair assay with the plasmid pJD1

The plasmid pJD1 (courtesy of S. Moertl) is a derivate from the *E. coli* yeast shuttle plasmid Ycp50 (Kuo and Campbell 1983). The *TRP1* and *URA3* genes presented in pJD1 were used as selection markers due to the absence of these functional genes in *MKP0* yeast strains. Whereas the *TRP1* gene remained unchanged, a gap of 169 bp was introduced in *URA3* gene by digestion with *ApaI* and *NcoI* restriction enzymes, as described in section 3.2.2.1. The *ura3-52* mutation presented in *MKP0* yeast strain is a “non- reverting Ty insertion” and it is situated outside of the sequence removed from the plasmid. Therefore, there is a homologous sequence in the chromosomal DNA of the host cells to the removed sequence in the plasmid.

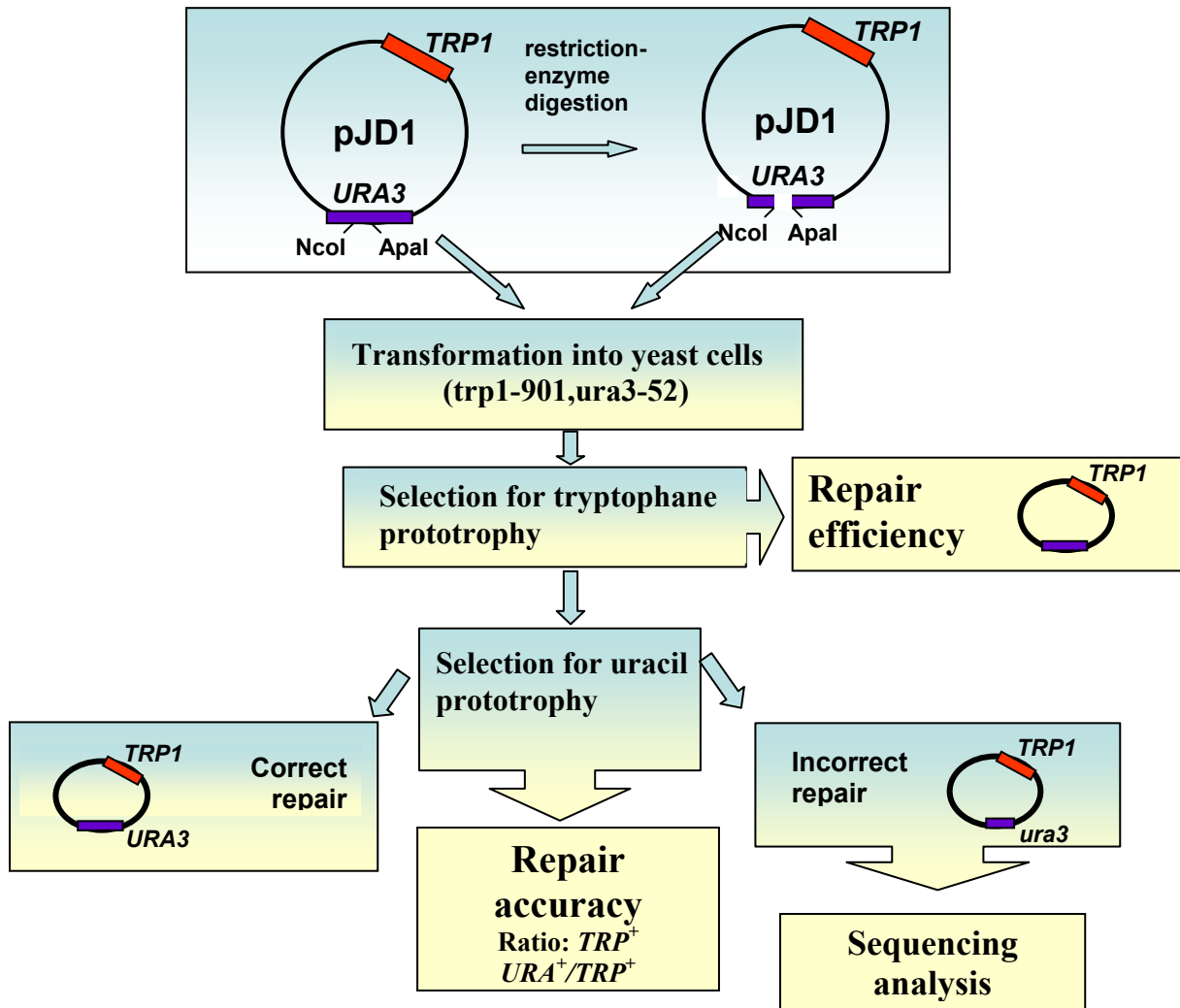


Figure 14: Plasmid repair assay. See text for more information.

In the repair assay 1 μ g uncut and 1 μ g gapped pJD1 plasmid was transformed (see 3.1.2.4) in WT and repair deficient yeast mutants. Then the transformed cells were plated on *trp*⁻ medium and incubated for 3 days at 30°C. Subsequently, the number of transformants was determined. Only recircularized pJD1 could complement the *TRP1* auxotrophy of the *MKP0* strain. Therefore, initial selection for *TRP*⁺ prototrophs allowed the identification of clones that had recircularized the gapped plasmid independently of the accuracy of the repair. Using the uncut plasmid as control it was possible to calculate the repair efficiency of each strain.

$$\text{Repair efficiency} = \frac{\text{Number of transformants obtained with cut plasmids}}{\text{Number of transformants obtained with uncut plasmids}}$$

In the next step, the transformants were selected for *URA3* expression by transferring individual *TRP*⁺ colonies on *ura*⁻ medium. Only colonies able to repair the *URA3* gene correctly can grow in this medium. Uracil-proficiency was therefore taken as an indicator of the correct repair of restriction enzyme-generated gaps. The repair accuracy was calculated by determining the number of *TRP*⁺*URA*⁺ colonies in relation to the number of transferred *TRP*⁺ colonies.

$$\text{Repair accuracy} = \frac{\text{Number of } TRP^+URA^+ \text{ colonies}}{\text{Number of transferred } TRP^+ \text{ colonies}}$$

Subsequently the plasmid was isolated from the *ura*⁻ colonies and the gap region was amplified by PCR analysis. The fragment size of the gapped region depends on the repair pathway used by the cells. Finally, the gapped regions of *ura*⁻ plasmids were sequenced.

3.5. DSB Quantification by Pulsed Field Gel Electrophoresis¹¹

3.5.1. Streaking, irradiation and cultivation of yeast cells

The original protocol of Pohlit and Heyder (Pohlit and Heyder 1977) was modified to obtain high stationary cells (with less than 3% budding cells). Each strain was inoculated in 20 ml of YPD. After 16 h incubation at 30°C and 190 rpm 100 µl of a titer of 10⁶ c/ml was streaked in triplicate on rich medium plates¹² and incubated for 5 - 7 days at 30°C. Then stationary growth cells were rinsed with potassium phosphate and washed three times (Frankenberg-Schwager, Frankenberg et al. 1980).

Cells were resuspended in 2 ml of potassium phosphate buffer to a final concentration of 7.5*10⁸ cells/ml and held on ice until the irradiation with 400 Gy was finished. After irradiation cells were incubated in Liquid Holding Recovery (LHR) buffer to promote DSB repair in the cells without growth. 1.5 *10⁹ of irradiated and unirradiated cells were diluted in 200 ml LHR buffer in a 1 l flask (2.7.3) and incubated at 190 rpm at 30°C for 23 h.

¹¹ Protocol modified according Friedl et al. 1995.

¹² Plates should be inverted in the incubator to prevent condensation from dripping on the colonies.

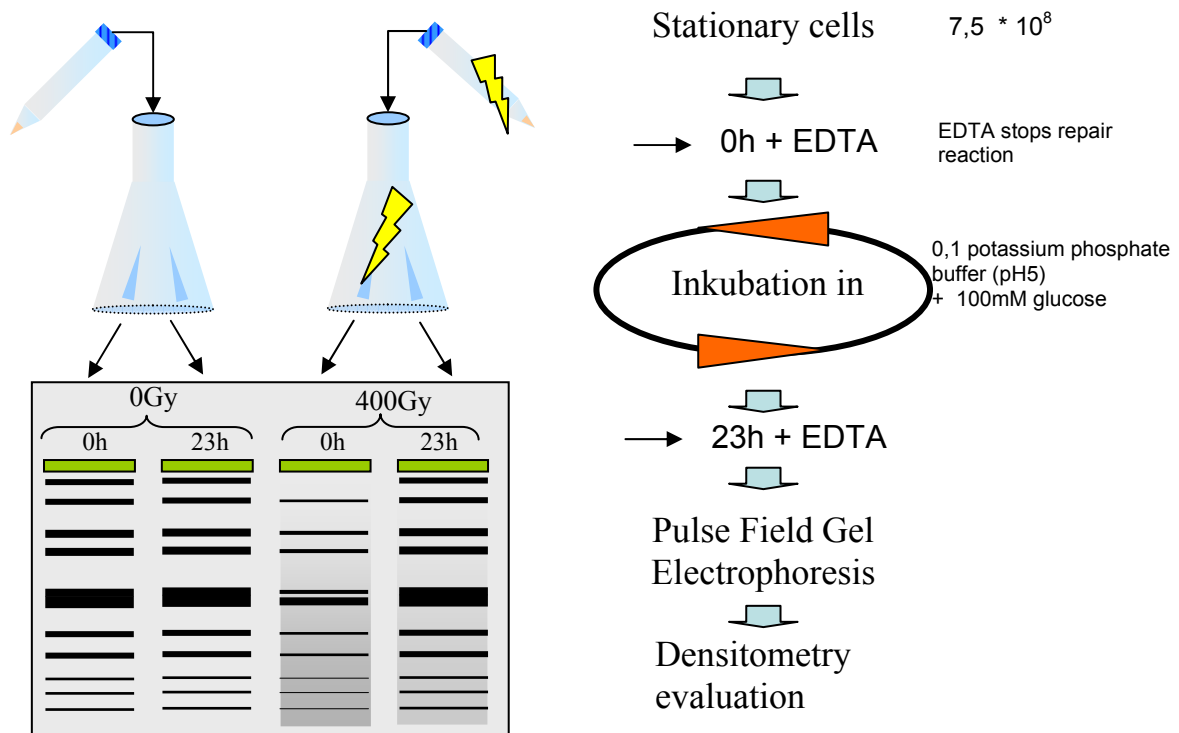


Figure 15: DSB determination under non growth conditions. For the determination of DSB repair under non growth condition, a sample of irradiated stationary cells is immediately taken after irradiation (0h). This sample is mixed with EDTA, to avoid repair processes from that moment. These samples are prepared for their use in PFGE and the rest of the cells is then incubated in Liquid Holding Recovery Puffer (LHR) for 23h, which allows repair but not growth. After 23h incubation samples are taken and prepared for PFGE. Irradiated cells should show a smear of chromosome fragments after irradiation. This smear will decrease in repair proficient cells in the course of time and depending on their repair capacity. Unirradiated cells, used as control, are processed in the same way.

3.5.2. DNA preparation

¹³For genomic DNA preparation 100 ml of the LHR culture were mixed with 20 ml EDTA 0.5 M pH 9 to stop repair in the cells. Then cells were harvested at 4000 rpm and 4°C during 20 min and resuspended in 200 µl 50 mM EDTA pH8. Subsequently 66 µl SEC buffer, 4.7 µl lyticase (20.000 U/ml in 50 % glycerol) and 3.3 µl β-mercaptoethanol were added. The suspension was mixed with 267 µl LMP agarose solution (previously warmed at 50°C), vortexed thoroughly and pipetted quickly into plug molds¹⁴. The plugs were allowed to solidify during 20 min incubation at 4°C before their carefully transferring into screwtop tubes using plastic spatulas¹⁴.

¹³Genomic DNA must be prepared with great care in order to prevent artificial degradation. Gloves must also be worn to avoid nucleases contamination

¹⁴ Previously sterilised with 70% ethanol p.a.

For spheroblasting 2 ml of lyticase buffer were added into the tubes and the plugs were incubated at 37°C for 90 min. Then the buffer was substituted by 1 ml proteinase K solution and incubated at 50°C during a minimum of 18 h to allow digestion of proteins. Subsequently the plugs were washed to allow the removal of buffer remnants and cell debris. In the first washing step the proteinase K solution is replaced with 8 ml rinsing buffer, tilted several times and replaced with fresh 8 ml rinsing buffer. The next two days plugs were washed three more times by replacing and tiling of the previous buffer with fresh buffer. Finally plugs were stored up to one year in rinsing buffer at 4°C. More details about DNA preparation have been published by Friedl et al., 1995.

<u>SEC Buffer</u>	1M sorbitol 0.1 M EDTA in 0.01 M citrate-phosphate buffer dissolved pH 7 adjusted with NaOH
<u>0.01 M citrate phosphate buffer</u>	0.01 M Trisodium citrate (C ₆ H ₅ Na ₃ O ₇) 0.01 M Disodium hydrogen phosphate (Na ₂ HPO ₄)
<u>Agarose solution</u>	1.6 % LMP agarose in 0.125 M EDTA, pH 8
<u>Lyticase buffer</u> (pro sample)	2 ml 0.5 M EDTA, pH 9 20 µl 1 M Tris/HCl, pH 7.5 30 µl milli Q water
<u>Proteinase K solution</u> (pro sample)	1 ml 0.5 M EDTA, pH 9 10 mg sodium lauroylsarcosine 1 mg proteinase K
<u>Rinsing buffer</u>	10 mM Tris/HCl pH 7,5 10 mM EDTA, pH 8

3.5.3. Pulsed Field Gel Electrophoresis

Pulsed Field Gel Electrophoresis (PFGE) is a method used to separate DNA molecules larger than 50 kb according to their length. It works by alternating electric fields at regular intervals, so that DNA runs through a flat gel of agarose (Figure 16). Electrophoresis was carried out in a CHEF mapper system (BioRad).

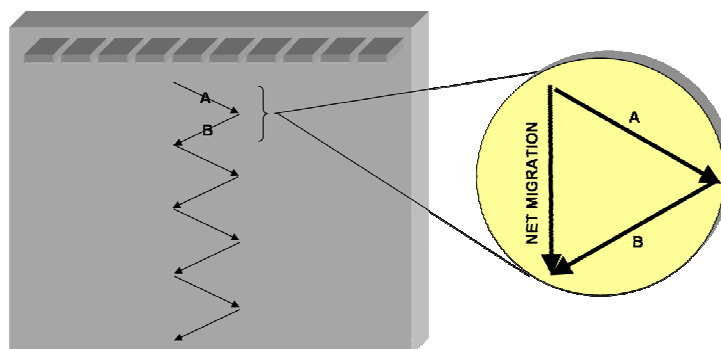


Figure 16: Pulsed Field Gel Electrophoresis. Large DNA molecules can run along the gel due to alternating electric fields.

For electrophoresis gels 100 ml 0.8 % agarose was boiled until the solution was completely clear and cooled up to 50°C under continuous swirling. The gel casting system and the comb were sterilised with 70 % ethanol and let air dried. Between the surface of the casting system and the comb was 1 mm space. Then agarose was poured into the system avoiding bubbles. The agarose plugs were trimmed up to a size of 10 mm x 5 mm using a cover glass and then they were loaded into the wells using a spatula. Parallel 1.9 l electrophoresis buffer (0.5M TBE) was cooled at 14°C before transferring the gel into the electrophoresis chamber. The gel running conditions were:

Period of time	8 h (first period)	13 h (second period)
Angle for field A:	60 °	60 °
Angle for field B:	- 60 °	-60 °
Switching interval:	Initial time	90 s
	Final time	150 s
Voltage gradient:	6 V/cm	6 V/cm

More details about conditions for Pulsed Field Gel Electrophoresis have been published by Friedl et al., 1995.

3.5.4. Gel staining and densitometry evaluation

Yeast chromosomal DNA separated by PFGE were stained with EB. The brightness of the individual bands varies in proportion to the length of the corresponding molecules. Furthermore *S. cerevisiae* has 16 chromosomes but only 11 bands appeared after PFGE, some of these bands being anomalously bright. This effect is due to the equal migration velocity of different chromosomes with similar lengths, which yield double bands.

Gels were stained ON by gentle shaking in 200 ml of 0.5 M TBE solution containing 15 μ l EB. Then gels were photographed and digitalized using the Bio-Rad Gel Doc 2000. Digital data can be evaluated using the program "Quantity one" provided with the Bio-Rad gel documentation system. This image analysis provides 256 grey levels for the incident light intensity at each pixel. A gel size of 500 x 500 pixels was enough for a satisfying spatial resolution. For the evaluation of each gel a lane frame was used, so that each lane had the same width oscillating between 37 - 42 pixels (equivalent to 9.635mm – 10.677 mm). Each lane was approximately 450 pixels long. For the densitometry analysis of the gel it was necessary to calculate the average of the light intensity of the pixels forming the width of a lane, so that we have so many average values as number of pixel a long the lane. A linear digitalization of the data was necessary for the evaluation of gels.

3.5.5. Quantification of DSB

3.5.5.1. Quantification using the program PULSE

The program PULSE was developed for the quantification of randomly distributed DSB in yeast. Observed and calculated DNA mass distributions were compared using a mathematical model, which allowed the determination of the break frequency in yeast chromosomal DNA (Friedl, Kraxenberger et al. 1995).

3.5.5.2. Quantification using the program Geltool

Geltool is a new program for the quantification of double strand breaks in haploid cells. The program is based on a simple densitometric evaluation of EB stained gels (For more information see results).

3.6. Determination of the mutation capacity

To compare the mutagenic effect after UV irradiation in repair proficient and repair deficient strains mutation experiments were carried out in *MKPO* strains which present mutations in the *LYS* and *ADE* gene (*lys2-1*, *ade2-1*). Locus mutations affect the DNA sequence in a defined place or locus, and therefore the probability of reverting both marker genes is negligible. Locus mutations are determined by the number of red mutants (*ade*⁻), which can grow in medium lacking lysine (*LYS*⁺). The determination of spontaneous and UV-induced locus mutations reveals the mutagenicity of yeast strains.

2 or 3 colonies were inoculated in 100 ml rich medium and grown till the stationary phase was achieved (max. 5-10% budding cells). Then cells were harvested and the pellet was washed twice with potassium phosphate buffer. After cell resuspension in 2 ml potassium phosphate buffer the cell number was determined (3.1.2.3). Next cells were adjusted with potassium phosphate buffer up to a concentration of 2×10^9 c/ml. Subsequently a dilution serie was prepared up to 2×10^3 c/ml starting with the 2×10^9 c/ml concentration. For the survival curve 100 µl cells were plated 3 times on rich medium and for the mutation rate experiments 100 µl cells were plated 3 times on SC-lys with 0.5 g adenine medium. Then cells were irradiated with UV doses of $1 \text{ J/m}^2 \cdot \text{s}$ ($\lambda = 254 \text{ nm}$) for 5, 10, 20, 40 and 80 sec. Control cells were not irradiated. After incubation for 72 h at 30°C colonies were counted. Red colonies in the SC-Lys plates were counted. The spontaneous and UV-induced mutation frequency was calculated as:

Spontaneous mutation frequency:

$$M_{(0)} = \frac{Nm_0}{N_0}$$

UV-induced mutation frequency:

$$M_{(x)} = \frac{Nm_z - Nm_0 * S(x)}{Ns(x)}$$

Nm_0 : Number of mutants prior irradiation (0J/m^2)

N_0 : Survivors prior irradiation (0J/m^2)

Nm_z : Number of mutants after a defined UV doses (x)

$S(x)$: Survival after a defined UV doses (x)

$Ns(x)$: Number of survivors after a defined UV-doses (x)

4. RESULTS

4.1. Role of Rad5 in the HR and NHEJ repair pathways

Taking into consideration the sensitivity of the *rad5* mutant towards ^{60}Co -gamma rays, it is important to study the role of Rad5 in DSB repair and its putative interaction with the main DSB repair pathways, HR and NHEJ. Therefore, the interplay between Rad5 and the most important HR and NHEJ proteins, Rad52 and yKu70, was studied by the analysis of the *rad5*, *rad52*, *rad52rad5*, *yku70rad52*, *yku70* and *yku70rad5* mutants.

4.1.1. Generation of *rad52* mutants using the cassette *KANMX6*

To avoid any kind of residual activity of truncated protein fragments, mutants were generated by complete deletion of *RAD52*. The gene cassette *KANMX6* from plasmid pFA6 (2.5.2) was used for the creation of geneticin resistant yeast mutants (Wach, Brachat et al. 1994; Wach 1996). The cassette *KANMX6* was amplified with the primers “*rad52 KANMX fw*” and “*rad52 KANMX rev*” (see sequences on page 31). These primers possess a 5'-end (~40 nt) homologous to the 5'-end of the *RAD52* gene sequence and a 3' end (~20nt) homologous to the *KANMX6* marker gene (Longtine, McKenzie et al. 1998). The amplified cassette was transformed in WT, *rad5* and *yku70* strains to generate *rad52*, *rad52rad5* and *yku70rad52* mutants. The correct integration of the disruption cassette was examined by PCR. Moreover, the *rad52* mutant phenotype was confirmed by analysis of gamma sensitivity experiments.

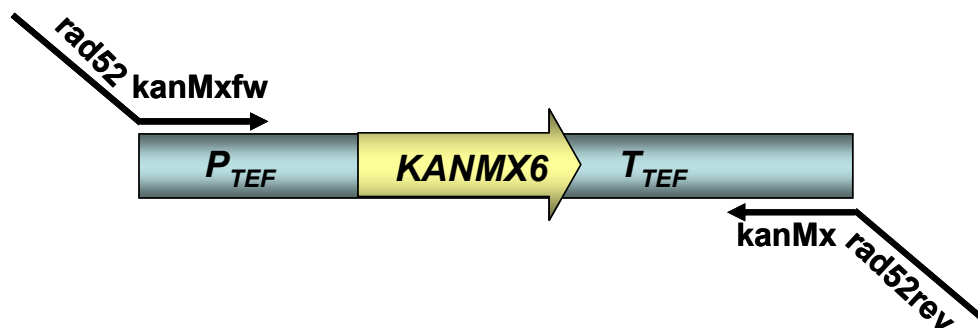


Figure 17: Cassette *KANMX6* from the plasmid pFA6a (Wach 1996). *KANMX6* is a selection marker, which confers resistance against geneticin (G418). P_{TEF} and T_{TEF} are the promoter and terminator regions of the *KANMX6* gene. For primer sequences see page 31.

4.1.2. Survival capacity after gamma and UV radiation

Gamma irradiation produces different kinds of damage such as oxidative base damage, SSB, and DSB. In yeast, DSB are mainly repaired by HR, while NHEJ is of minor importance. As the balance between these DSB repair pathways differs during cell cycle (Karathanasis and Wilson 2002; Ira, Pellicioli et al. 2004), the study of cellular responses to gamma-induced damage in logarithmically growing and stationary phase cells is necessary. On the other hand, UV irradiation generates thymine dimers and 6-4 photoproducts, which are repaired by NER and, in replicating DNA, by PRR, where *RAD5* is involved. The determination of the survival of repair deficient mutants after irradiation allows studying the roles of various repair proteins for the repair of irradiation-induced lesions.

Dose reduction factors (DRF) for 10% of survival are used to compare the survival rates of the different strains. The DRF of a strain 1 is calculated with respect to a strain 2 from the irradiation doses $D_{\text{strain 1}}$ and $D_{\text{strain 2}}$ necessary to reduce the survival of the strains to 10% as

$$\text{DRF} = D_{\text{strain 2}} / D_{\text{strain 1}}.$$

For example, the DRF of a mutant with respect to the WT is calculated as

$$\text{DRF} = D_{\text{WT}} / D_{\text{mutant}}.$$

4.1.2.1. Survival capacity after gamma irradiation

In **logarithmic growth phase**, *rad5*, *rad52*, *yku70*, *rad52rad5*, *yku70rad52* and *yku70rad5* mutants present very different survival capacities (Figure 18). As expected, a high gamma survival capacity (between 8% and 18% after 500Gy) is shown by the HR-proficient WT and *yku70* strains. This confirms that yKu70 does not play a role for the repair of gamma-induced damage in a HR-proficient background. Furthermore, the *yku70* mutant presents a slightly higher survival capacity than the WT, with a DRF of 0.6. The *rad5* mutant, also HR-proficient, shows a lower survival capacity than the WT (DRF = 3.6), revealing a minor role of Rad5 for the repair of gamma-induced damage. This phenotype, also observed in a *rad5* mutant presenting a truncated Rad5, is suppressed by the additional deletion of *YKU70*, the *yku70rad5* mutant having a DRF with respect to the WT of 1.2.

In the *rad52* mutant, which has a DRF with respect to the WT of 12, the sensitivity to gamma irradiation increases due to the incapacity of these cells to use HR for repairing the induced DSB. Unexpectedly, this gamma sensitivity is only slightly increased with the additional *YKU70* deletion, which is in contrast with previous results in a different genetic background (Boulton and Jackson 1996; Mages, Feldmann et al. 1996; Siede, Friedl et al. 1996). However, the double mutant *rad52rad5* is more sensitive than the *rad52* mutant, with a DRF with respect to the WT of 16 and a DRF between the two mutants of about 1.3.

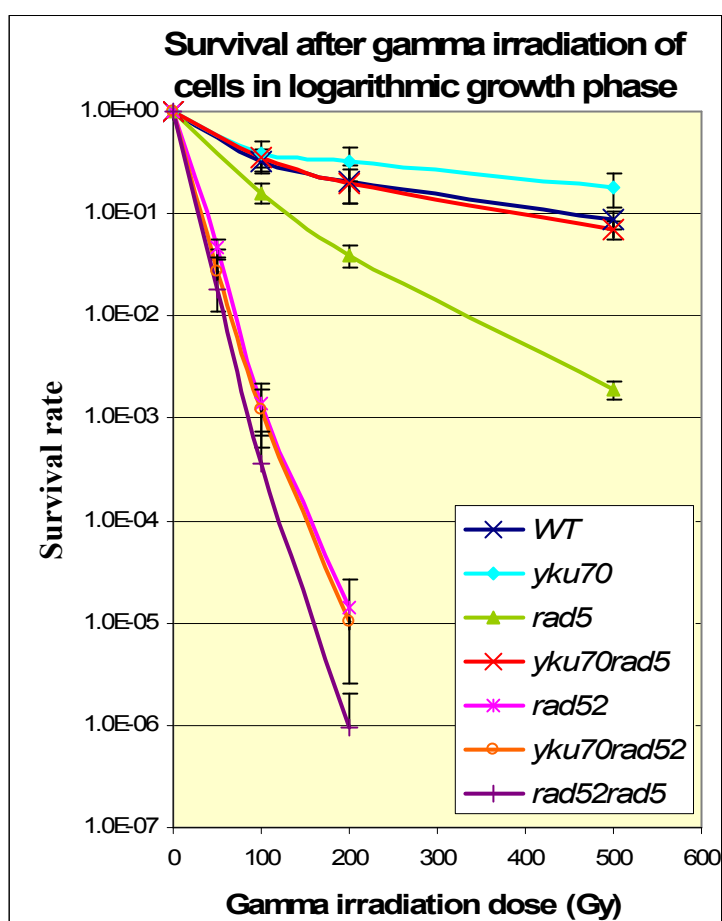


Figure 18: Survival curves after gamma irradiation of logarithmic cultures. The graphic shows the mean survival rates and standard deviations of three to five experiments per strain.

The interaction between two different genes can be classified into epistatic, additive and synergistic, by comparing the sensitivity of the double mutant with the sensitivities of the single mutants. In an epistatic interaction, the double mutant shows the same sensitivity as the single mutants, while in an additive or synergistic interaction, the sensitivity of the double mutant is increased. However, the distinction between additive and synergistic is not always made, and both types of interaction are then called synergistic. For survival curves showing

an exponential behaviour, if the DRF of the double mutant is lower than the sum of the DRFs of the single mutants, the interaction is called additive, while it is called synergistic if the DRF of the double mutant is higher than this sum (Haynes 1975). Using this differentiation, a comparison of the sensitivities of the *rad52rad5* double mutant with the sensitivity of the *rad5* and the *rad52* single mutants shows an interaction that is at the border between additive and synergistic. In any case, the data indicate the involvement of *RAD5* and *RAD52* in different repair pathways for the repair of gamma-induced damage.

The survival capacity was also analysed in cells in the **stationary growth phase** (Figure 19). Both growth phases are compared regarding the DRF with respect to the WT in logarithmic growth phase. In the stationary growth phase, the HR-proficient WT, *yku70* and *yku70rad5* strains are more sensitive to irradiation than in the logarithmic growth phase, showing a DRF of around 4. In contrast, the HR-deficient mutants are much less sensitive in the stationary growth phase, presenting a DRF of around 3, i.e. reduced about 4 times with respect to the logarithmic growth phase.

The *rad5* mutant shows nearly the same survival values in logarithmic and stationary growth phases (Figure 19), indicating that repair in these mutants is mostly independent of the growth phase. Again, the *YKU70* deletion suppresses the *rad5* phenotype in the *yku70rad5* mutant to WT levels.

The additional *RAD5* deletion in the *rad52* mutant increases slightly its gamma sensitivity, confirming the results of the survival experiments in logarithmic growth phase. However, a precise differentiation into additive and synergistic is problematic in the stationary growth phase, due to the strong deviation of the survival curves from exponential behaviour.

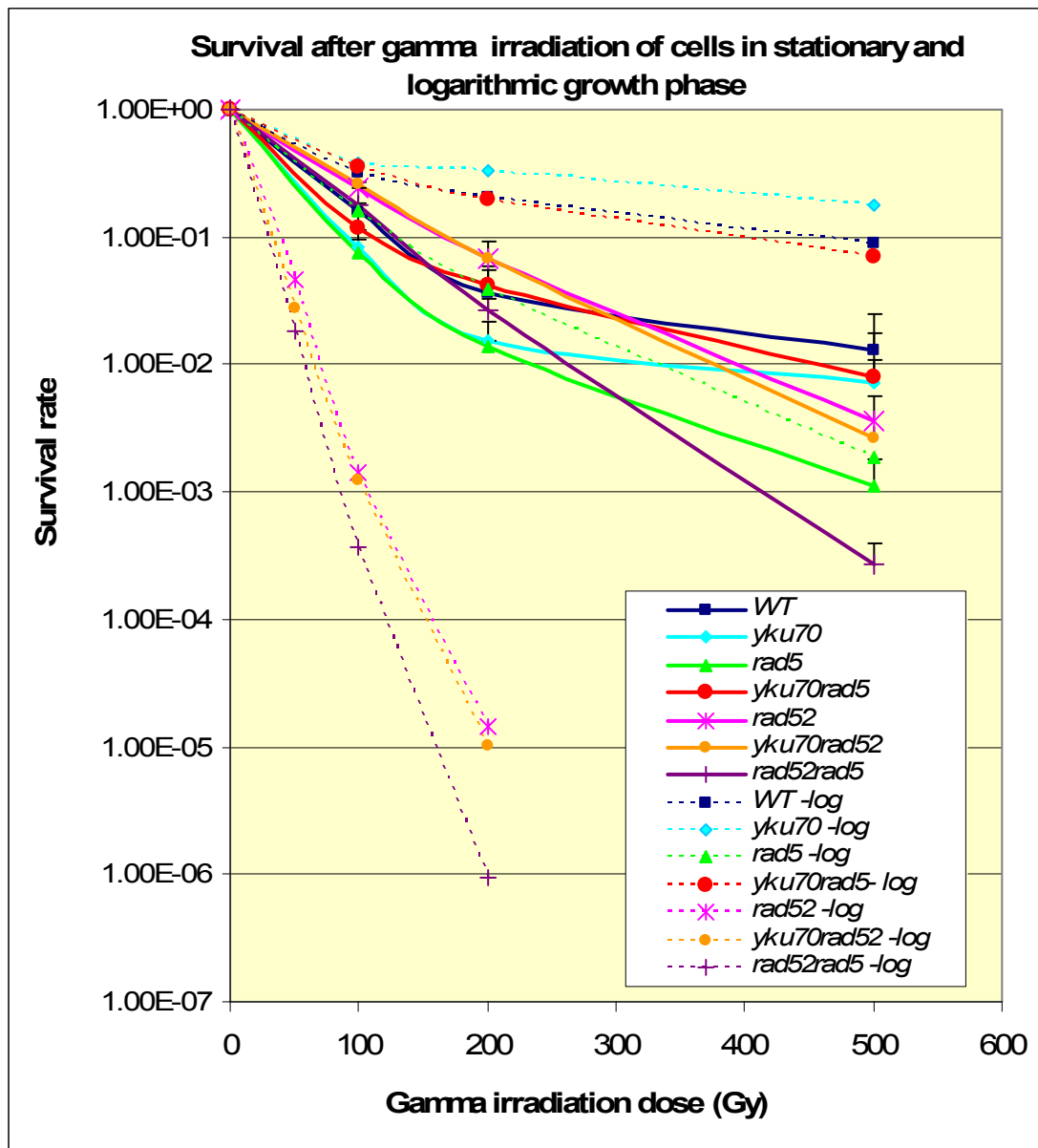


Figure 19: Survival curves after gamma irradiation of MKP0 WT and its derivative mutants in stationary growth phase, compared with the survival curves in logarithmic growth phase shown as dashed lines. This graphic shows the mean survival rates and standard deviations of two to six experiments per strain. For more clarity, only the plus values of the standard deviations are shown.

4.1.2.2. Survival capacity after UV irradiation

Because of the known UV sensitivity of the *rad5* mutant, survival experiments after UV irradiation were carried out in cells of the stationary growth phase to further characterise the *yku70rad5* and *rad52rad5* mutants.

The survival experiments (Figure 20) show two groups of UV sensitivities. The first one is composed of the WT, which presents the lowest UV sensitivity, followed by the *yku70*, *yku70rad52* and *rad52* mutants. The low sensitivity in these mutants is expected since UV does not induce DSBs. The second group is composed of the *rad5* mutant, with its known moderate UV sensitivity, and by its double mutants, *yku70rad5* and *rad52rad5*. The UV survival of the *yku70rad5* is slightly higher than the survival of the *rad5* mutant, which is similar to the suppression of the *rad5* phenotype seen in the gamma irradiation experiments. Moreover, survival further decreases with the deletion of *RAD52* in the *rad5* mutant, indicating a role for *RAD52* in the repair of UV-induced damage in *Rad5* deficient cells.

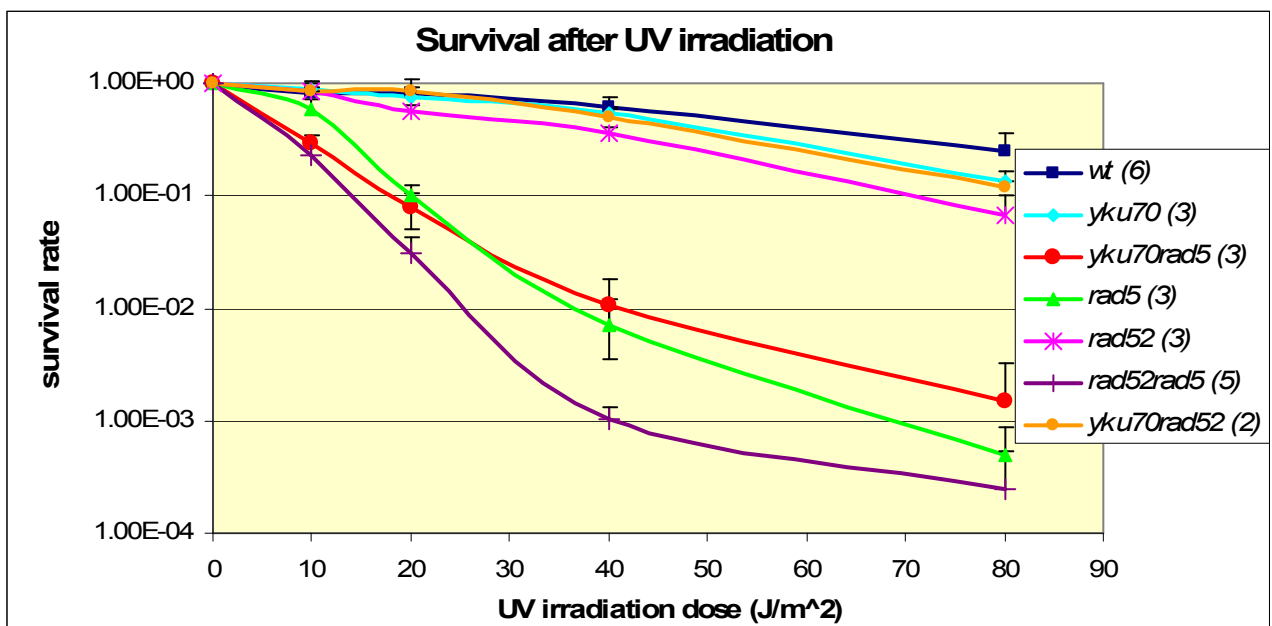


Figure 20: Survival curves after UV irradiation of HR and NHEJ deficient mutants. The values between brackets indicate the number of experiments number with the different strains. For more clarity, only the plus values of the standard deviation are shown.

4.1.3. Role of Rad5 for the repair of chromosomal DSB

The survival experiments reveal a potential role of Rad5 in the repair of gamma-induced damage, but they do not allow the identification of the specific underlying damage. To study the role of Rad5 for DSB repair, PFGE experiments were carried out.

4.1.3.1. Detection of DSB by PFGE

The number of DSB can be quantified by PFGE, which allows the separation of yeast chromosomes and their fragments (see 3.5). Since chromosomal DNA presents different densitometry profiles depending on the fragmentation grade of the chromosomes, it is possible to calculate the number of DSB from PFGE gels (Figure 21). So far, DSB repair using PFGE has been studied in diploid yeast cells (Geigl and Eckardt-Schupp 1991; Kraxenberger, Friedl et al. 1994) or mammalian cells (Longo, Nevaldine et al. 1997; Foray, Arlett et al. 1999; Gauter, Zlobinskaya et al. 2002; Stenerlow, Karlsson et al. 2003; Gradzka and Iwanenko 2005). Even though DSB repair is strongly reduced in haploid yeast cells, it can be observed by PFGE (Fellerhof, 1999).

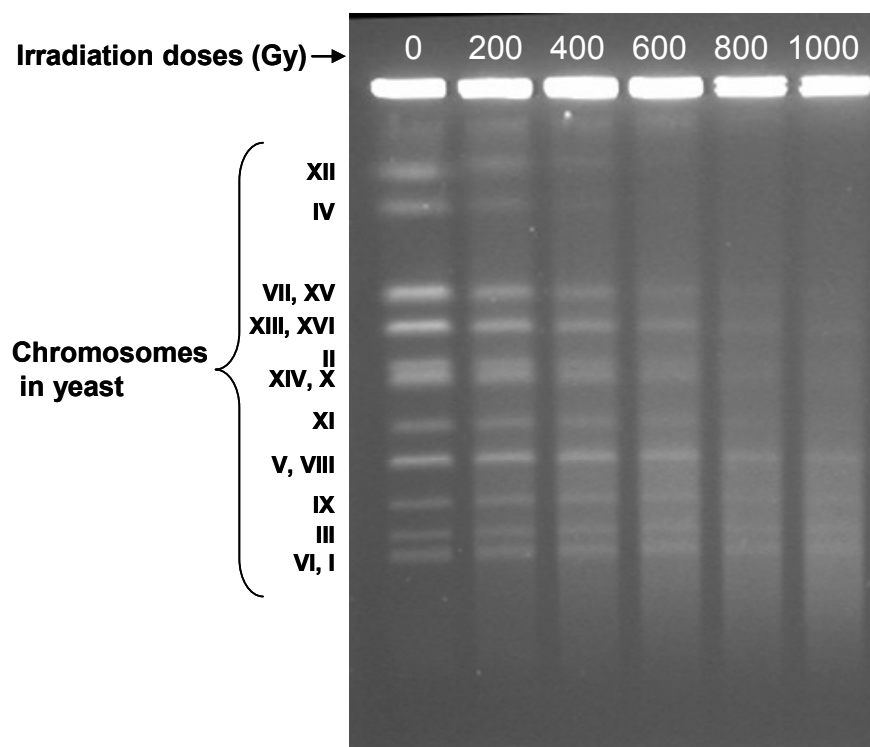


Figure 21: PFGE of wild-type haploid cells after irradiation with different gamma doses (Gy). The intensity of bands representing individual chromosomes decreases with higher irradiation doses, whereas the chromosomal fragmentation (smear) increases. Roman numbers indicate the *S. cerevisiae* chromosomes.

Different methods are used to calculate the number of DSB from PFGE densitometric data. However, some methods are quite imprecise because they exclusively determine the DSB number from changes in the band intensity of chromosome IV (Potter and Kohnlein 2001) or from the observation of several chromosomal bands but ignoring the chromosomal degradation (Moore, McKoy et al. 2000). Another method based on a mathematical model and known as PULSE determines DSB by comparing the observed DNA mass distribution in gel lanes with a theoretical mass distribution (Friedl, Beisker et al. 1993; Friedl, Kraxenberger et al. 1995). PULSE was originally developed for the quantification of chromosomal fragmentation in diploid yeast cells. In haploid yeast cells, DSB repair was observed in interruption mutants (Barbara Fellerhoff, 1999). To confirm that this repair was not due to any remaining enzymatic activity of the interrupted genes, analysis in mutants with complete deletion was necessary. However, PULSE was not sensitive enough for the quantification of chromosomal degradation in the haploid strains used in this work that lack the complete gene, since the results were not reproducible for most of the PFGE gels. Furthermore, the PULSE-program could not be adapted to the new PFGE digitalization equipment. Therefore, it was a main goal of this work to develop a new procedure for the digitalization of PFGE gels and a new software for the direct quantification of DSB repair from the degradation of chromosomal DNA. This software, called Geltool, was elaborated in collaboration with Herbert Braselmann (GSF, Institute of Molecular Radiobiology - Cytogenetics Group).

4.1.3.2. Digitalization of PFGE gels

For the quantification of the number of induced DSB and their repair in haploid yeast cells, it is necessary to digitalise the PFGE gels for further analysis. The documentation device GelDoc 2000 and the corresponding software “Quantity one” (BioRad) was used for this purpose. However, this evaluation program does not have built in functions for the kind of densitometric evaluation necessary for the quantification of DSB¹⁵: “Quantity one” can graphically display a densitometric profile of a lane, but it does not deliver the corresponding densitometric data for further evaluation. Moreover, “Quantity one” can calculate the luminosity of a band, but it does not supply the background luminosity between bands. For this reason, a special procedure was necessary in order to evaluate densitometrically PFGE gels using “Quantity one”. Once the PFGE gel is photographed, this procedure starts with the establishment of the best lane frame for the PFGE gel starting from the slots to the end of the gel (see Figure 22-A). Each lane has to be defined as a single band of a length of approx. 450-500 pixels (Figure 22-B).

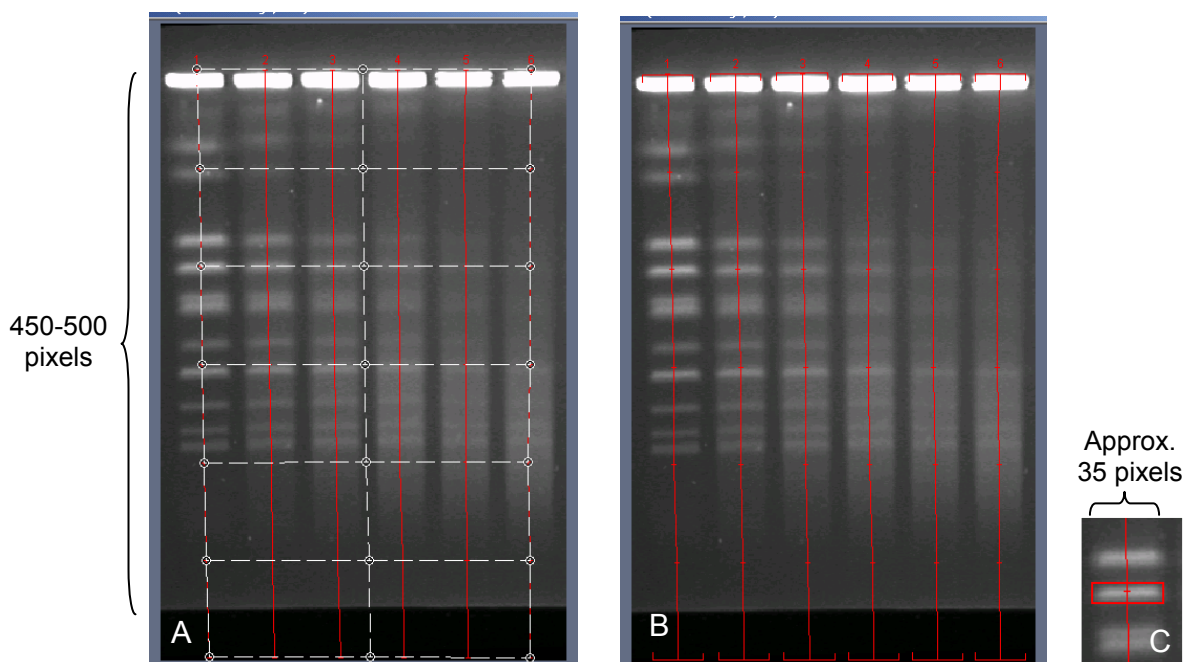


Figure 22: Densitometric evaluation by „Quantity one“ (BioRad). (A) Establishment of the best lane frame for the data by „Quantity one“. In this case, six lanes were recognized. (B) Each lane is composed of a single band approx. 450 - 500 pixel long, generating approx. 400- 500 luminosity values per lane. (C) Each luminosity value is calculated as the average of the pixel luminosity within the width of the lane (approx. 35 pixels).

¹⁵ Personal communication with BioRad’s professionals

Then, a chromosomal band in the gel is manually chosen to establish the correct band width (of approx. 35 pixels, Figure 22-C). Hereby, the Gauss distribution of the pixel luminosity of the chosen band has to be taken into consideration. This width is used for each lane in the gel. Then, the average of the luminosity values of each pixel included in the width of the band is calculated. Thus, the densitometry analysis of a lane is composed of 450-500 values, each of which is the average of the luminosity values presented by the approximately 35 pixels of the width of a band. This densitometric analysis displays a curve (Figure 23), that can be saved and then be used for further analysis by Geltool.

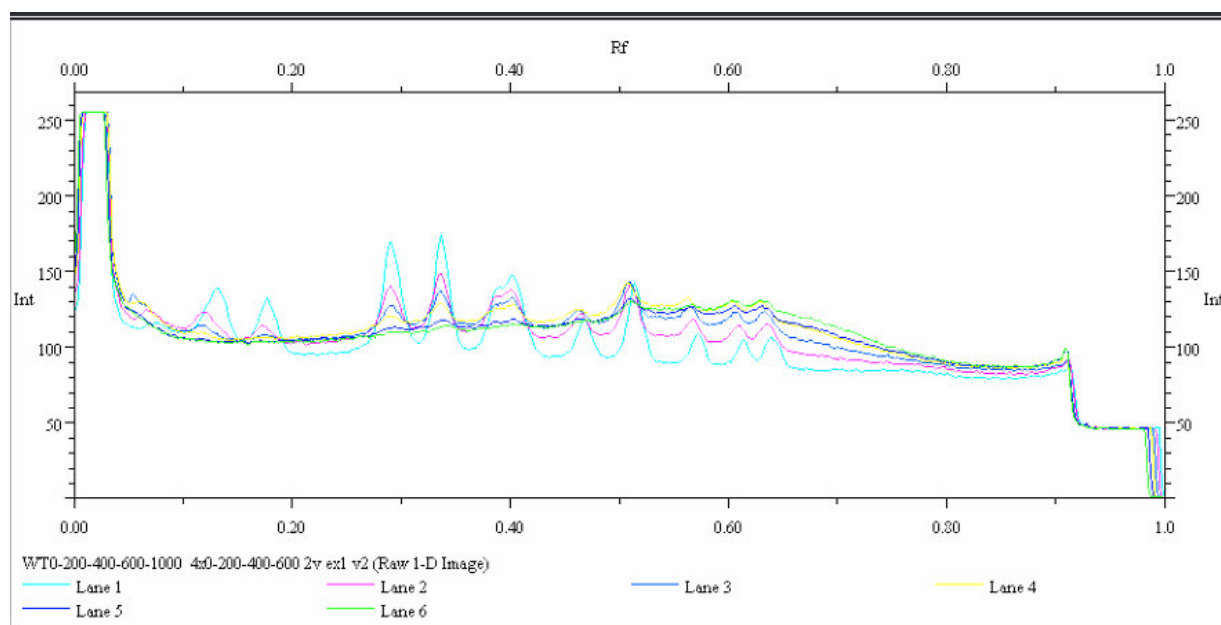


Figure 23: Display of densitometric profiles by “Quantity one”. Lane 1 shows the densitometric profile of chromosomes from non irradiated cells, lane 2, 3, 4, 5 and 6 show the profiles of cells irradiated with 200, 400, 600, 800 and 1000 Gy respectively. These profiles correspond to the PFGE gel shown in Figure 22.

4.1.3.3. DSB quantification by Geltool

Geltool is a software tool written in Delphi that evaluates the densitometric data from PFGE gels by the quantification of chromosomal degradation. For this purpose, the densitometric data are plotted (Figure 24) and a region is established between the double band of the chromosomes XV and VII and the end of the gel (Figure 24-1, Tl and Tr). The two largest chromosomes XII and IV were not used for the evaluation in order to increase the sensitivity of the quantification. Next, the intensity of the highest and lowest points (Figure 24-1, H and L) in this region is calculated to normalize the data (Figure 24-2).

This normalization is necessary to avoid that differences in the DNA amount in the gel influence the evaluation. After normalization, the minima (Figure 24-3, M) of the selected region are detected. Using these minima, a line contouring the degradation under the chromosome peaks (Figure 24-4, P) can be traced. Subsequently, the length of this line (in pixels) is normalized with the length (in pixels) of the region to study on the X- axis (Figure 24-4, Hp), resulting in a profile value (Pv).

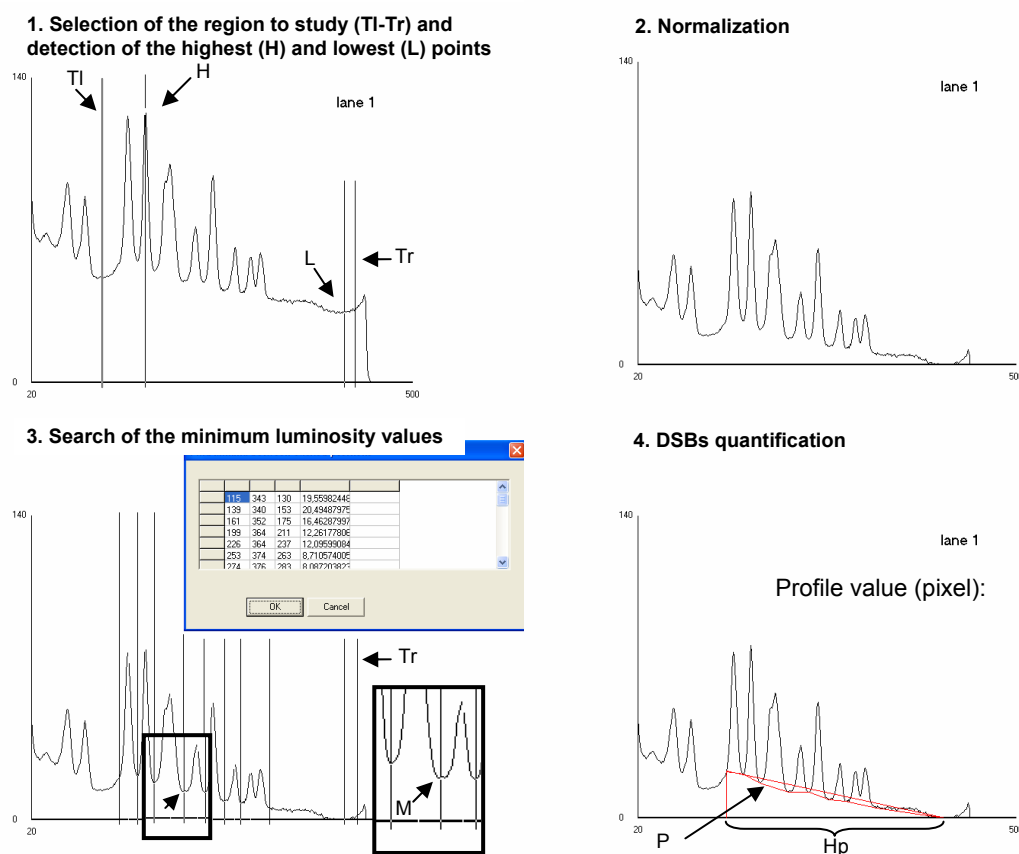


Figure 24: Chromosomal profile evaluation from “Quantity one” data. 1. Establishment of the region to study using a left (TI) and a right (Tr) threshold and determination of the highest (H) and lowest point (L) 2. The normalization of raw data allow to eliminate the gel background. 3. Search of the points of lowest luminosity (M). 4. Geltool calculates a profile line (P) which is normalized with the horizontal profile (Hp), generating a profile value (Pv) in pixels.

Relation between profile value and radiation dose

To check the applicability of Geltool it was necessary to verify the relationship between the gamma irradiation doses and the profile values calculated by Geltool. Therefore cells were irradiated with doses between 200 Gy and 1000 Gy and their chromosomal profiles and profile values were evaluated (Figure 26). Plotting the profile values against the doses shows proportionality between the irradiation doses and the calculated profile values (Figure 25). This indicates that the profile values calculated by Geltool are linearly related to the number of DSBs. However, it is recommended to avoid the evaluation of gels presenting heavily degraded DNA. In these gels, small fragments run out of the gel and they are absent in the profile evaluation (Figure 26, lane 6). In these cases, the profile value increases with the accumulation of fragments at the end of the gel, while the normalization parameter (H_p) remains constant. This produces very high profile values. However, the use of correction factors (available in future versions of Geltool) would rectify these profile values.

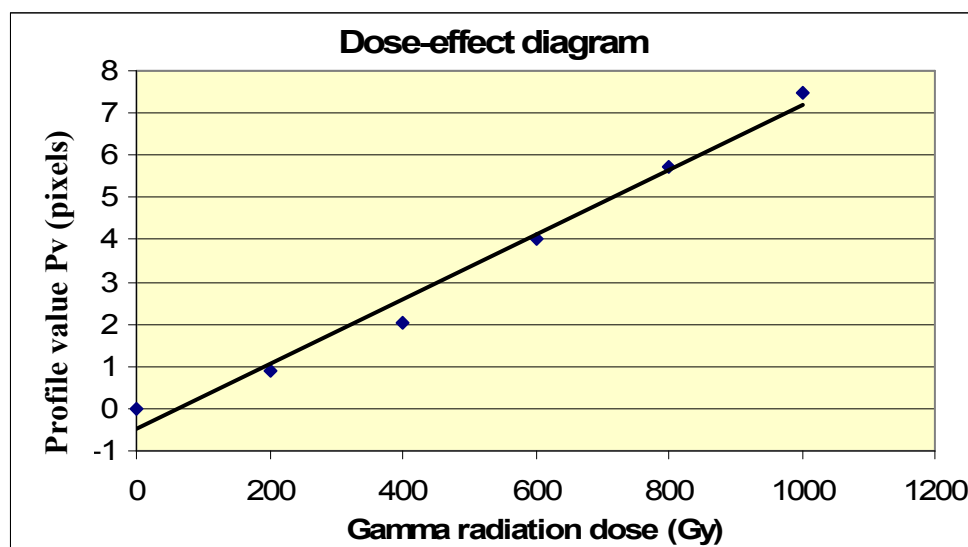
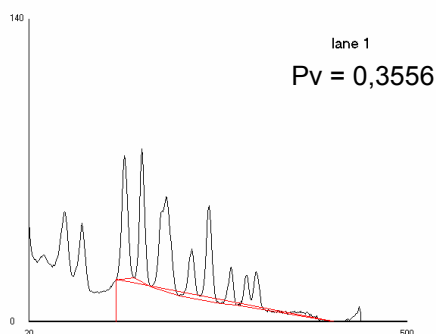
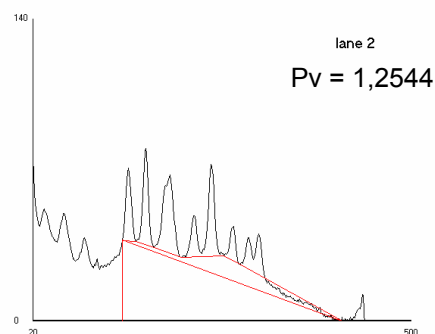


Figure 25: Dose-effect diagram: Geltool shows a linear relationship between the irradiation dose (Gy) and the profile values. For clarity reasons, the values have been corrected with the control value at 0 Gy.

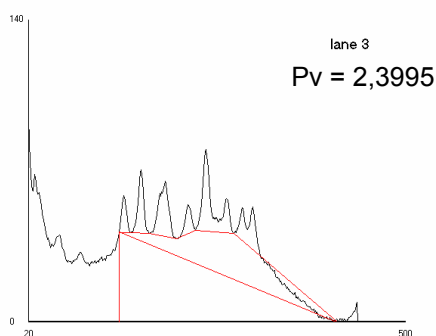
0 Gy = 0 DSB/Genome



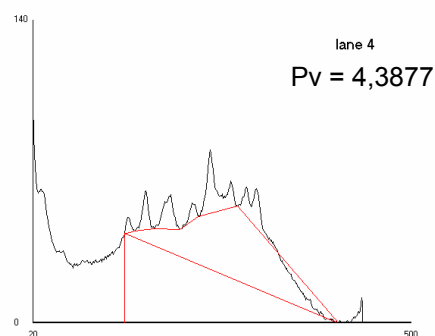
200 Gy = 5.42 DSB/Genome



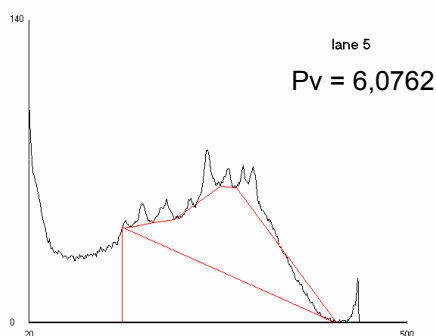
400 Gy = 10.5 DSB/Genome



600 Gy = 19.2 DSB/Genome



800 Gy = 26.7 DSB/Genome



1000 Gy = 34.5 DSB/Genome

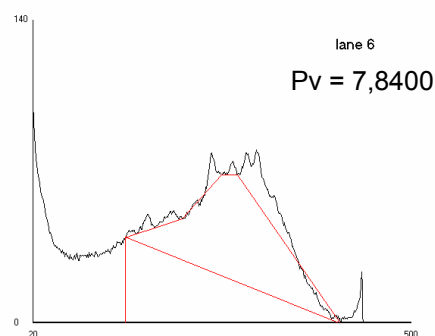


Figure 26: Evaluation of chromosomal fragmentation after different gamma doses by Geltool. Peaks represent chromosomes. The peak height decreases with irradiation, whereas the chromosomal fragmentation (background) increases. Pv is the profile value generated by Geltool. The induced DSB/genome value was calculated by a correlation equation (see page 75).

Correlation between PULSE and Geltool

At the beginning of this work, some PFGE gels of the strains of interest could be evaluated successfully with the previously described evaluation program PULSE. This program allows the quantification of DSB/Mbp (Friedl, Beisker et al. 1993). The PULSE data were then correlated with the data obtained by Geltool. Hence, the comparison of approx. 40 values, generated after the evaluation of 5 gels with both programs shows a linear relationship between the data obtained (Figure 27), which is defined by the equation:

$$y = 0.3198x + 0.1054$$

Where...

- y = equivalent PULSE values (DSB/ Mbp)
- x = measured Geltool values

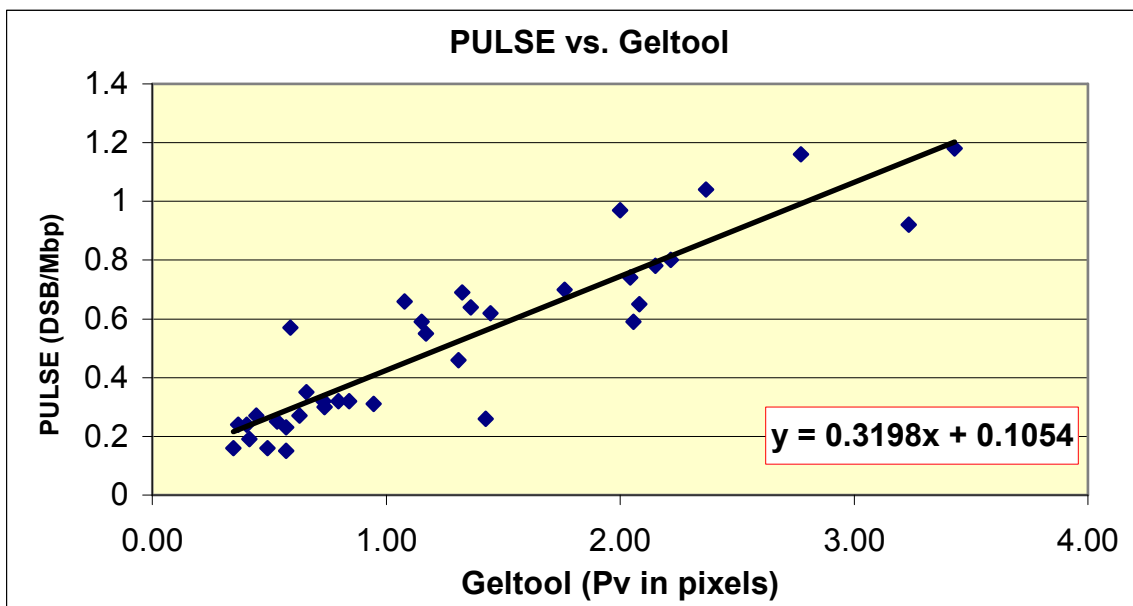


Figure 27: Correlation between PULSE (DSB/ Mbp) and Geltool (Pixels).

Taking into consideration that the yeast genome of the used strains has a size of 13.8 Mbp, it is possible to calculate the number of produced DSB per genome for 400 Gy. The average of 36 independent measurements of the DSB induced by 400 Gy in air (without extra addition of oxygen or nitrogen) was 10.2 DSB/ genome or $1.84 \text{ DSB} * 10^{-9} \text{ bp} * \text{Gy}^{-1}$ (Table 3).

These results fit with previous ones when the different experimental conditions are taken into account. If cells are gassed with oxygen prior to radiation, which promotes the creation of DSB by oxygen radicals, the DSB/genome rate increases up to 18.5, which is equivalent to $3,35 \text{ DSB} \cdot 10^{-9} \cdot \text{Gy}^{-1}$ (Friedl, Beisker et al. 1993). If cells are gassed prior to and during irradiation with nitrogen, eliminating the oxygen content of a normal atmosphere, the DSB/genome rate decreases to 5.14 or to $0.93 \text{ DSB} \cdot 10^{-9} \cdot \text{Gy}^{-1}$ (Fellerhoff 1999). These values support Geltool as adequate software for DSB quantification.

Table 3: Calculated DSB/Genome after irradiation with 400 Gy and $\text{DSB} \cdot 10^{-9} \cdot \text{Gy}^{-1}$ in different studies.

Conditions	DSB/ Genome for 400Gy	DSB* 10^{-9} bp* Gy^{-1}
In air (this work, see Figure 27)	10.2	1.84
20 min gassed with oxygen prior to irradiation (Fellerhoff 1999)	18.5	3.35
30 min gassed with nitrogen prior to and during irradiation (Friedl, Beisker et al. 1993)	5.14	0.93

4.1.3.4. Calculation of the repair capacity after incubation under non-growth conditions

To quantify the repair capacity of different mutants, the percentage of DSB induced by irradiation with 400 Gy and repaired during 23h incubation in LHR buffer was calculated. This percentage is calculated as the ratio between the number of repaired DSB (R) and the induced DSB (I). Unirradiated cells were necessary as a control to correct possible fluctuations in the DSB content during the incubation. The repair capacity determination is carried out by the following steps:

1°. Calculation of the induced DSB (I) after 400 Gy.

$$I = 400 \text{ Gy}_{0h} - 0 \text{ Gy}_{0h}$$

0 Gy_{0h} = DSB in unirradiated cells without incubation in LHR buffer

400 Gy_{0h} = DSB after 400 Gy without incubation in LHR buffer

2°. Calculation of the repaired DSB after 23h (R):

$$R = (400 \text{ Gy}_{0h} - 400 \text{ Gy}_{23h}) - (0 \text{ Gy}_{0h} - 0 \text{ Gy}_{23h})$$

0 Gy_{23h} = DSB in unirradiated cells after 23h incubation in LHR buffer
 400 Gy_{23h} = DSB after 400 Gy after 23h incubation in LHR buffer

3°. Calculation of the percentage of the repaired DSB (PR):

$$PR [\%] = R * 100 / I$$

4.1.4. Repair of DSB in HR and NHEJ deficient mutants

Once the applicability of Geltool had been proven, it was used to determine the repair capacity for gamma-induced DSB in NHEJ- and HR-deficient haploid mutants. For this purpose the number of gamma-induced-DSB was determined previous to and after an incubation time. The experimental procedure, originally developed for diploid cells and survival experiments (Frankenberg-Schwager, Frankenberg et al. 1980; Friedl, Beisker et al. 1993; Friedl, Kraxenberger et al. 1995), has also been applied to haploid cells (Fellerhoff, 1999). Cell cultures have to be in high stationary growth phase, where a maximum of 3 % of the cell population possesses buds. The absence of cell growth during this phase is crucial for the accurate quantification of DSB repair by PFGE (Fellerhoff, 1999). Furthermore, experiments with haploid cells in the stationary growth phase provide the optimal conditions to study the contribution of NHEJ to the repair of DSB. First, NHEJ is promoted in haploid cells by Nej1 (Valencia, Bentele et al. 2001) and second, the absence of sister chromatids handicaps repair by HR.

After gamma irradiation cells were incubated at 30°C in liquid holding recovery (LHR) buffer, which keeps cells in stationary growth phase by inhibiting cell growth while allowing repair processes¹⁶ (Frankenberg-Schwager, Frankenberg et al. 1980; Dardalhon, Nohturfft et al. 1994, Fellerhoff 1999). Since repair of DSB at chromosomal level (Figure 28) is calculated in cells in the stationary growth phase, the results can be compared with survival experiments of cells in this phase (Figure 19).

¹⁶ For more information see also 3.5

The quantification of DSB after a repair period reveals a significant DSB repair capacity in haploid strains in stationary phase. Especially the HR-proficient strains repair far better than the HR-deficient mutants. This shows a vital role for HR in the repair of DSB in haploid cells in spite of the lack of homologous chromosomes and sister chromatids. The high repair capacity of the *yku70* and the *yku70rad5* mutants in comparison with the *yku70rad52* mutant indicates that NHEJ does not play a crucial role for repair of DSB in a HR-proficient background, while the additional *YKU70* deletion in the *rad52* mutant reduces about 2 times its repair capacity. The *RAD5* deletion also does not significantly affect the repair of HR-proficient strains, whereas it reduces the repair capacity of the *rad52rad5* mutant (only 6% of the DSB are repaired).

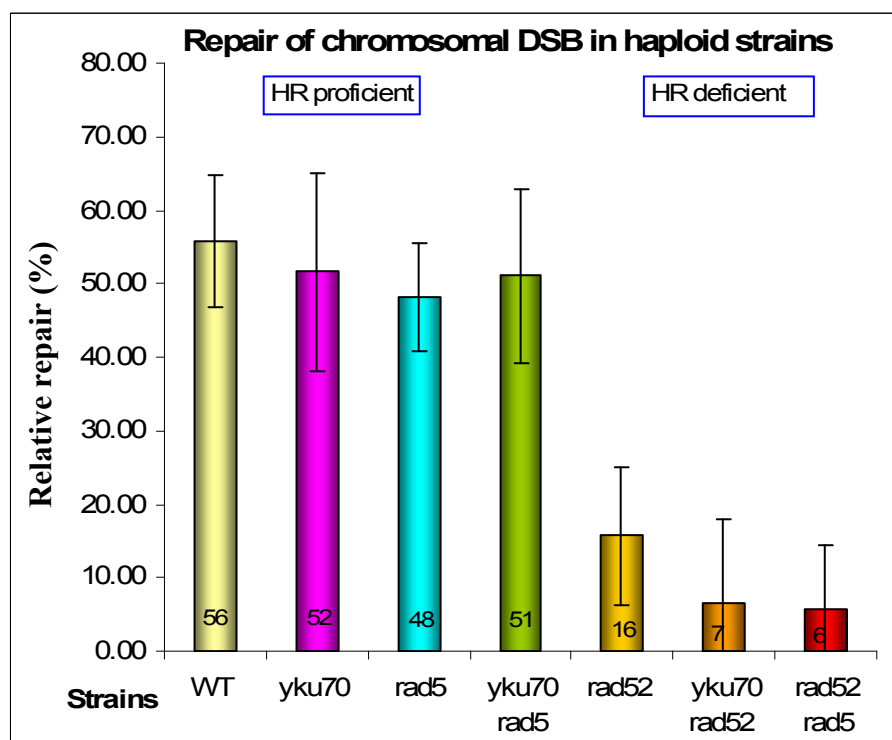


Figure 28: Repair of chromosomal DSB in haploid strains in stationary phase. After irradiation with 400 Gy, cells were incubated at 30°C in LHR buffer during 23h. Samples were taken previous to irradiation and after an incubation time to determine the percentage of the repaired DSB (see 4.1.3.4). The average and standard deviations of 3 - 4 experiments are shown. In WT, the average corresponds to 10 experiments.

4.1.5. Repair of plasmidial gaps

The interplay of Rad5 with HR and NHEJ proteins was studied in more detail by a plasmid assay (Jha, Ahne et al. 1993). In contrast to studying chromosomal DSB repair, this assay allows the exact identification of the particular pathway used for the repair of a plasmidial gap, HR or NHEJ, and its efficiency and accuracy. In this assay, cells were transformed with the episomal plasmid pJD1, which possesses the independent marker genes *TRP1* and *URA3*. In the *URA3* marker gene a 169 bp long gap was induced by restriction enzymes (see Figure 14 in page 55). Since yeast cells in G₀/G₁ can not be transformed, cells in the logarithmic growth phase were used.

4.1.5.1. Repair efficiency of plasmidial gaps

The efficiency of plasmid repair was determined in the MKP0 WT, *yku70*, *rad5*, *rad52*, *yku70rad5*, *yku70rad52* and *rad52rad5* strains using the plasmid pJD1. Abutting ends were created by cleavage with the RE *ApaI* and *NcoI*. The recirculation of the plasmid is necessary for propagation of the plasmids and colony formation of the transformed *trp⁻* cells on medium without tryptophan. The ratio between the number of clones transfected with gapped plasmid and the number of clones transfected with uncut plasmid defines the efficiency for plasmidial gap repair. Figure 29 shows the results for the determination of repair efficiencies of gapped plasmids for the various mutants and WT strains. The HR proficient strains WT, *yku70* and *rad5* show a high gap repair efficiency ranging between 0.08 and 0.09, whereas the double mutant *yku70rad5* presents a 2-fold reduction of the efficiency rate. The efficiency in the *rad52* single mutant is reduced 45-fold in comparison with the WT. The additional deletion of *RAD5* or *YKU70* aggravates the *rad52* phenotype. In the *rad52rad5* mutant the repair efficiency is 180 times lower than in WT while in the *yku70rad52* double mutant hardly any transformant was recovered (9000 times lower than in the WT).

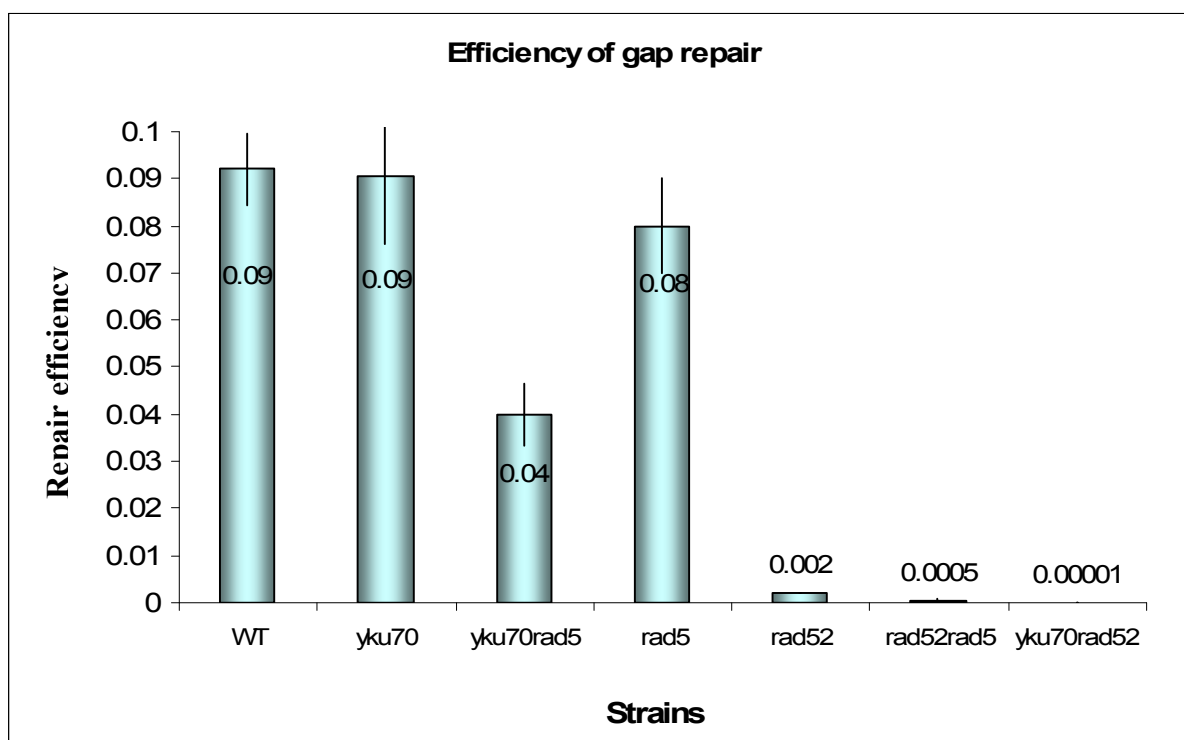


Figure 29: Efficiency of gap repair in MKP0 WT and its derived mutants. Average and standard error of 2 to 5 experiments are shown. Some standard errors are too small to be visible.

4.1.5.2. Repair accuracy of plasmidial gaps

The accuracy of plasmidial gap repair was determined in the MKP0 WT, *yku70*, *rad5*, *rad52*, *yku70rad5*, *yku70rad52* and *rad52rad5* strains by their capacity to repair the *URA3* selection marker accurately, necessary for survival in medium without uracil. Gap repair can be performed correctly by homology-dependent repair, which uses an inactive chromosomal *ura3-52* sequence to repair the plasmidial gap. This leads to the expression of a functional *URA3* gene from the plasmid (URA^+ clones). The plasmidial gap can also be repaired incorrectly by end joining mechanisms or by error-prone homology dependent repair, generating *ura⁻* clones. The ratio of the number of URA^+ clones with correctly repaired plasmids (TRP^+URA3^+) to the total number of clones with recircularized plasmids (TRP^+) defines the accuracy of plasmidial gap repair. Figure 30 shows that WT repairs correctly in 97 % of the events, whereas both of the HR proficient *yku70* and *yku70rad5* mutants present a 20-25 % lower repair accuracy. Surprisingly, this high accuracy of the *yku70rad5* double mutant contrasts with its low repair efficiency. On the other hand and as expected, the *RAD52* deletion decreases the repair accuracy drastically.

Hence, the repair of the *rad52* mutant is approx. 64 times more inaccurate than the repair of the WT. Moreover, the additional *RAD5* deletion aggravates the *rad52* phenotype. Thus, only few transformants could be recovered from *rad52rad5* double mutant, which shows a repair accuracy around 200 times lower than the WT. Hardly any *yku70rad52* mutants were recovered. None of them repaired the *URA3* gene correctly.

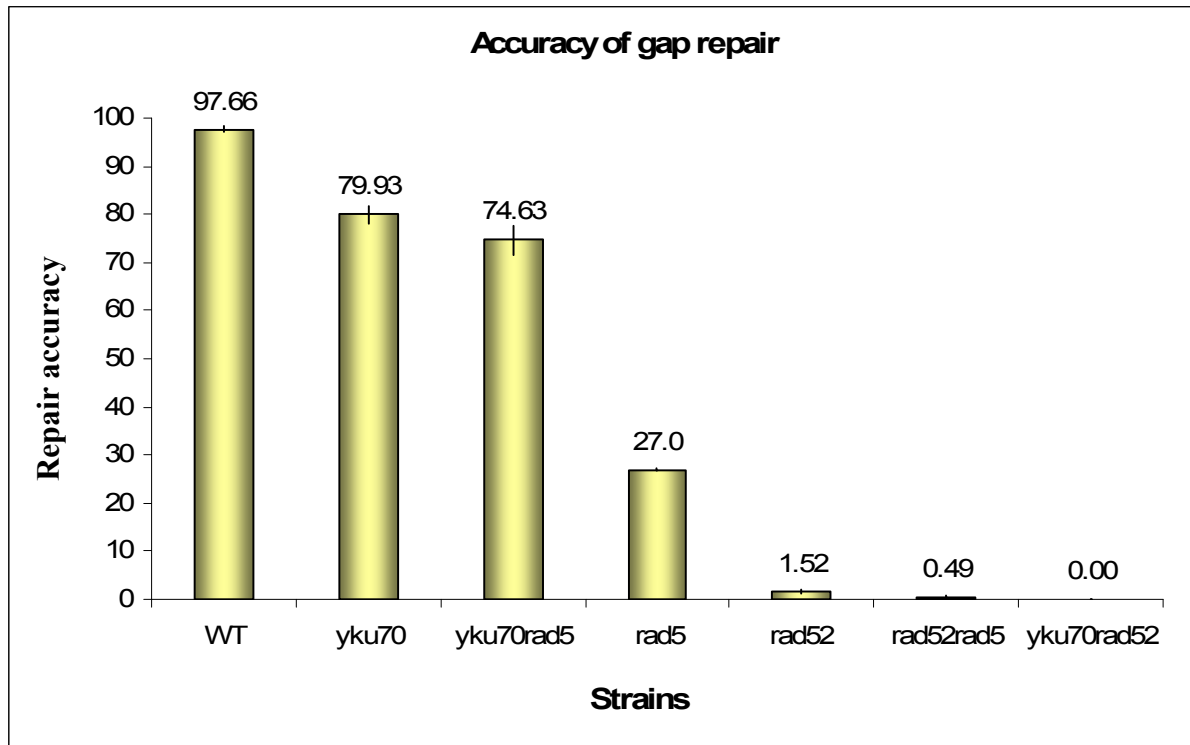


Figure 30: Accuracy of gap repair in MKP0 WT and its derived mutants. Average and standard error of 2 to 5 experiments are shown. Some standard errors are too small to be visible.

4.1.5.3. NHEJ vs. HR in misrepaired plasmids

To further confirm the type of misrepair a PCR analysis of the incorrectly repaired plasmids isolated from *ura⁻* clones was carried out. The size of the fragments corresponding to the incorrectly repaired region allows distinguishing between repair by HR or NHEJ. Plasmids repaired by HR present the same size as the uncut plasmid. However, if the gap is repaired by NHEJ, the deletion in the plasmidial *URA3* remains and the recovered fragments are shorter (Figure 31). Furthermore, fragments repaired through NHEJ can present an additional shortening due to DNA end degradation. PCR analysis was carried out using primers localized approx. 460 bp upstream of the *NcoI* site (*ura3-1*) and 75 bp (P2) or 430 bp (*sonde rev*) downstream of *ApaI* (Figure 31). Alternatively, primers sited approx. 520 bp upstream (*ura3-3*) and 2000 bp downstream (*INV5*) of the gapped region were necessary.

PCR Analysis of incorrectly repaired gapped plasmids

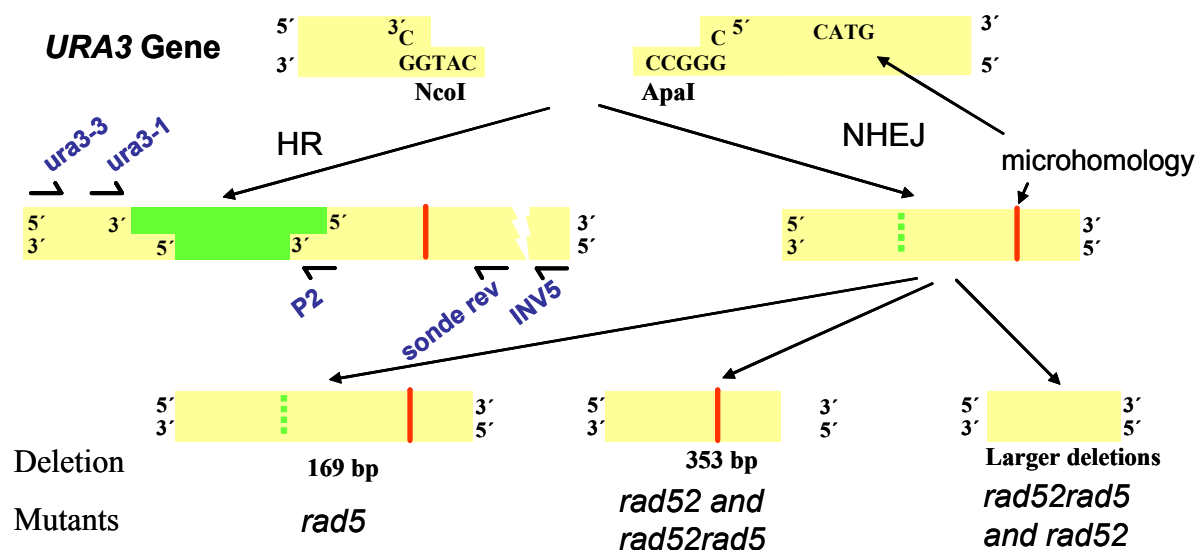


Figure 31: PCR analysis of incorrectly repaired gapped plasmids. The recovered PCR fragments present different sizes depending on the repair pathway used. DNA degradation can arise during the NHEJ process, which generates deletions up to 2300 bp.

PCR results show that incorrect gap repair is due to error-prone HR in all plasmids derived from *ura⁻* clones of the WT and approximately 90% of the plasmids from *ura⁻* clones of *yku70* and *yku70rad5* strains (figure 32). This is in contrast with results for the *rad5* mutant, in which 85 % of the repair events are due to NHEJ. Thus, in accordance with the results for repair accuracy, the *rad5* phenotype is suppressed in the double mutant *yku70rad5*. Plasmids of the *rad52* mutants are repaired exclusively by NHEJ (Figure 31). This use of NHEJ is independent of the strain background, as results from three different *rad52* strains (MKP0, SX560 and SX95) confirm. All the PCR fragments (primers *ura3-1* and *sonde rev*) from *rad52* mutants presented larger degradation of approx. 350 bp, except in one case, where the degradation reached approx. 1300 bp (primers *ura3-3* and *INV5*). The analysis of repair products from plasmids isolated from *rad52rad5* was hardly possible due to the low transformant recovery of these mutants and the difficulty to obtain PCR products; only 3 transformants of 10 showed fragments after PCR. Two of the plasmids, which also were successfully sequenced, were recovered after PCR with the primers *ura3-1* and *sonde rev* and presented a 350 bp long degradation. One of the fragments was only visible by PCR with primers localized approx. 520 bp upstream (*ura3-3*) and 2000 bp downstream (*INV5*) of the gapped region, presenting an approx. 2300 bp long deletion that possibly impeded its sequencing. Only 3 plasmids were obtained from the *yku70rad52* mutant. From none of them a PCR fragment could be recovered, possibly as a consequence of very large deletions.

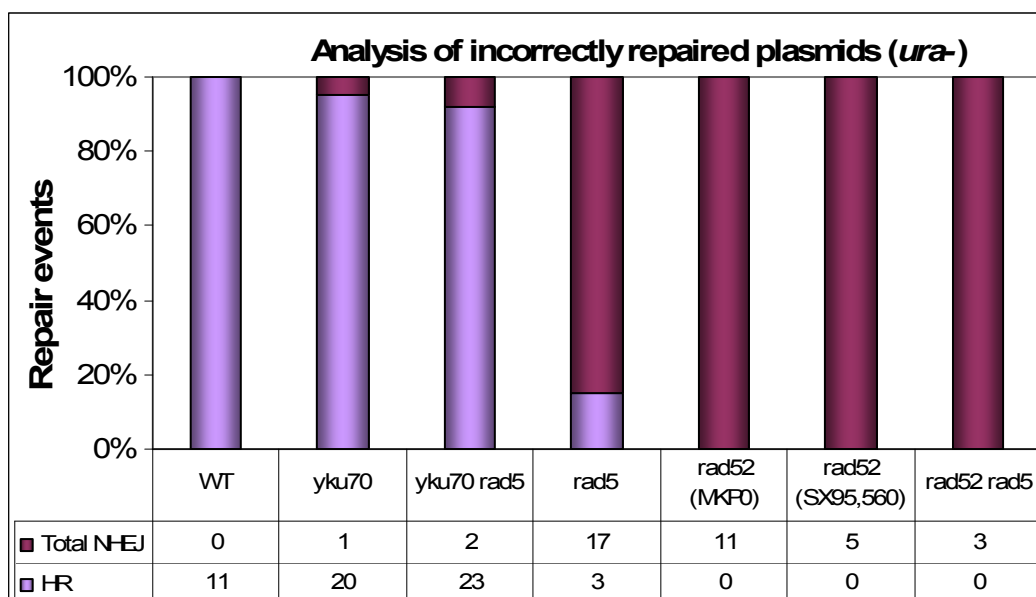


Figure 32: Balance between HR and NHEJ in MKP0 WT and repair deficient haploid mutants after PCR analysis of incorrectly repaired plasmids. *SX95* and *SX560 rad52* mutants were also studied to confirm the independence between *rad52* phenotype and the strain background.

4.1.5.4. Sequence analysis of plasmids incorrectly repaired by NHEJ

Previous studies with a *rad5* interruption mutant have revealed that 70-80% of the plasmids were repaired by NHEJ after degradation of the protruding ends followed by rejoining of the blunt ends (Ahne, Jha et al. 1997; Moertl, S., unpublished data). In this work, the role of Rad5 in NHEJ was further analyzed in *yku70*, *yku70rad5*, *rad52* and *rad52rad5* mutants by sequencing of fragments recovered from plasmids of *ura*- colonies. Table 4 sums up the results from the sequence analysis of the NHEJ events.

Table 4: NHEJ events in incorrectly repaired plasmids from *ura*⁻ clones. Since DNA ends can be degraded before rejoining takes place, different rejoining products are possible. To analyze them more accurately, PCR fragments from the recovered plasmids were sequenced. By sequencing, repair by direct joining and by microhomology was found. Other plasmids presenting more extensive deletions could not be sequenced. This table summarises the different sequencing products and the fragments presenting extensive deletions.

Fragments presenting:	<i>yku70</i>	<i>rad5</i>	<i>yku70rad5</i>	<i>rad52</i>	<i>rad52rad5</i>
Repair by direct joining	0	16	1	3	0
Repair by microhomology	1	1	1	12	2
Extensive deletions	0	0	0	1	1
Total	1	17	2	16	3

HR proficient WT, *yku70* and *yku70rad5* strains present none or few repair events by NHEJ, in contrast to the *rad5* and the HR-deficient *rad52* and *rad52rad5* mutants (figure 32). After NHEJ different products were found depending on the grade of DNA end processing. Direct rejoining with small deletions was found in one *yku70rad5* mutant and three *rad52* mutants of different strains (Table 4 and Table 5). Larger deletions arose due to a 5'->3' degradation of the 5'-end up to a 5 bp microhomology of the NcoI cut site, which is localized 353 bp downstream of the NcoI cut site. This repair by microhomology was found only in one case in the *yku70* and *yku70rad5* mutants respectively, in most events in the *rad52* mutant and in two of three events in the *rad52rad5* mutant. More extensive deletions were found in one case in the *rad52* mutant and one case in the *rad52rad5* mutant by PCR. However, a further analysis by sequencing was not possible. Moreover, in the *rad52rad5* mutant, from out of 10 isolated plasmids, 7 could not even be analysed by PCR, possibly due to strong degradations of the DNA ends before repair (Table 5).

Table 5: Sequences of joined ends. Sequences in yellow show the remainders of the restriction sites NcoI and ApaI after repair. The NcoI-microhomology region localized 353 bp downstream of the NcoI cut site is shown in blue.

REPAIR BY DIRECT JOINING WITH SMALL DELETIONS	
WT	5' CTGATTTTTC CCATGG ---169 bp--- GGCCCCAG ---184 bp--- CATGGG 3'
<i>yku70rad5</i>	5' CTGATTTTTC CCATG ----- CAG ----- CATGGG 3'
<i>rad52</i> (SX560)	5' CTG ----- CAG ----- CATGGG 3'
<i>rad52</i> (SX95)	5' CTGATTTTTC ----- C CAG ----- CATGGG 3'
<i>rad52</i> (MKP0)	5' CTGATTTTTC ----- G ----- CATGGG 3'
REPAIR BY MICROHOMOLOGY DEPENDENT END JOINING	
<i>yku70</i>	
<i>yku70rad5</i>	
<i>rad52</i> (SX560)	
<i>rad52</i> (SX95)	5' CTGATTTTTC -----353 bp----- CATGGG 3'
10 * <i>rad52</i> (MKP0)	
2 * <i>rad52rad5</i>	
REPAIR WITH EXTENSIVE DELETIONS	
<i>rad52</i> (SX560)	5' ???????? ----- >1300 bp----- ???????? 3'
<i>rad52rad5</i>	5' ???????? ----- >2300 bp----- ???????? 3'

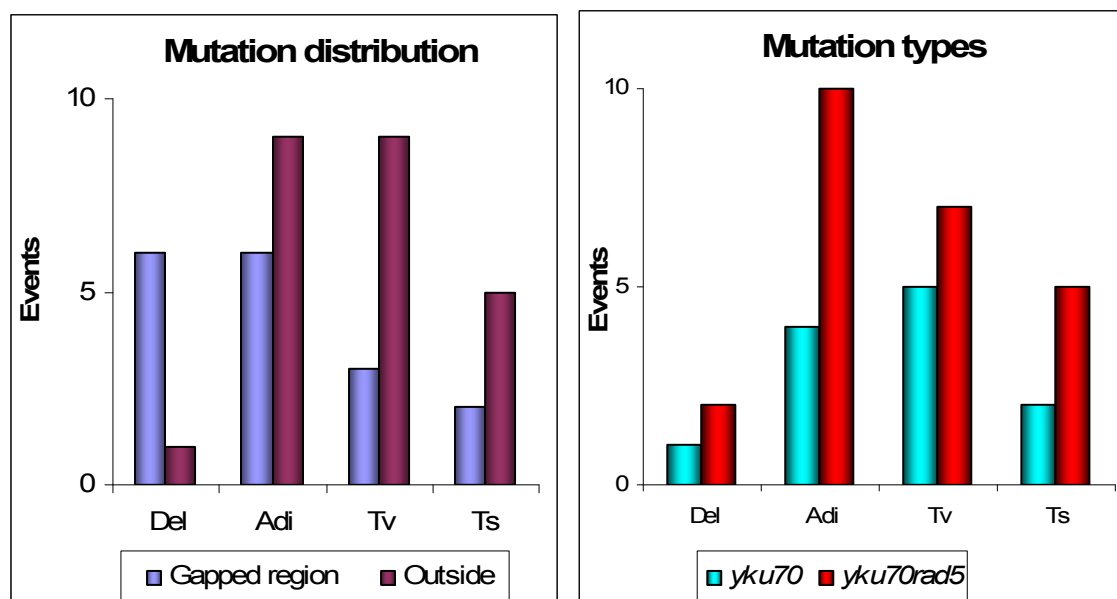


Figure 33: Mutation distribution and type. 11 *ura⁻* plasmids from *yku70* and 13 *ura⁻* plasmids from *yku70rad5* mutants were sequenced and analysed. Del: deletions; Adi: additions; Tv: transversions and Ts: transitions.

4.1.5.5. Analysis of plasmids incorrectly repaired by HR

Sequences of the *URA3* gene from incorrectly repaired plasmids were isolated from the *yku70* mutant (11 sequences) and from the *yku70rad5* mutant (13 sequences) and analysed to study error prone repair by HR. Most of the sequences were analysed from the ATG-start codon to 755 bp downstream using the primer sonde rev. The sequence analysis reveals a slightly higher mutation frequency in the *yku70rad5* double mutant than in the *yku70* single mutant (Figure 33-right). The most common mutations are additions, localized in and outside the repaired gap region, transversions, predominantly outside, and deletions, mainly localised at the *ApaI* cut site (Figure 33-left and Figure 34).

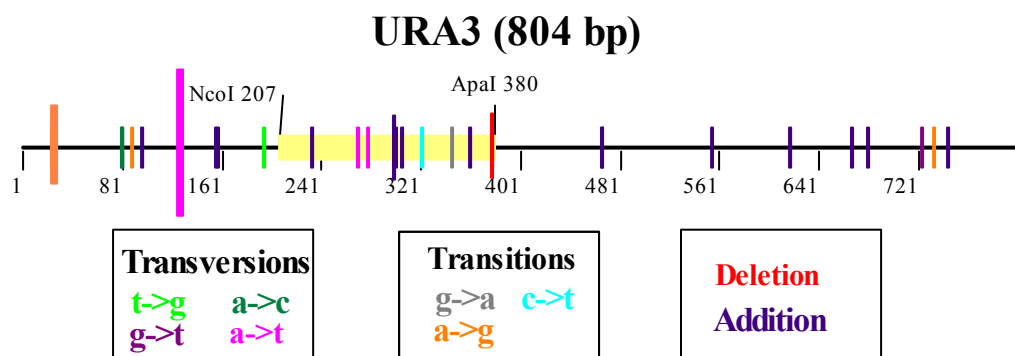


Figure 34: Spatial distribution of mutations generated after error-prone HR. 11 plasmids from *yku70* and 13 plasmids from *yku70rad5* mutants were sequenced and analysed. The yellow bar represents the gapped region. Different colours and sizes of the bars represent the mutations types and their frequency respectively.

4.1.5.6. Summary of the results of the plasmidial gap repair assay

Deletion of *YKU70* does neither affect the gap repair efficiency nor the accuracy, explained by the use of HR for the repair of plasmidial gaps in the *yku70* mutant. The *rad5* mutant repairs with high repair efficiency but low repair accuracy by NHEJ. The additional deletion of *YKU70* suppresses the *rad5* phenotype; the *yku70rad5* mutant repairs by HR, presents high repair accuracy and low repair efficiency. This low efficiency is surprising in a mutant that predominantly uses HR, however it can be explained if the absence of the regulation function of Rad5 influences the efficiency or if Rad5 has a role for the recirculation of gapped plasmids when NHEJ is suppressed.

On the other hand, *rad52* mutants use exclusively NHEJ as gap repair pathway independently of the strain background, confirming the central role of Rad52 for HR. Long deletions accompanied with microhomology mediated end joining (MMEJ) suggests a role of Rad52 in the protection of DNA ends. The long deletions would explain the very low efficiency in *rad52* mutants, and indicate that in these mutants, NHEJ does not guarantee the direct rejoining of the broken ends of a gap. Furthermore, the additional deletion of *RAD5* strongly reduces the recircularization capacity and it seems to increase the end degradation. Hence, in the *rad52rad5* mutant, only 3 PCR fragments could be analysed and they presented 353 bp up to 2300 bp long deletions. However, more studies with the *rad52rad5* double mutant are necessary to explain the role of Rad5 for DSB rejoining in HR deficient mutants. In the *yku70rad52* mutant, gap repair was almost not existent, indicating a severe disturbance of plasmid recirculation when both processes, HR and NHEJ, are abolished.

4.2. Role of Rad5 in base excision repair

The *rad5* mutant shows a high repair capacity of DSB in stationary phase cells and also a high efficiency in the repair of plasmidial gaps in the logarithmic phase cells. However, this high repair capacity is in contrast to its gamma sensitivity in the stationary as well as in logarithmic phase cells. Taking into consideration that gamma irradiation produces not only DSB but also oxidative base damage, which is mainly repaired by BER, the study of the repair after gamma irradiation in a BER-deficient background could help to explain this sensitivity.

4.2.1. Generation of knockout mutants

To study the role of Rad5 for BER, the *apn1ntg1ntg2* and the *apn1ntg1ntg2rad5* mutants were generated. Although these mutants lack the most important BER N-glycosylases and AP-endonucleases (Apn1, Ntg1 and Ntg2), a back up BER activity is possible due to the action of other BER specific proteins such as Apn2 and Ogg1. However, only a minimal BER residual activity is expected, as the *apn1ntg1ntg2* mutant has been described previously as BER-deficient (Swanson, Morey et al. 1999; Doetsch, Morey et al. 2001).

For the generation of BER-deficient mutants three plasmids were constructed and used for the transformation of MKP0 WT and *rad5* strains. In these plasmids, the *LEU2*, *URA3* and *TRP1* yeast markers are inserted between the start and end sequences of the *APN1*, *NTG1* and *NTG2* genes, respectively. This allows an almost complete deletion of the chromosomal gene (with less than 325 bp remaining), which avoids any residual activity by these proteins. Correct integration of the marker in the chromosomes of the MKP0 WT and the *rad5* mutant was confirmed by auxotrophy and PCR experiments.

4.2.1.1. Plasmid *papn1a6::LEU2*

The *papn1a6::LEU2* plasmid is a derivative of the pUC19 plasmid (Fermentas). A PCR fragment of the *APN1* gene was amplified using the “fw apn1-667 upstr” and “rev apn1 EcoR1” primers. Subsequently the fragment was digested with BamHI and EcoRI prior to integration in the plasmid pUC19, which generates the new plasmid *pUC19-apn1* (*papn1a*) with a size of approx. 4.8 kb. Then, the *LEU2* gene was isolated by BglII digestion from pSM20 (gift of David Schild, Berkeley) and inserted in *papn1a* at the BglII cut site. The plasmid was amplified in medium containing ampicillin and identified by gel electrophoresis according to its size (approx. 7.7 kb). In a next step the plasmid *papn1a* containing *LEU2* (*papn1a6::LEU2*) was digested with the RE BamHI and StuI and the 3870 bp fragment was transfected in the *MKP0 WT* and *MKP0 rad5* strains. Strains were grown in media lacking leucine and single clones were picked. Finally the correct integration of the *LEU2* fragment in the chromosome was checked by PCR analysis.

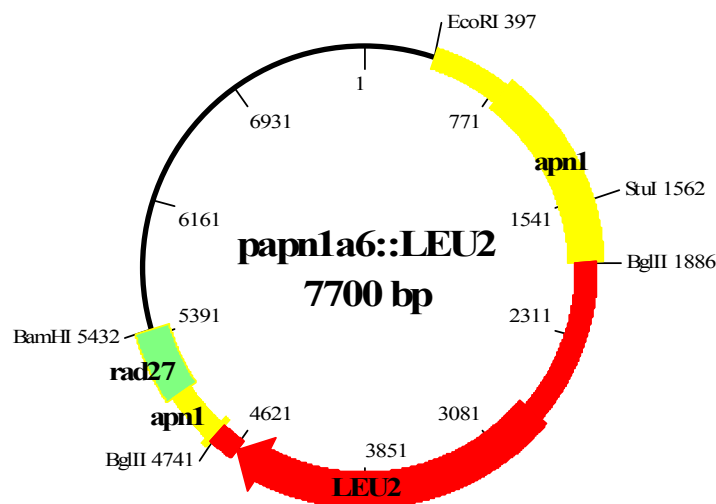


Figure 35: Plasmid *papn1a6::LEU2*. The *LEU2* gene from the plasmid pSM20 was inserted at the BglII cut site of the *apn1* fragment. This fragment was inserted previously at the BamHI/EcoRI cut sites of the pUC19.

4.2.1.2. Plasmid pGEM-T *ntg1::URA3*

The pGEM-T *ntg1::URA3* plasmid is a derivative of the pGEM-T plasmid (Promega). A PCR fragment of the *NTG1* gene was amplified using the primers “fw -225 NTG1” and “rev +254 NTG1” (approx. 1.6 kb). Then the PCR fragment was directly inserted at overhanging T ends of the pGEM-T plasmid producing the pGEM-T *ntg1* plasmid. After ampicillin selection the pGEM-T *ntg1* plasmid was identified by gel electrophoresis according to its size (approx. 4.6 kb). Subsequently a 3.2 kb BamHI-EcoRI *URA3* fragment (from pSM22, courtesy of David Schild, Berkeley) was inserted at the BglII-MunI cut sites creating the 7.1 kb pGEM-T *ntg1::URA3* plasmid. Finally an approx. 4 kb PCR fragment was amplified using the primers mentioned above and transfected in *MKP0 WT* and *rad5* strains. Strains were grown in medium lacking uracil and single clones were picked. The correct integration of the *URA3* fragment in the chromosome of the cells was checked by PCR analysis.

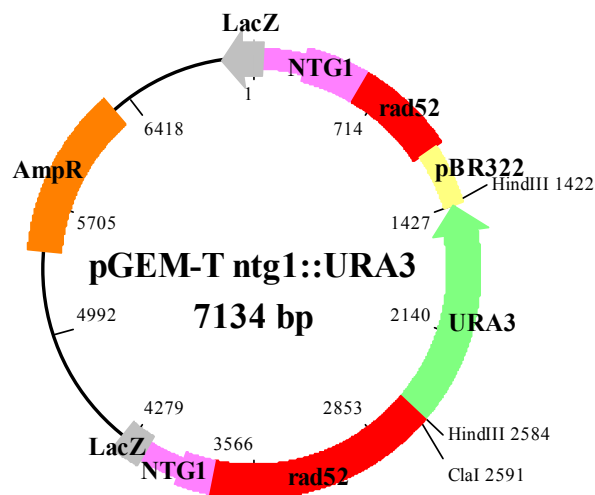


Figure 36: Plasmid pGEM-T *ntg1::URA3*. The BamHI/EcoRI *URA3* fragment from pSM22 was inserted at the BglII/MunI cut sites of the pGEM-T*ntg1* plasmid. The disrupted *LacZ* gene and the Amp^r marker are also shown.

4.2.1.3. Plasmid pGEM-T *ntg2::TRP1*

pGEM-T *ntg2::TRP1* is a derivative of the 3.0 kb pGEM-T plasmid (Promega). A PCR fragment of the *NTG2* gene was amplified from chromosomal DNA using the primers “fw - 474 NTG2” and “rev +237 NTG2” (approx. 1.9 kb). Then the PCR fragment was directly inserted at overhanging T ends of the pGEM-T producing the pGEM-T *ntg2* (4.9 kb) plasmid. After ampicillin selection the pGEM-T *ntg2* plasmid was identified by gel electrophoresis. Subsequently a 0.83 kb EcoRI-BglIII *TRP1* fragment (from pSM21, courtesy of David Schild, Berkeley) was inserted at the EcoRI-BglIII cut sites creating the 4.9 kb pGEM-T *ntg2::TRP1* plasmid. Then a 1.3 kbp fragment was isolated using the RE HincII/RsaI and transfected into MKP0 WT and *rad5* strains. Strains were grown in medium lacking tryptophan and single clones were picked. The correct integration of the *TRP1* fragment in the chromosome of the cells was checked by PCR analysis.

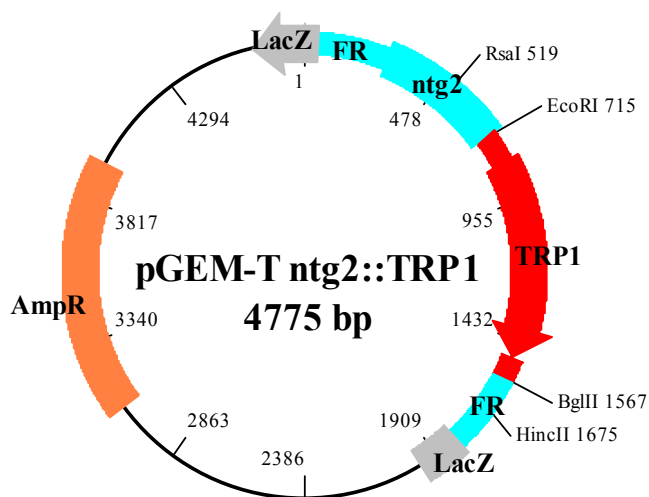


Figure 37: pGEM-T *ntg2::TRP1*. The EcoRI/BglIII *TRP1* fragment from the plasmid pSM2 was inserted in the plasmid pGEM-T *ntg2*. The disrupted *LacZ* gene and the Amp^r marker are also shown.

4.2.2. Survival capacity after gamma irradiation

To explain the gamma sensitivity of the *rad5* mutant in spite of its lack of important DSB repair deficiencies, gamma survival experiments have been carried out in a BER-deficient background with the *apn1ntg1ntg2* and *apn1ntg1ntg2rad5* multiple mutants. Hence, the repair of gamma-induced damage was studied by survival curves of cells in the logarithmic phase and compared with survival of cells in the stationary phase, which is used simultaneously as control for PFGE studies.

Logarithmic cells of BER deficient mutants do not show enhanced gamma sensitivity, behaving in a similar way as the WT. The survival capacity of the triple mutant *apn1ntg1ntg2* in comparison with the WT is similar after 100 Gy and even slightly higher after 500 Gy. Surprisingly, the *apn1ntg1ntg2rad5* quadruple mutant presents a 2-fold enhanced survival capacity as compared to the WT after 200 Gy. This contrasts with the 10.4 times lower survival capacity after 200 Gy of the *rad5* single mutant. Thus, there is a complete suppression of the *rad5* phenotype in the *apn1ntg1ntg2rad5* quadruple mutant (Figure 38).

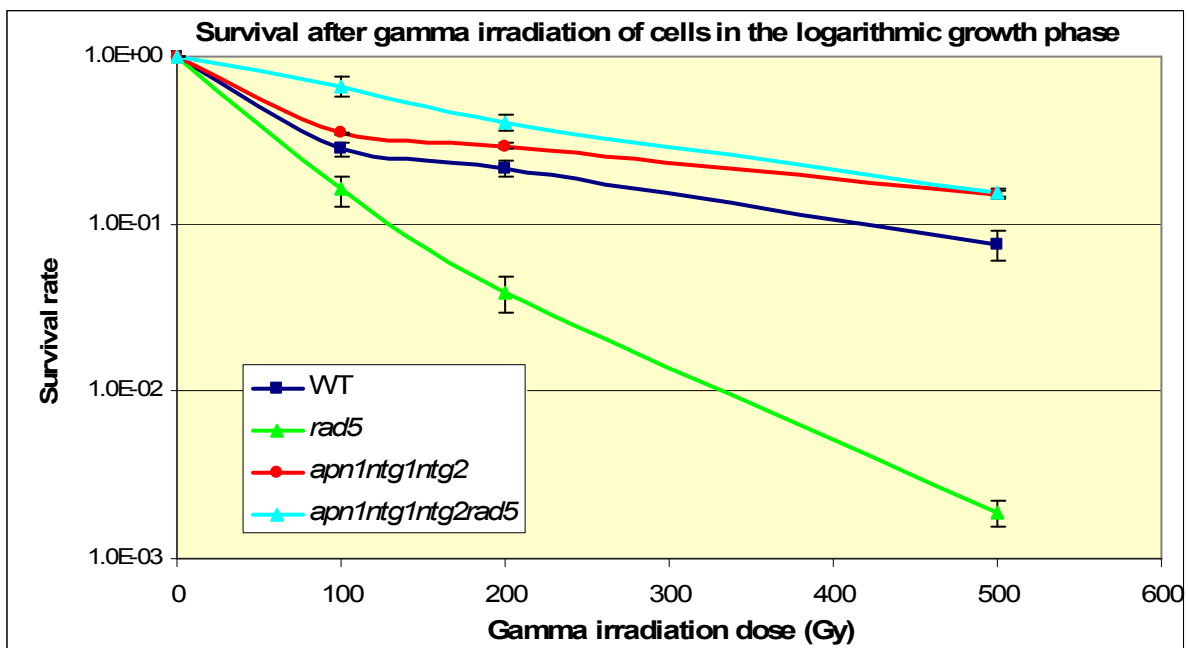


Figure 38: Gamma survival curve of BER deficient mutants. Data and standard deviations from two independent experiments are shown. The WT and the *rad5* mutant were used as controls in the two experiments. Gamma survival in cells in the logarithmic and stationary phase are shown in (Table 6).

Studies with cells in the **stationary phase** were performed as a control for PFGE experiments, but they also allow the study of a relation between *rad5* phenotype suppression and the growth phase (Table 6). Since cells in the stationary phase had been recollected from plates, whereas logarithmic cells were grown in fluid medium, parallel experiments were carried out with stationary cells from plates and fluid medium to be sure that possible differences depend on the growth phase but not on the cultivation conditions. A higher sensitivity in cells in the stationary phase in comparison to cells in the logarithmic phase was found in BER deficient mutants. This enhanced sensitivity was independent of the cultivation conditions.

Table 6 shows that after 100 Gy the sensitivity is 1.5 - 2.3 times higher in stationary cells than in logarithmic cells, whereas after 200 Gy the difference between stationary and logarithmic cells increases to 9 - 15 times, except in the *rad5* mutant, where stationary cells only show a 3 times higher sensitivity. After 500 Gy, WT and BER-deficient mutants present an even higher sensitivity in stationary cells, contrasting with the *rad5* mutant, where the sensitivity is similar.

Table 6: Gamma survival in cells in the logarithmic and stationary phase (%). Values indicate the survival capacity of *apn1ntg1ntg2* and *apn1ntg1ntg2rad5* mutants after different gamma doses in logarithmic (Log) and stationary cells from fluid medium (St-F) and from plates (St-P). Logarithmic values are displayed in Figure 38.

Strains	0 Gy	% Survival								
		100 Gy			200 Gy			500 Gy		
		Log	St-F	St-P	Log	St-F	St-P	Log	St-F	St-P
WT	100	28.01	12.18	13.65	21.36	1.7	2.31	7.59	0.57	0.2
<i>rad5</i>	100	16.07	11.4	7.6	3.9	1.43	1.41	0.19	0.12	0.11
<i>apn1ntg1ntg2</i>	100	34.71	21.03	19.36	29.3	3.19	2.18	14.85	0.07	0.16
<i>apn1ntg1ntg2rad5</i>	100	66.66	40.33	36.9	40.62	2.64	4.13	15.38	0.68	0.48

To summarise, the *rad5* phenotype suppression in the *apn1ntg1ntg2rad5* mutant indicates an interplay between Rad5 and BER proteins for the gamma-induced repair. Hence, the absence of BER mechanism seems to be advantageous for the *rad5* mutant. Whereas the moderate gamma sensitivity of the *rad5* mutant is nearly independent of the growth phase, *apn1ntg1ntg2* and *apn1ntg1ntg2rad5* mutants are more sensitive in stationary phase than in logarithmic phase. Finally, the growth conditions do not play a role in the sensitivity after gamma irradiation.

4.2.3. Repair at chromosomal level

To investigate whether the increased gamma survival of the BER-deficient mutants is due to an enhanced DSB repair, PFGE experiments were carried out for the the *apn1ntg1ntg2* and the *apn1ntg1ntg2rad5* mutants and compared to the results for the BER proficient strains (Figure 39).

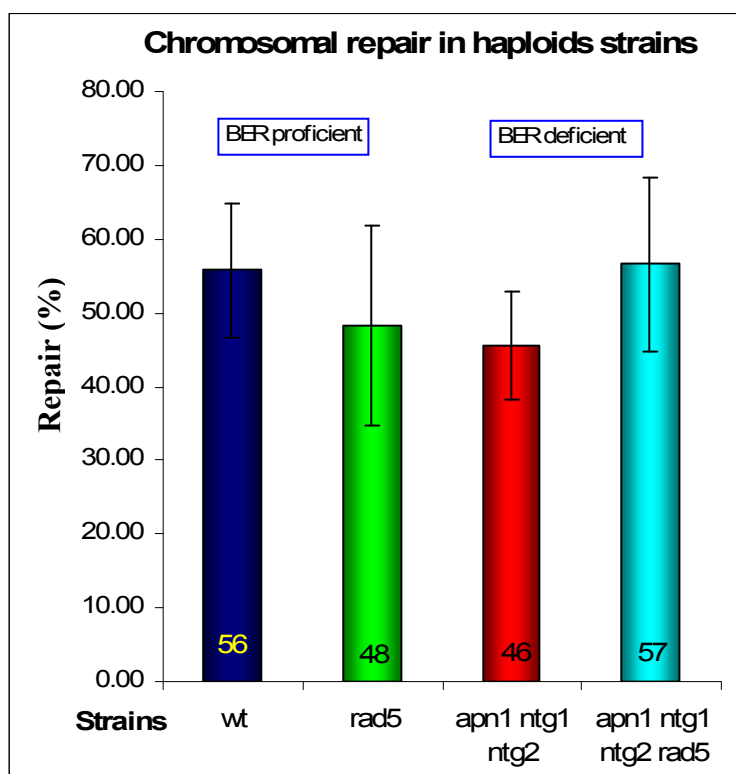


Figure 39: DSB repair capacity at chromosomal level in BER deficient mutants. After irradiation with 400 Gy, cells were incubated at 30° in LHR during 23h. Samples were taken previous to irradiation and after an incubation time to determine the percentage of the repaired DSB (see 4.1.3.4). The average of 2-3 experiments (10 in WT) and the corresponding standard deviations are shown.

Figure 38 shows that BER-proficient and the BER-deficient strains present comparable results for their DSB repair capacities, the *apn1ntg1ntg2* triple mutant even having a tendency towards lower values. The results indicate that the increased survival after gamma irradiation of the BER deficient mutants is not due to a more efficient DSB repair.

4.2.4. Survival capacity after UV irradiation

UV-induced lesions are mainly repaired by the nucleotide excision repair (NER) and by the post-replication repair (PRR) pathways. Little is known about a possible interplay between PRR proteins and BER proteins, which both repair small disturbances in the DNA structure, such as formamidopyrimidine or 8-oxo-guanin. Thus, the study of the UV-induced repair in BER deficient mutant lacking or presenting Rad5 can reveal possible interactions between proteins involved in BER and PRR. Hence, survival curves were carried out with *apn1ntg1ntg2* and *apn1ntg1ntg2rad5* with UV doses ranging from 0 - 80 J/m².

After 80 J/m² UV irradiation the BER deficient *apn1ntg1ntg2* and *apn1ntg1ntg2rad5* mutants have a slightly higher survival capacity than the WT, whereas the survival capacity of the *rad5* mutant is significantly reduced. As in the gamma survival experiments, the additional deletion of *APN1*, *NTG1* and *NTG2* in the *rad5* mutant completely suppresses the *rad5* phenotype in the *apn1ntg1ntg2rad5* mutant. Hence, these results indicate a minor role of BER in the repair of UV-induced damages and suggest an advantage for the *rad5* mutant concerning survival after UV irradiation when BER is inhibited.

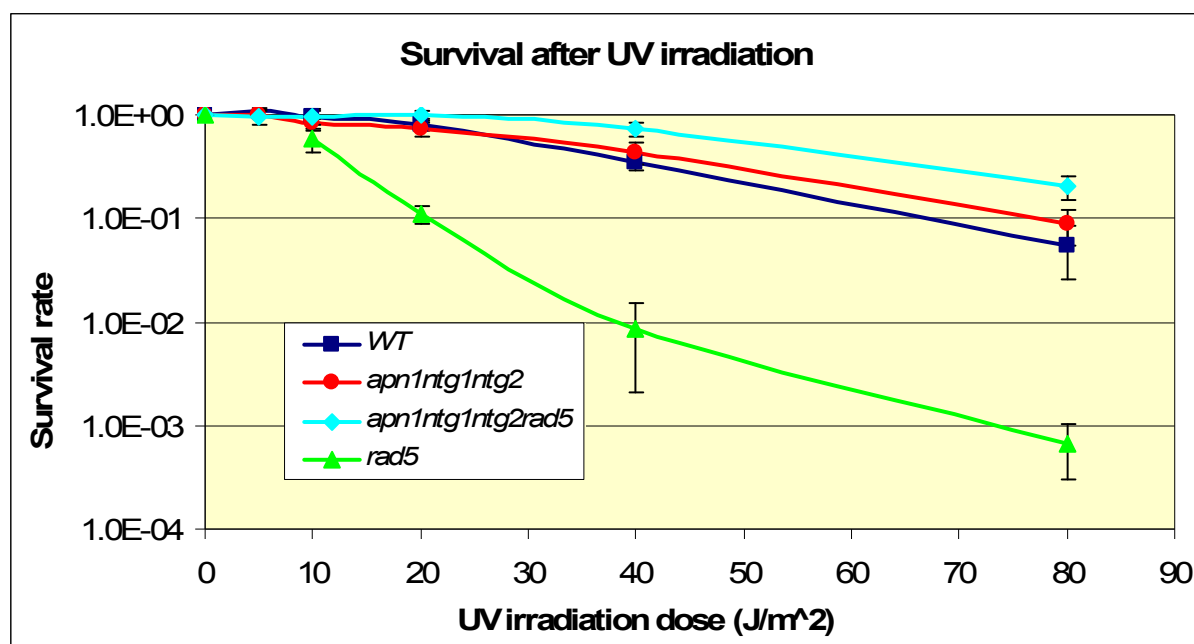


Figure 40: UV survival curves of the MKP0 WT, *rad5* and *apn1ntg1ntg2* and *apn1ntg1ntg2rad5* strains. Data and standard deviations from three to six independent experiments are shown.

4.2.5. UV-mutagenicity in BER mutants

To further characterize the interplay between Rad5 and BER deficient mutants, mutagenicity experiments were carried out (see 3.6). In these experiments, the reversion of a stop codon in the *lys2* gene of MKP0 strain derivatives was analysed. Colonies that have reverted this codon by a locus mutation present a red phenotype. The effect of *RAD5* deletion on the mutagenicity in a BER deficient background was studied with the *apnIntgIntg2* and *apnIntgIntg2rad5* mutants. Figure 41 shows the number of colonies with locus mutations per $2 \cdot 10^7$ cells plated.

Spontaneous mutagenicity:

In agreement with prior experiments (Schüller 1995), the MKP0 WT and *rad5* strains show a very low number of spontaneous locus mutations. In contrast, *apnIntgIntg2* and *apnIntgIntg2rad5* deficient mutants present 240 and 168 times more spontaneous locus mutations, indicating the necessity of the BER mechanism for the repair of damage arisen during metabolism.

UV-induced mutagenicity:

The WT and the *rad5* mutant present a similar number of induced locus mutations up to 10 J/m^2 (see Figure 41). At 20 J/m^2 and 40 J/m^2 the number of induced locus mutations of the WT in comparison with the *rad5* mutant is 3 times and even 17 times higher, respectively. The determination of the mutagenicity of the *rad5* mutant at higher doses was not possible due to its reduced UV survival capacity.

After irradiation with 5 J/m^2 the difference between BER mutants and the WT decreases strongly. After 10 J/m^2 BER mutants present only 2 times more locus mutations than the WT. However, from now on the behaviour of BER deficient mutants differs (Figure 41). The triple mutants present a similar number of locus mutations to the WT at 20 J/m^2 and 40 J/m^2 and even less mutations at 80 J/m^2 . In contrast, the quadruple mutant presents 3, 4 and 8 times more locus mutations than the WT at 20 J/m^2 , 40 J/m^2 and 80 J/m^2 respectively. Thus, in the *apnIntgIntg2* mutant the number of locus mutations in relation with the WT decreases with the dose, whereas it increases with the additional deletion of *RAD5*.

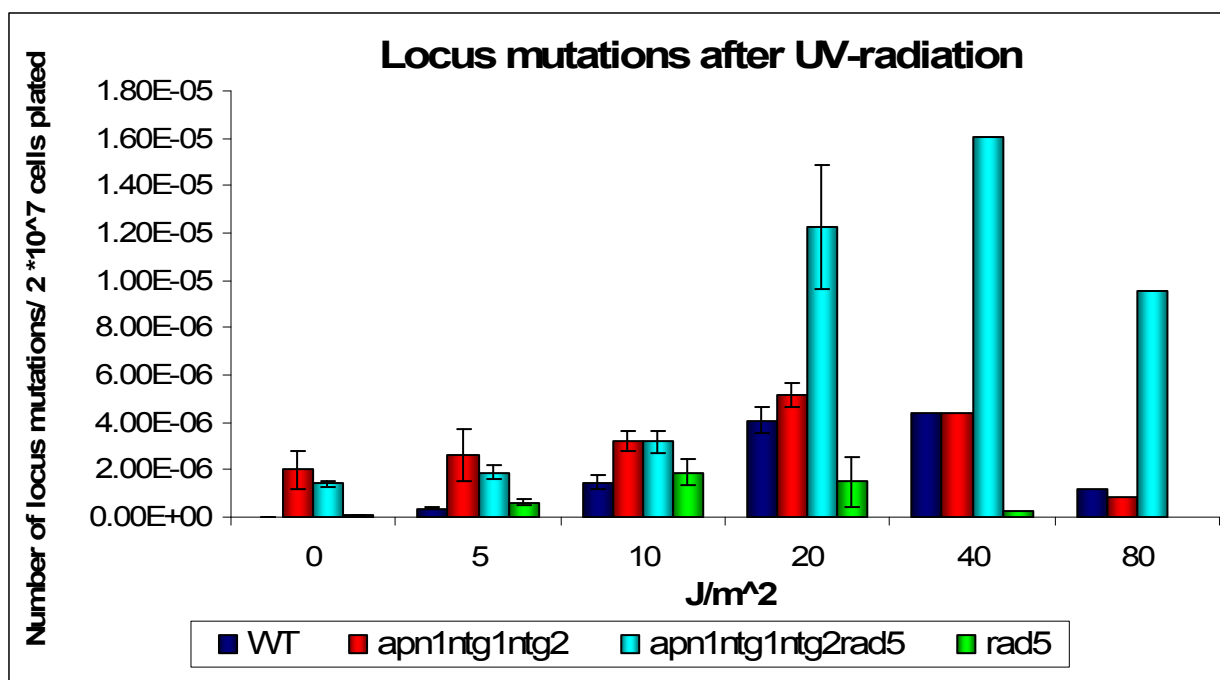


Figure 41: Number of locus mutations (*LYS*⁺) per $2 \cdot 10^7$ cells plated after different UV doses in WT *apn1ntg1ntg2*, *apn1ntg1ntg2rad5* and *rad5* strains. The average and standard error of at least three experiments is shown.

Since the survival capacity influences the absolute number of locus mutations, the mutation frequency after UV irradiation was calculated by correlating the number of locus mutations to the survival capacity of the strains (for further details see chapter 3.6). Results in Figure 42 show a linear increase of the mutation frequency with the UV dose in the WT, the *rad5* and *apn1ntg1ntg2rad5* strains. This relation between the mutation frequency and the UV dose is very similar in the *rad5* and *apn1ntg1ntg2rad5* mutants, indicating that the absence of Rad5 increases the mutation frequency independently of the BER proficiency. In contrast, the mutation frequency of the triple mutants shows a flattening at 40 J/m² and becomes 2.3 times lower than the mutation frequency of the WT at 80 J/m².

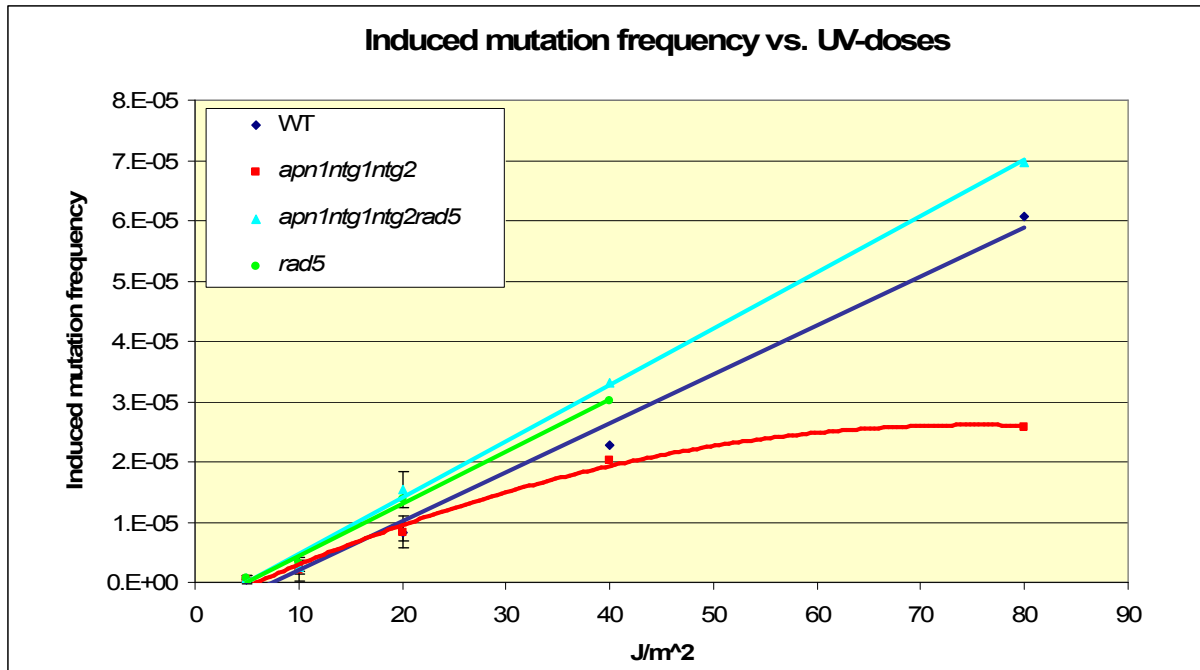


Figure 42: Relation between induced mutation frequency and UV-doses for the WT, *rad5*, *apn1ntg1ntg2* and *apn1ntg1ntg2rad5* strains. The average of at least three experiments is shown.

Taken together, the WT and the *rad5* mutant show a similar number of spontaneous locus mutations, while the elimination of the BER pathway increases the spontaneous mutagenicity. After UV irradiation, the triple mutant shows a reduced mutation frequency in comparison to WT. This phenotype is suppressed by the additional deletion of Rad5 in the *apn1ntg1ntg2rad5* mutant, which is in agreement with its high mutagenicity.

5. DISCUSSION

The main goal of this work was the study of the function of Rad5 for the repair of gamma induced lesions, since the *rad5* mutant presents a moderate sensitivity towards this agent. This gamma sensitivity has also been observed in other mutants deficient in the PRR, which is an important pathway for repair of UV-induced damages. Rad5 has also an influence in other repair pathways: it targets repair factors to minor groove adducts (Kiakos, Howard et al. 2002), which are usually repaired by NER. In addition, a regulatory role of Rad5 for the balance between HR and NHEJ has also been proposed (Ahne, Jha et al. 1997), possibly through its role in the ubiquitination (Simone Mörtl, forthcoming publication). However, there are no studies about the interaction of Rad5 with proteins of the BER, which is responsible for repair of base damage. Hence, this work focuses on the role of Rad5 for the repair of DSB, small deletions and base damage in a HR-, NHEJ- and BER- deficient background.

5.1. Role of Rad5 in the HR and NHEJ repair pathways

Cells have developed different mechanisms to repair DSB, of which the most relevant are HR and NHEJ. In *S. cerevisiae* DSB are mainly repaired by HR, which facilitates an efficient and accurate repair. NHEJ allows the direct rejoining of DNA ends usually in a homology-independent manner, although microhomologies presented in the broken DNA ends can facilitate this rejoining. Mutations can arise if wrong or modified DNA ends are rejoined. For a long time it has been thought that in *S. cerevisiae*, DSB repair occurs by NHEJ only when HR is suppressed. However, recent studies have suggested that the balance HR-NHEJ can depend on the ploidy type through Nej1 (Kegel, Sjostrand et al. 2001; Valencia, Bentele et al. 2001; Jazayeri and Jackson 2002; Wilson 2002), on the substrate (Frank-Vaillant and Marcand 2002), on the cell cycle (Takata, Sasaki et al. 1998; Karathanasis and Wilson 2002) or also on the action of proteins such as Cdk1 (Ira, Pellicoli et al. 2004) or Rad5 (Ahne, Jha et al. 1997).

In this work, survival curves after gamma and UV irradiation were used for the analysis of the putative interplay between Rad5 and proteins of the HR (Rad52) and NHEJ (yKu70) pathway. By PFGE experiments, the gamma induction of DSB and their repair after an incubation time was calculated. Finally, repair efficiency and accuracy of DSB repair pathways was studied in more detail by a plasmid assay.

5.1.1. Synergism between Rad5 and Rad52

The role of Rad5 for UV-induced damage repair (Xiao, Chow et al. 2000; Cejka, Vondrejs et al. 2001) was confirmed in UV survival experiments (Figure 20). The *rad5* mutant presents a significantly higher UV sensitivity than the WT, explained by the role of Rad5 in PRR. On the contrary, survival of the *rad52* mutant decreases only slightly, indicating a minor role of Rad52 for UV damage repair. However, there was an increase of the UV sensitivity in the *rad5* mutant after the additional deletion of *RAD52*. The enhanced UV sensitivity of the double mutant indicates that the Rad52 and Rad5 proteins act in different pathways for UV damage repair.

This interplay was also studied for the repair of gamma-induced damage. Therefore, survival curves in different growth stages were carried out after gamma irradiation in mutants deficient for HR (Figure 18 and Figure 19). Survival curves of logarithmically growing *rad52* mutants show high gamma sensitivity due to their inability to repair DSB by HR. Furthermore, the *rad5* mutant, which is HR proficient, presents moderate gamma sensitivity in comparison to other HR proficient strains. The gamma sensitivity increases significantly with the additional *RAD52* deletion. This synergistic effect after deletion of both *RAD5* and *RAD52* was observed in survival curves of cells of logarithmic and stationary growth phase, and it indicates the involvement of Rad5 in a different repair pathway than Rad52 competing for the same damage. This enhanced sensitivity is also present in other PRR-deficient mutants such as *rad6* and *rad18* (Broomfield, Hryciw et al. 2001). Moreover, a similar synergistic effect was found in *rad52rad18* and *rad52rad6* double mutants (Game 2000), indicating a role of Rad5 and other Rad6 members for the repair of gamma damage, which is independent from repair by HR.

Gamma irradiation produces a variety of DNA damages, such as base damages, SSB, DSB, and MDS. If they remain unrepaired, all damages can contribute to the reduced survival capacity of irradiated cells. DSB are usually analysed by PFGE (Geigl and Eckardt-Schupp 1991; Friedl, Beisker et al. 1993; Dardalhon, Nohturfft et al. 1994; Lobrich, Ikpeme et al. 1994; Longo, Nevaldine et al. 1997). In this work, PFGE was carried out to study the role of Rad5 in comparison to the other genes of interest in the repair of DSB (Figure 28). These chromosomal repair experiments have revealed that the *rad5* mutant presents a similar DSB repair capacity (48 %) in comparison with the WT (56 %). The *rad52* mutant repairs only 16% of the DSB. An additional deletion of *RAD5* in the *rad52rad5* double mutant reduces the repair capacity by a factor of 2. This indicates a role of Rad5 for the remaining DSB repair capacity of the HR-deficient *rad52* mutant.

To further study this role, the efficiency and accuracy of gap repair events were studied by a plasmid assay (Jha, Ahne et al. 1993; Ahne, Jha et al. 1997). The *rad5* mutant was HR proficient but repaired 85% by NHEJ, which agrees with the 70%- 80% found for a *rad5* interruption mutant (Ahne, Jha et al. 1997). The *rad5* mutant presented a high efficiency for the repair of plasmidial gaps, which cannot be exclusively explained by the 15% of repair by HR, indicating that NHEJ is very efficient for rejoining of DSB.

This high efficiency of the *rad5* mutant contrasts with the low efficiency of the *rad52* mutant, which also repairs DSB by rejoining mechanisms. This difference could be explained by different types of rejoining mechanisms in the *rad5* and the *rad52* mutants. Hence, Daley et al. has recently proposed that DSB can be rejoined by NHEJ, by a Rad52-dependent SSA-like pathway and by a mechanism that is independent of NHEJ proteins and Rad52 but depending on the length of the overhanging end (Daley and Wilson 2005).

Results of the plasmid assay and sequencing analysis show that in the *rad52* mutant, 75 % of the repaired plasmids present large deletions up to a microhomology, revealing a joining mechanism different from the NHEJ used by the *rad5* mutant, where such deletions have not occurred. This effect has been previously observed (Boulton and Jackson 1996; Ma, Kim et al. 2003) and is usually called microhomology mediated end joining (MMEJ). The degradation of DNA ends can be responsible for the decrease of the repair efficiency in the *rad52* mutant and it also indicates a role of Rad52 for the protection of DNA ends, which could be due to a DNA-end-binding function (Van Dyck, Stasiak et al. 1999; Stasiak, Larquet et al. 2000).

All these microhomology-mediated events showed the same DNA end degradation up to a 5 bp long microhomology to the NcoI site localized 184bp downstream of the ApaI site. The absence of other microhomology end-joining products can only be explained if the overhanging ends are protected. Moreover, no end degradation of the NcoI overhanging end - and therefore no ApaI site microhomology-mediated end joining - was observed. The lack of rejoining products by microhomology with the ApaI overhanging end could be explained by a protective function of Rad52 limited to the 3' overhanging end, which is supported by the activity of Rad52 and Rad59 for the annealing of 3' nucleofilament for SSA (Ivanov, Sugawara et al. 1996; Shinohara, Shinohara et al. 1998; Sugawara, Ira et al. 2000). Furthermore, the recombination roles of Rad52 involve only 3' overhangs (Prado, Cortes-Ledesma et al. 2003). Another possibility would be the lack of a homology with the ApaI site in the sequence upstream of the NcoI site. In this case, the NcoI end could be degraded but in the absence of an ApaI microhomology, no end-joining could take place.

The kind of protruding ends, 3' or 5', might in general play a role for end degradation. Hence, recent experiments in the *rad52* mutant have described a microhomology-dependent degradation of non complementary DNA ends, where both of the degraded ends were 3' overhangs (Ma, Kim et al. 2003). This rejoining results in deletions of up to 302 bp followed by annealing by means of different imperfect microhomologies of about 8-10 bp (Ma, Kim et al. 2003). This kind of rejoining is dependent on Mre11, Rad50 and Rad1, and is still active after *YKU70* and *RAD52* deletion. Ku- and Rad52- independent end joining has also been described in other studies (Wang, Perrault et al. 2003; Yu and Gabriel 2003).

The additional *RAD5* deletion in the *rad52* mutant reduces the repair efficiency and also the repair accuracy of gapped plasmids. Hardly any transformant could be recovered. From 10 transformants only 3 showed fragments after PCR, which is an indication of severe degradation. Two of the plasmids, which could be analysed by PCR with primers localized approx. 460 - 430 bp from the gapped region and sequenced successfully, were repaired by microhomology mediated end joining. A third fragment was only visible after PCR with primers localized approx. 520 bp upstream and 2000 bp downstream of the gapped region; in this case sequence analysis was not possible. If in these mutants the lack of Rad5 promotes repair of DSB by NHEJ, the lack of Rad52 impedes the protection of the DNA ends and probably leads repair to MMEJ. Hence, DNA ends are massively degraded in absence of both, Rad5 and Rad52, explaining the low efficiency as well as the low accuracy presented in the *rad52rad5* double mutant. Moreover, this massive degradation due to the additional Rad5 deletion in *rad52* mutants could indicate a role for Rad5 in end protection.

Altogether, results in all assays reveal a synergistic effect in the *rad52rad5* mutant as compared to the *rad5* and *rad52* single mutants. This effect could indicate a common role for both Rad5 and Rad52 in the repair of gap and DSB, since one of them can compensate the loss of the other, but when both are missing the double mutant shows a severe effect. Comparison of plasmids repaired by the *rad52* and *rad5* mutants indicates that this compensatory function could be end protection and that loss of Rad5 and Rad52 could trigger different end joining mechanisms; the *rad52* mutant could repair by MMEJ and the *rad5* mutant by NHEJ. However it is not clear if this is due to different types of NHEJ or due to differences in DNA end degradation.

5.1.2. *rad5* phenotype suppression in NHEJ deficient mutants

Survival experiments after gamma irradiation show similar sensitivities of *yku70* and WT strains, the sensitivity of the *yku70* mutant in the logarithmic phase even being 10 % lower than the sensitivity of the WT. A similar positive effect for cell survival due to *YKU70* deletion was observed in haploid strains for the repair of a single HO nuclease-induced DSB (Clikeman, Khalsa et al. 2001). This has been explained either by competition for DSB between HR and NHEJ or by interferences of yKu70 with HR, in which yKu70 would block a certain amount of DNA ends from HR, which are then repaired by NHEJ.

YKU70 deletion suppresses the moderate gamma sensitivity of the *rad5* mutant (Figure 18) in the *yku70rad5* double mutant in the logarithmic phase. That could be explained taking into consideration the regulatory role of Rad5, which promotes DSB by HR. *rad5* mutants repair DSB mostly by inaccurate NHEJ, which had already been observed in a *rad5* interruption mutant (75% NHEJ, Ahne, Jha et al. 1997). This reduces its survival capacity after gamma irradiation. In the *yku70rad5* mutant, NHEJ is eliminated due to *YKU70* deletion and therefore, they must repair DSB by accurate HR, which increases the survival capacity of this mutant to a WT level.

This suppression is not as pronounced in cells in the stationary phase (Figure 19) as in the logarithmic phase. The sensitivities of the *yku70* and *yku70rad5* mutants strongly increase in the stationary phase in comparison to the logarithmic phase, whereas the sensitivity of the *rad5* mutant remains almost the same. The higher sensitivity of the strains that repair DSB by HR is due to the absence of sister chromatids in the stationary phase (see chapter 5.1.3), having only a small influence in the *rad5* mutant, which mainly repairs by NHEJ (Ahne, Jha et al. 1997). Since in PFGE experiments cells are in high stationary growth phase, this would also explain that the DSB repair efficiency of the *rad5* mutant is comparable to the efficiency of the WT, *yku70* and *yku70rad5* strains (Figure 28). Due to this high DSB repair capacity of the *rad5* mutant in PFGE experiments, it is not possible to confirm the *rad5* phenotype suppression in the *yku70rad5* mutant.

To confirm the repair pathways used by the *yku70*, *rad5* and *yku70rad5* mutants, plasmids assays would be necessary. However, plasmid assays in high stationary cells have not been successful till now. This can be a consequence of the higher resistance of the cell wall in this growth phase, which impedes the transfection of plasmids. Plasmid assay experiments with cells in the logarithmic phase show that the *yku70rad5* mutant repairs mainly by HR, explaining the suppression of the *rad5* phenotype in this mutant (Figure 32).

Results on the efficiency of plasmid gap repair show that the *rad5* cells present a high effectiveness of rejoining, indicating that NHEJ can be very effective (Ahne, Jha et al. 1997). This high efficiency of NHEJ has been previously shown for repair of intact ends that present 4 nt complementary overhanging ends (Frank-Vaillant and Marcand 2002) and for 3' cohesive overhanging ends in Ku80 deficient cells (Feldmann, Schmiemann et al. 2000). In this work a high efficiency for end joining was found, even though the DNA ends to be rejoined were non-cohesive. Surprisingly, the HR proficient *yku70rad5* double mutant shows a rather low efficiency for plasmid gap repair (Figure 29). This could be explained by the disturbance of the balance between DSB repair pathways in favour of NHEJ in cells lacking Rad5 (Ahne, Jha et al. 1997); the impossibility to repair by this way in the *yku70rad5* mutant induces the “redirection” of repair to HR (Figure 32). Thus, although HR is the final repair pathway, it was also the second choice for repair; the loss of decisive time during this redirection process could be the reason of the reduction in repair efficiency in the *yku70rad5* mutant.

The *rad5* mutant shows a strong decrease in gap repair accuracy in comparison with WT, *yku70* and *yku70rad5* strains, which repair almost exclusively by accurate HR. This decrease might be due to the predominant use of NHEJ by the *rad5* mutant for the repair of gaps (Figure 32). This confirms, first, the correctness of HR in general, and second, the minor role of *YKU70* for the accuracy of DSB repair in a HR proficient background. In the *yku70rad5* mutant, the possible “redirection” of the repair does not affect its accuracy.

Further studies were carried out by sequencing plasmids that were incorrectly repaired (*ura-*) by the *yku70* and *yku70rad5* mutants (Figure 32, Figure 33 and Figure 34). 91% and 95% of the *ura-* plasmids from the *yku70rad5* and *yku70* mutants, respectively (100% from WT) were repaired by error-prone HR. Sequence analysis of the 11 recovered *ura-* plasmids from *yku70* and 13 from *yku70rad5* strains reveal only minor differences between these

mutants, confirming the *rad5* phenotype suppression also for error-prone HR events. The induced point mutations were distributed inside and outside of the repaired gap region; additions were the most widespread mutation (Figure 33-left and Figure 34), deletions were concentrated at the restriction site and transversions outside of the repaired gap region.

Accurate end joining was observed in one clone out of 2 of the *yku70rad5* mutant, the recovered plasmid having been repaired by direct end joining without any end processing. The influence of Ku in accurate rejoining has been discussed controversially in *xrs6* cells: whereas Kabotyanski found no influence in the accuracy (Kabotyanski, Gomelsky et al. 1998), Feldman indicated a reduction in absence of Ku80 depending on the type of ends being joined (Feldmann, Schmiemann et al. 2000). Feldmann has shown that the accuracy of non-cohesive ends 5'/3' is completely reduced in *xrs6* mutants due to nucleotide deletions at DSB ends. In this work, MMEJ was observed in one clone from the *yku70* and one from the *yku70rad5* strains (Table 4).

In summary, a suppression of the *rad5* phenotype in the *yku70rad5* mutant was found in survival experiments with cells in the logarithmic and stationary growth phase. Plasmid assays revealed that the *yku70rad5* mutant repairs plasmidial gaps by HR. This means that the deletion of *YKU70* in the *rad5* mutant leads to repair by HR in cells that would otherwise repair 75 % by NHEJ, confirming the regulatory role of the Rad5 protein.

5.1.3. Gamma-induced repair depends on the growth phase

After gamma irradiation, cells have to repair the induced damage, especially DSB in order to survive. The survival capacity depends on the efficiency and accuracy to repair DSB, which also depends on the repair pathways used. During HR damages are repaired using homologous templates from sister chromatids (Gonzalez-Barrera, Cortes-Ledesma et al. 2003), from homologous chromosomes (Palmer, Schildkraut et al. 2003) or from homologous sequences anywhere in the genome (Inbar and Kupiec 1999; Aylon, Liefshitz et al. 2003). The search for homology implicates more complexity in the repair process but also more accuracy. In NHEJ the DNA ends are directly rejoined (Critchlow and Jackson 1998), simplifying the process but increasing the mutability if the DNA ends are degraded or “false” ends are rejoined.

In this work, survival after gamma irradiation differed depending on the cell growth phase, confirming previous studies (Karathanasis and Wilson 2002). In stationary growth phase (G1/G0), WT and the HR proficient mutants *yku70* and *yku70rad5* are more gamma sensitive than cells in the logarithmic phase, when sister chromatids are available for repair by HR. The lack of sister chromatids in stationary phase could force cells to repair by ectopic recombination, which may lead to chromosomal rearrangements, reducing the survival capacity (Inbar and Kupiec 1999; Aylon, Liefshitz et al. 2003). Another possible explanation could be a dependence of the DSB repair pathway on the growth phase, which was previously observed in the chicken B-cell line DT40 (Takata, Sasaki et al. 1998). Thus, the increased gamma sensitivity in stationary phase could be due to a promotion of NHEJ (Karathanasis and Wilson 2002). NHEJ is very effective and correct if the DNA ends to be joined are intact, but NHEJ becomes mutagenic if the DNA ends are degraded. Therefore, the use of NHEJ for gamma-induced DSB repair implies an increase in the mutation rate, since gamma-induced DSB normally present modifications such as base or nucleotid losses.

In logarithmic growth phase, cells in G1, S, G2, and mitosis are present simultaneously if they are not synchronised. This explains the high survival capacity of cells in logarithmic growth phase of the HR proficient strains WT, *yku70* and *yku70rad5* (Figure 18), since cells in G2 phase possess two sister chromatids and consequently, they can repair DSB by effective and accurate HR. The use of HR during the logarithmic phase in WT, *yku70* and *yku70rad5* was confirmed in plasmid assays (Figure 32).

In contrast, cells of the HR deficient *rad52*, *rad52rad5* and *yku70rad52* mutants present a relative high survival capacity in the stationary growth phase in comparison with the low one of the logarithmic growth phase (Figure 19). Since these mutants can not repair by HR, cell survival depends on end joining events. Cells in stationary growth phase are almost metabolically inactive, showing no (or little) DNA synthesis and as compared to dividing cells, a reduced number of endogenous DSB. It has been estimated that up to 10 DSB are generated in human cells during each cell cycle, especially during replication of DNA (S phase) caused by frequent stallings of the replication fork (Haber 1999; Franchitto 2002). That leads to a lower number of endogenous DSB in cells in the stationary phase in comparison to cells in the logarithmic phase and therefore to a better survival in spite of the inaccuracy of NHEJ. This is in accordance with studies of Karathanasis (Karathanasis and

Wilson 2002), who showed that stationary *rad52* mutants became resistant against ionizing radiation with increasing of culture density, due to a promotion of NHEJ as the cultures aged.

In logarithmic phase the higher cellular activity of cells implies a higher number of endogenous DSB. If cells are not capable to repair the high number of DSB, unrepaired lesions can block the replication process, arresting cells in G2 phase and impeding mitosis and colony formation. The use of NHEJ or another end joining mechanism during logarithmic growth phase has been confirmed in the *rad52* and the *rad52rad5* mutants in plasmid assay experiments (Figure 32).

The *rad5* mutant shows moderate gamma sensitivity, which is very similar during the logarithmic and stationary growth phase. This sensitivity indicates some role of Rad5 for gamma-induced damage repair that is independent of the growth phase. As plasmid assay data have shown, the *rad5* mutant repairs 75% of the gaps by NHEJ (Ahne, Jha et al. 1997). Thus, the moderate sensitivity in logarithmic cells can be explained since the *rad5* mutant does not entirely profit from the existence of sister chromatids for HR, unlike the WT, *yku70* and *yku70rad5* strains. The remaining 25% repair by HR bestows the *rad5* mutant a higher survival than the *rad52* mutant, which can not carry out HR. In the stationary growth phase, the sensitivity of the *rad5* mutant does not increase, unlike the sensitivity of the strains repairing by HR.

5.2. Role of yKu70 for DSB repair in a HR deficient background

In this work, survival experiments after gamma irradiation show similar sensitivities of *yku70* and WT strains in both stationary and logarithmic phase; the *yku70* mutant in the logarithmic phase exhibits even 10 % lower sensitivity than the WT. This minor role of yKu70 for gamma-induced repair in a HR proficient background has been previously described (Boulton and Jackson 1996; Siede, Friedl et al. 1996) and contrasts with the sensitivity to ionizing radiation presented in the human homologs *ku70* mutants (Koike 2002). In addition, PFGE studies presented in this work show a similar DSB repair capacity in *yku70* and WT strains, which confirms previous results (Fellerhoff 1999).

The additional deletion of *YKU70* decreases the DSB repair capacity of the *rad52* mutant by a factor of 2 in PFGE experiments (Figure 28). However, no severe degradation/accumulation of small fragments was observed in the *yku70rad52* mutant, which is in contrast with previous studies using haploid yeast strains with a different genetic background (Fellerhoff 1999). Furthermore, plasmid assays corroborate the importance of *YKU70* in a HR deficient background. The *rad52* mutant, which already shows a 45-fold lower repair efficiency than the WT, was nearly unable to repair gapped plasmids when additionally *YKU70* was deleted. These results confirm the idea that *YKU70* is required for the recircularization of gapped plasmids in a HR deficient background (Boulton and Jackson 1996). Hardly any repaired plasmids from the *yku70rad52* mutant could be recovered and none of the recovered plasmids was repaired correctly. Analysis by PCR of any of the recovered plasmids was not possible, which indicates large degradations of the DNA ends.

The decrease in the DSB and gap repair capacity of the *rad52* mutant after the additional *YKU70* deletion can be explained by the simultaneous loss of HR and Ku-dependent end joining (Yu and Gabriel 2003). This reduced repair capacity for gamma-induced DSB and gaps induced by restriction enzymes contrasts with the survival experiments after gamma irradiation. Hence, neither in logarithmic nor in stationary growth phase, a further decrease of the survival capacity of the *yku70rad52* mutant as compared to the *rad52* mutant was found, which is not in agreement with previous studies (Boulton and Jackson 1996; Mages, Feldmann et al. 1996; Siede, Friedl et al. 1996).

However, these studies have been carried out with strains with a different genetic background, such as the cryptic *rad5* mutation found in the W303 strains, which were used in studies by Boulton and Mages (Clikeman, Khalsa et al. 2001). In summary, *yku70* plays an essential role for DSB repair and plasmid recircularization in a HR-deficient background. This role, however, seems not to be decisive for survival after gamma irradiation.

5.3. Haploid strains can repair DSB in high stationary phase

For a long time, it had been assumed that haploid cells were unable to repair induced DSB in stationary phase due to the lack of sister chromatids and homologous chromosomes. So far, DSB quantification was carried out in diploid yeast cells (Geigl and Eckardt-Schupp 1991; Friedl, Beisker et al. 1993; Dardalhon, Nohturfft et al. 1994; Friedl, Kraxenberger et al. 1995; Moore, McKoy et al. 2000) or mammalian cells (Whitaker, Ung et al. 1995; Longo, Nevaldine et al. 1997; Ozawa, Wang et al. 1999; McMillan, Tobi et al. 2001). Then, the discovery of Ku70 in yeast suggested the possibility of end joining repair, which had to be visible in G0 cells. Studies by Fellerhoff in this stage have shown repair in the haploid WT, *yku70* and *rad52* strains (Fellerhoff 1999), contrasting with previous studies, where no DSB repair was found in this growth phase (Geigl and Eckardt-Schupp 1991). In this work, it could be shown that even in stationary phase HR is still the predominant DSB repair pathway in haploid yeast cells. For this purpose, the repair capacity of a strain was determined after an incubation time in LHR buffer. Buffer holding suppresses growth but allows repair events, and therefore it has been used for analysis of cell recovery and DSB repair (Fellerhoff 1999).

DNA was extracted before and after gamma irradiation and additional incubation in LHR buffer, and it was prepared for PFGE using a previously described protocol, which avoids any kind of DNA degradation (Friedl, Kraxenberger et al. 1995). Then, PFGE gels were evaluated by scanning and DSB were calculated by PULSE (Friedl, Beisker et al. 1993), which was developed for the determination of DSB. PULSE determinates DNA mass distributions using a model for the spatial distribution of DSB and random values for the DSB frequency per unit length. The mass distributions calculated for the random values are compared with the observed mass distributions and the deviations between both of them are minimized in order to obtain the best fit, which allows the determination of the DSB frequency. However, PULSE was not sufficiently sensitive to deliver reproducible data for most of the haploid strains studied in this work. Moreover, compatibility problems occurred between the hardware required (PC 486) and the technologies nowadays available.

Therefore, it was necessary to develop new software. Geltool is a user friendly software written in Delphi (Borland). Delphi was chosen as computer language because it presents two fundamental advantages. First, Delphi is easier to learn and to manage than other languages such as c++, thus, software can be written in a short time. Second, the compilation in Delphi is very quick in contrast to other easy languages as Visual Basic, saving time during the program developing. Furthermore, Geltool can process data delivered by common Gel documentation systems such as the “Gel 2000 device” manufactured by BioRad and, the evaluation method proposed in this work can save the high costs that are involved in the adquisition of expensive gel documentation system and software specialized in densitometry evaluation.

Geltool calculates the chromosomal fragmentation by the establishment of a degradation profile measured in pixels. The linearity between chromosomal fragmentation and dose was confirmed up to doses of 1000 Gy (Figure 25). The correlation of Geltool with PULSE allows the degradation profile to be related to the number of DSB/Mbp (Figure 27). For instance, Geltool has calculated 10.16 DSB/genome after 400 Gy irradiation in air, which is equivalent to $1.84 \text{ DSB} \cdot 10^{-9} \text{ bp} \cdot \text{Gy}$. This correlates well with previous results, when the irradiation conditions are also considered (see Table 3): samples gassed with oxygen, which can produce DSB due to the generation of reactive oxygen species (ROS), present 18.5 DSB/genome after 400 Gy or $3.35 \text{ DSB} \cdot 10^{-9} \text{ bp} \cdot \text{Gy}$ (Fellerhoff 1999), whereas samples gassed with nitrogen present 5.14 DSB/genome after 400Gy or $0.93 \text{ DSB} \cdot 10^{-9} \text{ bp} \cdot \text{Gy}$ (Friedl, Beisker et al. 1993).

PFGE experiments in this work were performed in haploid cells in the stationary phase according to the LHR procedure of Fellerhoff, which avoids any influence of replicating cells in the results. If cells are kept in LHR buffer for 23h, DSB repair of 57 – 46 % occurs in the HR proficient strains WT, *yku70*, *rad5*, *yku70rad5*, *apn1ntg1ntg2* and *apn1ntg1ntg2rad5* strains, whereas in the HR deficient *rad52*, *yku70rad52* and *rad52rad5* strains only 16 – 6 % of the DSB were repaired. This indicates that in the absence of sister chromatids, DSB can be repaired by allelic or ectopic recombination. The lower survival capacity of HR proficient cells in the stationary phase could be explained if, in the absence of sister chromatids, HR repairs in an error-prone manner in spite of its effectiveness.

The use of NHEJ, facilitated by the upregulation of NHEJ in haploids cells by Nej1 (Astrom, Okamura et al. 1999; Valencia, Bentele et al. 2001) and during stationary phase, (Karathanasis and Wilson 2002) could explain the residual repair in the HR deficient strains. The lower repair of the *yku70rad52* mutant in comparison to the *rad52* mutant is explained by the additional suppression of the *yku70*-dependent NHEJ.

These results in principle confirm previous studies of Fellerhoff suggesting repair in haploid yeast strains during stationary phase. However, Fellerhoff found a lower repair capacity in the HR-proficient WT and *yku70* strains of 33-30 % and a higher capacity in the HR-deficient *rad52* strain of 26 % in comparison to the repair capacities showed in this work (Fellerhoff 1999). Moreover, Fellerhoff found a strong DNA degradation after gamma irradiation in the *yku70rad52* double mutant, which was not found in the *yku70rad52* strain used in this work. The different genetic backgrounds of the strains could explain this discrepancy. Another possibility could be the different conditions during irradiation; whereas in studies of Fellerhoff cells were irradiated with 300 Gy in a saturated oxygen atmosphere, in this work cells were irradiated with 400 Gy in air (normal atmosphere composed of oxygen and nitrogen).

Altogether, these results confirm the applicability of Geltool for the sensitive quantification of DSB in haploid cells. This new tool has been used to unequivocally confirm the occurrence of DSB repair in haploid yeast cells in stationary phase (<3 % residual budding). The HR proficient strains can repair up to 56 % of the gamma-induced-DSB in the absence of sister chromatids. Wildtype yeast of different genetic backgrounds, mutants constructed according to different procedures and different irradiation conditions deliver in principle similar results.

5.4. Role of Rad5 in the BER repair

Reactive oxygen species can be generated during cellular metabolism or can be induced through the action of chemicals such as H₂O₂ or UV and gamma radiation, generating base damages. By impeding correct base pairing, base damages can affect replication and transcription. The main pathway to repair these lesions is the BER pathway. However, the overlapping of different repair pathways such as NER, BER, PRR and even HR for the repair of base damage has been proposed (Swanson, Morey et al. 1999). Moreover, repair of base damage generates AP sites, which can also arise spontaneously. These AP sites can either be repaired by the BER or NER pathways, be tolerated through Translesion Synthesis repair (TLS) or recombination or even remain unrepaired and generate SSB and even DSB (Boiteux and Guillet 2004).

In this work, the role of Rad5 has been studied in a BER deficient background through the generation of the *apn1ntg1ntg2* and *apn1ntg1ntg2rad5* mutants. The deletion of *NTG1*, *NTG2* and *APN1* impedes repair by BER in different steps and in a redundant manner (Figure 2). First, the elimination of Ntg1 and Ntg2 N-glycosylases prevents the repair of a wide spectrum of base damages and therefore the subsequent formation of AP sites necessary for the BER process. Second, if residual AP sites are present, the *APN1* deletion suppresses 97% of the AP-endonuclease and 3' phosphodiesterase activity involved in the repair of AP sites by 5' cleavage (Boiteux and Guillet 2004). Third, the repair of AP sites by 3' side cleavage is also impeded through *NTG1* and *NTG2* deletion and the suppression of the following step by the *Apn1* deletion. Other proteins involved in BER present only a residual activity. That is the case for *Apn2*, which presents only 3 % of the AP-endonuclease and 3' phosphodiesterase activity, and for *Ogg1*, a N-glycosylase specific for the repair of FapyG and 8-oxoG. FapyG can also be repaired by Ntg1 and Ntg2, whereas 8-oxoG can be repaired by Ntg1 when it is mispaired with a guanine (Senturker, Auffret van der Kemp et al. 1998; Gellon, Barbey et al. 2001) and even by *Apn1*, as recent studies have suggested (Ishchenko, Yang et al. 2005). Furthermore, in contrast to Ntg1 and Ntg2, *Ogg1* can only excise AP sites opposite to cytosine. Taken together, only a minimal BER residual activity can be possible in mutants lacking *Apn1*, *Ntg1* and *Ntg2*.

5.4.1. Suppression of *rad5* phenotype in BER deficient mutants for repair of gamma-induced damage

The most serious lesions after gamma irradiation are DSB (single or associated with other lesions). These lesions are mainly repaired through HR and NHEJ, whose balance is influenced by Rad5 (Ahne, Jha et al. 1997). Gamma irradiation can also cause base damages, which are predominantly repaired by BER. To study the role of Rad5 in the repair of these damages, the interplay between Rad5 and BER was investigated. Surprisingly, BER deficient mutants presented similar gamma sensitivity as the WT in this work, indicating that BER is not essential for survival after gamma irradiation in a HR-proficient background. The *apnIntgIntg2* triple mutant even shows a slightly higher survival capacity after 500 Gy in comparison to WT. This can be explained by the enhancement of homologous recombination in these mutants, as suggested by Swanson et al., who found an 18-fold increase in the recombination rate between chromosomes II and V in *apnIntgIntg2* mutants (Swanson, Morey et al. 1999). Furthermore, taking into consideration that gamma-induced AP sites are not cleaved by AP-endonucleases or Ntg-glycosylases in these mutants, the formation of SSB with blocked ends during the repair process is avoided (Friedberg 1995; Krokan, Standal et al. 1997; Boiteux and Guillet 2004). These blocked ends, which cannot be the substrate of DNA polymerases and ligases, can be converted into DSB during DNA replication, increasing the number of DSB (Boiteux and Guillet 2004). For this reason, the survival capacity after gamma irradiation can increase if no SSB with blocked ends are generated, as is the case in BER deficient mutants.

Taking into account that DSB are also substrate of NHEJ, blocked ends can also decrease the survival capacity in the *rad5* mutant, which mainly repairs DSB by NHEJ (Ahne, Jha et al. 1997). Since the *rad5* mutant can also profit by the hindering of BER process, this could explain in part the suppression of the *rad5* phenotype in the *apnIntgIntg2rad5* mutant after gamma irradiation.

Another possibility is that the additional BER suppression in the *apnIntgIntg2rad5* mutant leads to repair of DSB by HR, as is the case for the *yku70rad5* mutant. This assumption would explain the higher gamma sensitivity in stationary than in logarithmic growth phase in BER deficient mutants (as it has been seen for the HR proficient WT, *yku70*

and *yku70rad5* strains). To confirm this hypothesis, studies with plasmid assay would be necessary.

However, PFGE results show that the *apn1ntg1ntg2rad5* mutant has a DSB repair capacity comparable to the WT, indicating that its higher survival does not exclusively depend on the DSB repair but must have other causes. Studies by Liefshitz have suggested that the prevention of the error-free Rad5 dependent repair subpathway leads to the repair of intermediates by TLS and by HR (Liefshitz, Steinlauf et al. 1998). Thus, in the quadruple mutant, DSB could be repaired by HR, whereas other gamma-induced damage such as oxidative base damage or AP sites could be repaired effectively by TLS.

As will be described in the next chapter, the suppression of the *rad5* phenotype in the *apn1ntg1ntg2rad5* mutant also occurs after UV irradiation, indicating that this suppression might even be independent of the DSB repair.

5.4.2. Suppression of the *rad5* phenotype in BER deficient mutants after UV irradiation

UV damage is generally repaired by the PRR and by the NER pathway. The deletion of *RAD5* increases the UV sensitivity, indicating a role of Rad5 in the repair of UV damage. Mutants lacking Rad5 are not able to repair UV damage neither by the PRR error-free Rad5 dependent subpathway (Johnson, Henderson et al. 1992; Xiao, Chow et al. 2000; Broomfield, Hryciw et al. 2001; Broomfield and Xiao 2002; Hammet, Pike et al. 2002) nor by the recently proposed error-prone Rad5 dependent subpathway (Minesinger and Jinks-Robertson 2005). Therefore, the *rad5* mutant has to repair UV lesions through alternative pathways such as NER or other PRR subpathways. Among the possible PRR repair pathways used by the *rad5* mutant are the error-free POL30 dependent pathway and the error-prone *REV3*-dependent TLS pathway (Liefshitz, Steinlauf et al. 1998; Sonoda, Okada et al. 2003).

Therefore, to corroborate the hypothesis that the error-prone *REV3*-dependent PRR pathway is promoted in the *apn1ntg1ntg2rad5* mutant, the response of BER deficient mutants after UV irradiation was studied. Survival experiments presented in this work show similar UV sensitivities for the WT and the *apn1ntg1ntg2* mutant, indicating a minor role of BER pathway for the repair of UV damage. The UV sensitivity of the *rad5* mutant is suppressed by

the additional deletion of the three BER genes, the *apn1ntg1ntg2rad5* mutant presenting an even lower sensitivity than the WT. This lower sensitivity could be explained by a putative inhibition of UV repair by BER proteins, when UV lesions accumulate due to the absence of Rad5; the BER proteins Ntg1 or Ntg2 could compete for UV damage with proteins of NER or other PRR subpathways, impeding an effective UV repair. This theory is in agreement with recent studies (Heidenreich, Eisler et al. 2006) suggesting that the accumulation of UV damage activates the *REV3*-dependent TLS pathway, since UV irradiation in stationary cells generates substrates for Rev1 and Pol ζ (constituted by the catalytic subunit Rev3 and Rev7). This TLS pathway is also involved in the bypass of AP-sites (Broomfield, Hryciw et al. 2001).

The selective advantage of “adaptative mutations” introduced in stationary cells by the *REV3*-dependent TLS pathway (Heidenreich, Eisler et al. 2006) can explain how the promotion of an error-prone mechanism can be positive for cell survival. These adaptative mutations allow a restart of proliferation of stationary cells by relieving the growth-restraining conditions. Moreover, although *REV3*-dependent TLS is an error prone pathway, it can be faster than the repair pathways used by the WT, and therefore it can increase the UV repair efficiency. Higher repair efficiency can be more important than a higher accuracy when lesions are blocking DNA replication.

5.4.3. Mutagenic effect of the deletion of *RAD5* in a BER deficient background

Mutagenicity experiments allow the study of the genetic stability of a strain. The *rad5* mutant shows a similar number of spontaneous locus mutations in comparison with the WT, which confirms previous results (Schüller 1995). In contrast, BER deficient mutants show a strongly increased spontaneous mutagenicity, which is 168 - 240 times higher than that of WT. This confirms previous studies in *apn1* mutants which suggest unrepaired AP sites as the cause of the enhanced mutagenicity (Masson and Ramotar 1997). However, the mutagenicity after *NTG1* and *NTG2* deletion is controversial: Some authors found an increased spontaneous mutation frequency in *ntg1* and *ntg2* single and double mutants, which they explained by a requirement for repair of endogenous oxidative DNA damage (Alseth, Eide et al. 1999). In contrast, other authors found only a mutation rate enhancement in *apn1ntg1ntg2* triple mutants but not in the single and double mutant (Swanson, Morey et al. 1999; Doetsch,

Morey et al. 2001), and this enhancement was even higher after an additional NER or HR elimination. In studies by Swanson, it is also suggested that the majority of spontaneous mutations accumulating in *apn1ntg1ntg2* mutants are due the *REV3*-dependent TLS pathway. Taking into consideration that this pathway is also active in *apn1ntg1ntg2rad5* mutants, it would explain the similar number of spontaneous locus mutations in both BER deficient mutants that was found in this work.

In response to UV irradiation, the mutation frequency in the WT and the *rad5* mutant increases linearly with the doses, and it is slightly higher in the *rad5* mutant, confirming results by Schüller (Schüller 1995). In contrast, the *apn1ntg1ntg2* mutant presents a lower mutation frequency than the WT at higher doses. Taking into account that UV damage is repaired mainly by NER and PRR, this suggests that the accumulation of UV lesions in a BER deficient background triggers an alternative repair pathway, which may depend on Rad5. These results contrast with previous studies where an enhancement of the mutation frequency in *ntg1* and *ntg2* single and double mutants after peroxide treatment was found (Alseth, Eide et al. 1999).

The additional *RAD5* deletion leads to a suppression of this phenotype in the *apn1ntg1ntg2rad5* mutant, increasing the mutation frequency up to *rad5* level. Moreover, the *apn1ntg1ntg2rad5* mutant presents a 8 times higher mutagenicity in comparison with the WT at 80 J/m². The lower mutation frequency of the BER deficient *apn1ntg1ntg2* mutant could be explained by a repair of the UV-induced lesions by NER. However, the *apn1ntg1ntg2rad5* mutant shows a higher mutation frequency, even though this mutant could still repair by NER. This suggests that in the BER deficient mutants, UV-induced lesions are processed by PRR either by the Rad5-dependent subpathways, or in the absence of Rad5, by the error-prone *REV3*-dependent TLS pathway.

6. SUMMARY

Rad5 is a decisive protein in *S. cerevisiae* due to its role in the Post-replication repair (PRR) pathway, in which Rad5 is necessary for at least one error-free and one error-prone repair subpathway. In addition, Rad5 plays a role in other repair pathways; for instance, Rad5 regulates the balance between the double strand break (DSB) repair pathways, favoring the Rad52-dependent Homologous Recombination (HR) over the yKu70-dependent Non-Homologous-End Joining (NHEJ). Furthermore, since UV-induced damages are substrates for Rad5 but also for Base Excision Repair (BER) proteins, Rad5 is possibly involved directly or indirectly in the BER pathway.

To get a deeper insight into the interaction of Rad5 with HR, NHEJ and BER proteins, survival curves, plasmid assays, and mutagenicity experiments were carried out in this work. In addition, a new software tool has been developed for the quantification of DSB. This software, called Geltool, allows the quantification of DSB in haploid cells from PFGE gels, even if the number of DSB is small. This represents a decisive advantage in comparison with previous programs. The sensitivity of Geltool has permitted the quantification of DSB repair during the stationary growth phase in haploid cells, detecting a repair of 46 %- 57 % of the gamma-induced DSB in HR proficient strains against 6 % - 16 % in HR deficient strains.

Studies of the functional interactions of Rad5 with HR and NHEJ proteins revealed a synergistic effect between Rad5 and Rad52 proteins for the repair of DSB at chromosomal and plasmidial level. Differences in the repair of plasmids from the *rad52* and the *rad5* mutants revealed different end joining mechanisms for gap repair. Severe degradations found in plasmids from *rad52* and *rad52rad5* mutants could indicate an end protection function for Rad52 and also for Rad5, when Rad52 is absent. Moreover, the regulatory role of the Rad5 protein is confirmed, since the additional deletion of *YKU70* suppresses the *rad5* phenotype and forces the *yku70rad5* mutant to repair by HR.

The further study of the interplay of Rad5 with BER proteins shows that while BER only plays a minor role for the repair of gamma-induced damage, the *rad5* phenotype is suppressed in the BER deficient *apn1ntg1ntg2rad5* mutant. The same phenotype of suppression is also found for survival after UV irradiation. An enhanced mutagenicity of the *apn1ntg1ntg2rad5* mutant indicates a possible repair through the *REV3*-dependent Translesion Synthesis Repair (TLS) pathway, suggesting that an error-prone tolerance of UV-induced damage can be very effective for survival.

7. APPENDIX

7.1. Abbreviations

aa	Amino acid
Ab	Antibody
Amp	Ampicillin
AP	Alcaline phosphatase
AP site	Apurinic/apurimidinic sites
ARS	Autonomously Replicating Sequence
ATP	Adenosine -5'-triphosphate
BIR	Break-induced replication
bp	Base pair
CEN4	Centromeric region of chromosome 4
Da	Dalton
d (A, C, G, T) TP	2'-Deoxy-(Adenosine, Cytosine, Guanosine, Thymidin) -5'-Triphosphate
dd (A, C, G, T) TP	2',3'-Dideoxy-(Adenosine, Cytosine, Guanosine, Thymidin) -5'-Triphosphate
dd NTP	2',3'-Dideoxy-Nucleoside-5'-Triphosphate
Dei.	Deionized water
DEPC	Diethylpyrocarbonate
dist.	distilled
DMSO	Dimethylsulfoxide
DNA	Deoxyribonucleic acid
dNTP	2'-Deoxy-Nucleoside-5'- Triphosphate
DSBR	Double-strand break repair
ds	Double strand
DSB(s)	double strand break
DTT	Dithiothreitol
EB	Ethidium bromide
<i>E. coli</i>	<i>Escherichia coli</i>
EDTA	Ethylen diamine tetraacetate
Fig.	Figure
λ	Wave length
HMW Standard	High Molecular Weight Standard
HR	Homologous Recombination
IPTG	Isopropyl- β -D-thiogalactopyranoside
IR	Ionizing radiation
<i>KANMX/kanMX</i>	Kanamycin gene (functional/not functional)
kb	Kilobase pair
LB-Medium	Luria-Bertani-Medium
LMP	Low Melting Point
LHR	Liquid Holding Recovery Buffer
LMP	Low Melting Point

LMW Standard	Low Molecular Weight standard
mA	Milliampere
MCS	Multiple Cloning Site
MDS	Multiplly Damaged Sites
MMC	Mitomycin C
MMEJ	Microhomology mediated end joining
MMS	Methyl methanesulfonate
8-MOP	8-methoxypsoralen
MNNG	N-methyl-N'-nitro-N- nitrosoguanidine
NHEJ	Nonhomologous End Joining
nt	Nucleotide
OD	Optical Density
ORF	Open Reading Frame
p.a.	pro analysis
PBS	Phosphate Buffered Saline
PCI	Phenol/Chloroform/Isoamylalcohol [25 : 24 : 1]
PCR	Polymerase Chain Reaction
PDS	Potassium Dodecyl Sulfate
PEG	Polyethylenglycol
PRR	Post-replication repair
PFGE	Pulsed Field Gel Electrophoresis
RE	Restriction endonuclease
RNA	Ribonucleic acid
RNase	Ribonuclease
ROS	Reactive oxidative species
RPA	Replication protein A
RT	Room Temperature
<i>S.cerevisiae</i> or <i>Sc</i>	<i>Saccharomyces cerevisiae</i>
SDS	Sodium Dodecyl Sulfate
SDSA	Single dependent strand annealing
ss	Single strand
SSA	Single strand annealing
T _A	Annealing temperature
TAE-Buffer	Tris-Acetate-EDTA-Buffer
TBE-Buffer	Tris-Borate-EDTA-Buffer
TE-Buffer	Tris-EDTA-Buffer
TLS	Translesion Synthesis Repair
T _M	Melting temperature
Tris	Tris-(hydroxymethyl)-aminomethane
Triton X-100 [®]	Octylphenylpoly-(ethylenglycolether) _n
<i>TRP1/trp1</i>	Tryptophan gene (funtional/ not funtional)
ON	Over Night
<i>URA3/ura3</i>	Uracil gene (funtional/not funtional)
UV	Ultraviolet
v/v	Volume per volume
w/v	Weight per volume
YPD	Yeast peptone and Dextrose (rich medium)
YPDA	Yeast peptone, Dextrose and Adenine
X-Gal	5-bromo-4-chloro-3-indolyl-beta-D-galactopyranoside

7.2. References

- Ahne, F., B. Jha, et al. (1997). "The RAD5 gene product is involved in the avoidance of non-homologous end-joining of DNA double strand breaks in the yeast *Saccharomyces cerevisiae*." Nucleic Acids Res **25**(4): 743-9.
- Alseth, I., L. Eide, et al. (1999). "The *Saccharomyces cerevisiae* homologues of endonuclease III from *Escherichia coli*, Ntg1 and Ntg2, are both required for efficient repair of spontaneous and induced oxidative DNA damage in yeast." Mol Cell Biol **19**(5): 3779-87.
- Arai, N., D. Ito, et al. (2005). "Heteroduplex joint-formation by a stoichiometric complex of Rad51 and Rad52 of *Saccharomyces cerevisiae*." J Biol Chem.
- Asleson, E. N. and D. M. Livingston (2003). "Investigation of the stability of yeast rad52 mutant proteins uncovers post-translational and transcriptional regulation of Rad52p." Genetics **163**(1): 91-101.
- Astrom, S. U., S. M. Okamura, et al. (1999). "Yeast cell-type regulation of DNA repair." Nature **397**(6717): 310.
- Aylon, Y. and M. Kupiec (2003). "The checkpoint protein Rad24 of *Saccharomyces cerevisiae* is involved in processing double-strand break ends and in recombination partner choice." Mol Cell Biol **23**(18): 6585-96.
- Aylon, Y. and M. Kupiec (2004). "DSB repair: the yeast paradigm." DNA Repair (Amst) **3**(8-9): 797-815.
- Aylon, Y. and M. Kupiec (2005). "Cell cycle-dependent regulation of double-strand break repair: a role for the CDK." Cell Cycle **4**(2): 259-61.
- Aylon, Y., B. Liefshitz, et al. (2003). "Molecular dissection of mitotic recombination in the yeast *Saccharomyces cerevisiae*." Mol Cell Biol **23**(4): 1403-17.
- Ayyagari, R., K. J. Impellizzeri, et al. (1995). "A mutational analysis of the yeast proliferating cell nuclear antigen indicates distinct roles in DNA replication and DNA repair." Mol Cell Biol **15**(8): 4420-9.
- Bai, Y., A. P. Davis, et al. (1999). "A novel allele of RAD52 that causes severe DNA repair and recombination deficiencies only in the absence of RAD51 or RAD59." Genetics **153**(3): 1117-30.
- Bailly, V., S. Lauder, et al. (1997). "Yeast DNA repair proteins Rad6 and Rad18 form a heterodimer that has ubiquitin conjugating, DNA binding, and ATP hydrolytic activities." J Biol Chem **272**(37): 23360-5.
- Benson, F. E., P. Baumann, et al. (1998). "Synergistic actions of Rad51 and Rad52 in recombination and DNA repair." Nature **391**(6665): 401-4.
- Bertuch, A. A. and V. Lundblad (2003). "The Ku heterodimer performs separable activities at double-strand breaks and chromosome termini." Mol Cell Biol **23**(22): 8202-15.

- Boiteux, S. and M. Guillet (2004). "Abasic sites in DNA: repair and biological consequences in *Saccharomyces cerevisiae*." DNA Repair (Amst) **3**(1): 1-12.
- Bosco, G. and J. E. Haber (1998). "Chromosome break-induced DNA replication leads to nonreciprocal translocations and telomere capture." Genetics **150**(3): 1037-47.
- Boulton, S. J. and S. P. Jackson (1996). "Identification of a *Saccharomyces cerevisiae* Ku80 homologue: roles in DNA double strand break rejoining and in telomeric maintenance." Nucleic Acids Res **24**(23): 4639-48.
- Boulton, S. J. and S. P. Jackson (1996). "Saccharomyces cerevisiae Ku70 potentiates illegitimate DNA double-strand break repair and serves as a barrier to error-prone DNA repair pathways." Embo J **15**(18): 5093-103.
- Boulton, S. J. and S. P. Jackson (1998). "Components of the Ku-dependent non-homologous end-joining pathway are involved in telomeric length maintenance and telomeric silencing." Embo J **17**(6): 1819-28.
- Bressan, D. A., B. K. Baxter, et al. (1999). "The Mre11-Rad50-Xrs2 protein complex facilitates homologous recombination-based double-strand break repair in *Saccharomyces cerevisiae*." Mol Cell Biol **19**(11): 7681-7.
- Broomfield, S., T. Hryciw, et al. (2001). "DNA postreplication repair and mutagenesis in *Saccharomyces cerevisiae*." Mutat Res **486**(3): 167-84.
- Broomfield, S. and W. Xiao (2002). "Suppression of genetic defects within the RAD6 pathway by *srs2* is specific for error-free post-replication repair but not for damage-induced mutagenesis." Nucleic Acids Res **30**(3): 732-9.
- Brozmanova, J., V. Vlckova, et al. (1994). "Expression of the *E. coli* *ada* gene in *S. cerevisiae* provides cellular resistance to N-methyl-N'-nitro-N-nitrosoguanidine in *rad6* but not in *rad52* mutants." Nucleic Acids Res **22**(25): 5717-22.
- Cejka, P., V. Vondrejs, et al. (2001). "Dissection of the functions of the *Saccharomyces cerevisiae* RAD6 postreplicative repair group in mutagenesis and UV sensitivity." Genetics **159**(3): 953-63.
- Chen, L., K. Trujillo, et al. (2001). "Promotion of Dnl4-catalyzed DNA end-joining by the Rad50/Mre11/Xrs2 and Hdf1/Hdf2 complexes." Mol Cell **8**(5): 1105-15.
- Clikeman, J. A., G. J. Khalsa, et al. (2001). "Homologous recombinational repair of double-strand breaks in yeast is enhanced by MAT heterozygosity through yKU-dependent and -independent mechanisms." Genetics **157**(2): 579-89.
- Crespo-Hernandez, C. E. and R. Arce (2004). "Formamidopyrimidines as major products in the low- and high-intensity UV irradiation of guanine derivatives." J Photochem Photobiol B **73**(3): 167-75.
- Critchlow, S. E. and S. P. Jackson (1998). "DNA end-joining: from yeast to man." Trends Biochem Sci **23**(10): 394-8.
- Daley, J. M., P. L. Palmbo, et al. (2005). "Nonhomologous end joining in yeast." Annu Rev Genet **39**: 431-51.

- Daley, J. M. and T. E. Wilson (2005). "Rejoining of DNA double-strand breaks as a function of overhang length." Mol Cell Biol **25**(3): 896-906.
- Dardalhon, M., A. Nohturfft, et al. (1994). "Repair of DNA double-strand breaks induced in *Saccharomyces cerevisiae* using different gamma-ray dose-rates: a pulsed-field gel electrophoresis analysis." Int J Radiat Biol **65**(3): 307-14.
- Davis, A. P. and L. S. Symington (2001). "The yeast recombinational repair protein Rad59 interacts with Rad52 and stimulates single-strand annealing." Genetics **159**(2): 515-25.
- Davis, A. P. and L. S. Symington (2004). "RAD51-dependent break-induced replication in yeast." Mol Cell Biol **24**(6): 2344-51.
- de Morais, M. A., Jr., E. J. Vicente, et al. (1996). "Further characterization of the yeast *pso4-1* mutant: interaction with *rad51* and *rad52* mutants after photoinduced psoralen lesions." Curr Genet **29**(3): 211-8.
- Doetsch, P. W., N. J. Morey, et al. (2001). "Yeast base excision repair: interconnections and networks." Prog Nucleic Acid Res Mol Biol **68**: 29-39.
- Dolling, J. A., D. R. Boreham, et al. (1999). "Cisplatin-modification of DNA repair and ionizing radiation lethality in yeast, *Saccharomyces cerevisiae*." Mutat Res **433**(2): 127-36.
- Driller, L., R. J. Wellinger, et al. (2000). "A short C-terminal domain of Yku70p is essential for telomere maintenance." J Biol Chem **275**(32): 24921-7.
- Dudas, A. and M. Chovanec (2004). "DNA double-strand break repair by homologous recombination." Mutat Res **566**(2): 131-67.
- Feldmann, E., V. Schmiemann, et al. (2000). "DNA double-strand break repair in cell-free extracts from Ku80-deficient cells: implications for Ku serving as an alignment factor in non-homologous DNA end joining." Nucleic Acids Res **28**(13): 2585-96.
- Feldmann, H., L. Driller, et al. (1996). "HDF2, the second subunit of the Ku homologue from *Saccharomyces cerevisiae*." J Biol Chem **271**(44): 27765-9.
- Feldmann, H. and E. L. Winnacker (1993). "A putative homologue of the human autoantigen Ku from *Saccharomyces cerevisiae*." J Biol Chem **268**(17): 12895-900.
- Fellerhoff, B. (1999). "Die Rolle des *HDF1*-Gens für die Stabilität des Hefegenoms." Doktorarbeit der Fakultät für Biologie der LMU München.
- Fishman-Lobell, J., N. Rudin, et al. (1992). "Two alternative pathways of double-strand break repair that are kinetically separable and independently modulated." Mol Cell Biol **12**(3): 1292-303.
- Foray, N., C. F. Arlett, et al. (1999). "Underestimation of the small residual damage when measuring DNA double-strand breaks (DSB): is the repair of radiation-induced DSB complete?" Int J Radiat Biol **75**(12): 1589-95.

- Franchitto, A., Pichierri, P. (2002). "Protecting genomic integrity during DNA replication: correlation between Werner's and Bloom's syndrome gene products and the MRE11 complex " Human Molecular Genetics.
- Frank-Vaillant, M. and S. Marcand (2002). "Transient stability of DNA ends allows nonhomologous end joining to precede homologous recombination." Mol Cell **10**(5): 1189-99.
- Frankenberg-Schwager, M., D. Frankenberg, et al. (1980). "Repair of DNA double-strand breaks in irradiated yeast cells under nongrowth conditions." Radiat Res **82**(3): 498-510.
- Friedberg, E. C. (2003). "DNA damage and repair." Nature **421**(6921): 436-40.
- Friedberg, E. C., Walker, G. C. and Siede, W. (2006). "DNA repair and mutagenesis."
- Friedberg, E. C., Walker, G.C., Siede, W. (1995). "DNA Repair and Mutagenesis." ASM press, Washinton, DC.
- Friedl, A. A., W. Beisker, et al. (1993). "Application of pulsed field gel electrophoresis to determine gamma-ray-induced double-strand breaks in yeast chromosomal molecules." Int J Radiat Biol **63**(2): 173-81.
- Friedl, A. A., M. Kiechle, et al. (1998). "Radiation-induced chromosome aberrations in *Saccharomyces cerevisiae*: influence of DNA repair pathways." Genetics **148**(3): 975-88.
- Friedl, A. A., A. Kraxenberger, et al. (1995). "An electrophoretic approach to the assessment of the spatial distribution of DNA double-strand breaks in mammalian cells." Electrophoresis **16**(10): 1865-74.
- Friedl, A. A., B. Liefshitz, et al. (2001). "Deletion of the SRS2 gene suppresses elevated recombination and DNA damage sensitivity in rad5 and rad18 mutants of *Saccharomyces cerevisiae*." Mutat Res **486**(2): 137-46.
- Galli, A. and R. H. Schiestl (1998). "Effects of DNA double-strand and single-strand breaks on intrachromosomal recombination events in cell-cycle-arrested yeast cells." Genetics **149**(3): 1235-50.
- Game, J. C. (2000). "The *Saccharomyces* repair genes at the end of the century." Mutat Res **451**(1-2): 277-93.
- Gauter, B., O. Zlobinskaya, et al. (2002). "Rejoining of radiation-induced DNA double-strand breaks: pulsed-field electrophoresis analysis of fragment size distributions after incubation for repair." Radiat Res **157**(6): 721-33.
- Geigl, E. M. and F. Eckardt-Schupp (1991). "Repair of gamma ray-induced S1 nuclease hypersensitive sites in yeast depends on homologous mitotic recombination and a RAD18-dependent function." Curr Genet **20**(1-2): 33-7.
- Gellon, L., R. Barbey, et al. (2001). "Synergism between base excision repair, mediated by the DNA glycosylases Ntg1 and Ntg2, and nucleotide excision repair in the removal of

- oxidatively damaged DNA bases in *Saccharomyces cerevisiae*." Mol Genet Genomics **265**(6): 1087-96.
- Gonzalez-Barrera, S., F. Cortes-Ledesma, et al. (2003). "Equal sister chromatid exchange is a major mechanism of double-strand break repair in yeast." Mol Cell **11**(6): 1661-71.
- Gradzka, I. and T. Iwanenko (2005). "A non-radioactive, PFGE-based assay for low levels of DNA double-strand breaks in mammalian cells." DNA Repair (Amst) **4**(10): 1129-39.
- Gravel, S., M. Larrivee, et al. (1998). "Yeast Ku as a regulator of chromosomal DNA end structure." Science **280**(5364): 741-4.
- Guillet, M. and S. Boiteux (2002). "Endogenous DNA abasic sites cause cell death in the absence of Apn1, Apn2 and Rad1/Rad10 in *Saccharomyces cerevisiae*." Embo J **21**(11): 2833-41.
- Guo, Y., L. L. Breeden, et al. (2005). "Expression of a human cytochrome p450 in yeast permits analysis of pathways for response to and repair of aflatoxin-induced DNA damage." Mol Cell Biol **25**(14): 5823-33.
- Haber, J. E. (1999). "DNA recombination: the replication connection." Trends Biochem Sci **24**(7): 271-5.
- Haber, J. E. (2000). "Lucky breaks: analysis of recombination in *Saccharomyces*." Mutat Res **451**(1-2): 53-69.
- Hammet, A., B. L. Pike, et al. (2002). "Posttranscriptional regulation of the RAD5 DNA repair gene by the Dun1 kinase and the Pan2-Pan3 poly(A)-nuclease complex contributes to survival of replication blocks." J Biol Chem **277**(25): 22469-74.
- Hanna, M., B. L. Chow, et al. (2004). "Involvement of two endonuclease III homologs in the base excision repair pathway for the processing of DNA alkylation damage in *Saccharomyces cerevisiae*." DNA Repair (Amst) **3**(1): 51-9.
- Haracska, L., C. A. Torres-Ramos, et al. (2004). "Opposing effects of ubiquitin conjugation and SUMO modification of PCNA on replicational bypass of DNA lesions in *Saccharomyces cerevisiae*." Mol Cell Biol **24**(10): 4267-74.
- Haynes, R. H. (1975). "DNA Repair and the Genetic Control of Radiosensitivity in Yeast." Basic Life Sci. **5B:529-40: 5B:529-40.**
- Hays, S. L., A. A. Firmenich, et al. (1998). "Studies of the interaction between Rad52 protein and the yeast single-stranded DNA binding protein RPA." Mol Cell Biol **18**(7): 4400-6.
- Hefferin, M. L. and A. E. Tomkinson (2005). "Mechanism of DNA double-strand break repair by non-homologous end joining." DNA Repair (Amst) **4**(6): 639-48.
- Heidenreich, E., H. Eisler, et al. (2006). "Epistatic participation of REV1 and REV3 in the formation of UV-induced frameshift mutations in cell cycle-arrested yeast cells." Mutat Res **593**(1-2): 187-95.

- Heidenreich, E., R. Novotny, et al. (2003). "Non-homologous end joining as an important mutagenic process in cell cycle-arrested cells." Embo J **22**(9): 2274-83.
- Hoege, C., B. Pfander, et al. (2002). "RAD6-dependent DNA repair is linked to modification of PCNA by ubiquitin and SUMO." Nature **419**(6903): 135-41.
- Huang, H., A. Kahana, et al. (1997). "The ubiquitin-conjugating enzyme Rad6 (Ubc2) is required for silencing in *Saccharomyces cerevisiae*." Mol Cell Biol **17**(11): 6693-9.
- Inbar, O. and M. Kupiec (1999). "Homology search and choice of homologous partner during mitotic recombination." Mol Cell Biol **19**(6): 4134-42.
- Inbar, O., B. Liefshitz, et al. (2000). "The relationship between homology length and crossing over during the repair of a broken chromosome." J Biol Chem **275**(40): 30833-8.
- Innis, M. A., Gelfand, D.H., Sninsky, J.J., and White, T.J., eds. (1990). PCR Protocols: A guide to methods and applications, Academic Press, San Diego, CA:.
- Ira, G., A. Pellicioli, et al. (2004). "DNA end resection, homologous recombination and DNA damage checkpoint activation require CDK1." Nature **431**(7011): 1011-7.
- Ischenko, A. A. and M. K. Saporbaev (2002). "Alternative nucleotide incision repair pathway for oxidative DNA damage." Nature **415**(6868): 183-7.
- Ishchenko, A. A., X. Yang, et al. (2005). "The 3'->5' exonuclease of Apn1 provides an alternative pathway to repair 7,8-dihydro-8-oxodeoxyguanosine in *Saccharomyces cerevisiae*." Mol Cell Biol **25**(15): 6380-90.
- Ivanov, E. L., N. Sugawara, et al. (1996). "Genetic requirements for the single-strand annealing pathway of double-strand break repair in *Saccharomyces cerevisiae*." Genetics **142**(3): 693-704.
- Jazayeri, A. and S. P. Jackson (2002). "Screening the yeast genome for new DNA-repair genes." Genome Biol **3**(4): REVIEWS1009.
- Jeggo, P. A. (1998). "DNA breakage and repair." Adv Genet **38**: 185-218.
- Jha, B., F. Ahne, et al. (1993). "The use of a double-marker shuttle vector to study DNA double-strand break repair in wild-type and radiation-sensitive mutants of the yeast *Saccharomyces cerevisiae*." Curr Genet **23**(5-6): 402-7.
- Johnson, R. D. and M. Jasin (2001). "Double-strand-break-induced homologous recombination in mammalian cells." Biochem Soc Trans **29**(Pt 2): 196-201.
- Johnson, R. E., S. T. Henderson, et al. (1992). "Saccharomyces cerevisiae RAD5-encoded DNA repair protein contains DNA helicase and zinc-binding sequence motifs and affects the stability of simple repetitive sequences in the genome." Mol Cell Biol **12**(9): 3807-18.
- Johnson, R. E., S. Prakash, et al. (1994). "Yeast DNA repair protein RAD5 that promotes instability of simple repetitive sequences is a DNA-dependent ATPase." J Biol Chem **269**(45): 28259-62.

- Kabotyanski, E. B., L. Gomelsky, et al. (1998). "Double-strand break repair in Ku86- and XRCC4-deficient cells." Nucleic Acids Res **26**(23): 5333-42.
- Kagawa, W., H. Kurumizaka, et al. (2001). "Homologous pairing promoted by the human Rad52 protein." J Biol Chem **276**(37): 35201-8.
- Kanaar, R., J. H. Hoeijmakers, et al. (1998). "Molecular mechanisms of DNA double strand break repair." Trends Cell Biol **8**(12): 483-9.
- Karathanasis, E. and T. E. Wilson (2002). "Enhancement of *Saccharomyces cerevisiae* end-joining efficiency by cell growth stage but not by impairment of recombination." Genetics **161**(3): 1015-27.
- Kegel, A., J. O. Sjostrand, et al. (2001). "Nej1p, a cell type-specific regulator of nonhomologous end joining in yeast." Curr Biol **11**(20): 1611-7.
- Kiakos, K., T. T. Howard, et al. (2002). "*Saccharomyces cerevisiae* RAD5 influences the excision repair of DNA minor groove adducts." J Biol Chem **277**(46): 44576-81.
- Koike, M. (2002). "Dimerization, translocation and localization of Ku70 and Ku80 proteins." J Radiat Res (Tokyo) **43**(3): 223-36.
- Kramer, K. M., J. A. Brock, et al. (1994). "Two different types of double-strand breaks in *Saccharomyces cerevisiae* are repaired by similar RAD52-independent, nonhomologous recombination events." Mol Cell Biol **14**(2): 1293-301.
- Kraxenberger, A., A. A. Friedl, et al. (1994). "Computer simulation of pulsed field gel runs allows the quantitation of radiation-induced double-strand breaks in yeast." Electrophoresis **15**(2): 128-36.
- Krogh, B. O. and L. S. Symington (2004). "Recombination proteins in yeast." Annu Rev Genet **38**: 233-71.
- Krokan, H. E., R. Standal, et al. (1997). "DNA glycosylases in the base excision repair of DNA." Biochem J **325** (Pt 1): 1-16.
- Kuo, C. L. and J. L. Campbell (1983). "Cloning of *Saccharomyces cerevisiae* DNA replication genes: isolation of the CDC8 gene and two genes that compensate for the cdc8-1 mutation." Mol Cell Biol **3**(10): 1730-7.
- Laroche, T., S. G. Martin, et al. (1998). "Mutation of yeast Ku genes disrupts the subnuclear organization of telomeres." Curr Biol **8**(11): 653-6.
- Lawrence, C. (1994). "The RAD6 DNA repair pathway in *Saccharomyces cerevisiae*: what does it do, and how does it do it?" Bioessays **16**(4): 253-8.
- Le Page, F., A. Guy, et al. (1998). "Repair and mutagenic potency of 8-oxoG:A and 8-oxoG:C base pairs in mammalian cells." Nucleic Acids Res **26**(5): 1276-81.
- Le, S., J. K. Moore, et al. (1999). "RAD50 and RAD51 define two pathways that collaborate to maintain telomeres in the absence of telomerase." Genetics **152**(1): 143-52.

- Lee, S. E., J. K. Moore, et al. (1998). "Saccharomyces Ku70, mre11/rad50 and RPA proteins regulate adaptation to G2/M arrest after DNA damage." Cell **94**(3): 399-409.
- Lewis, L. K. and M. A. Resnick (2000). "Tying up loose ends: nonhomologous end-joining in *Saccharomyces cerevisiae*." Mutat Res **451**(1-2): 71-89.
- Liefshitz, B., R. Steinlauf, et al. (1998). "Genetic interactions between mutants of the 'error-prone' repair group of *Saccharomyces cerevisiae* and their effect on recombination and mutagenesis." Mutat Res **407**(2): 135-45.
- Lisby, M., U. H. Mortensen, et al. (2003). "Colocalization of multiple DNA double-strand breaks at a single Rad52 repair centre." Nat Cell Biol **5**(6): 572-7.
- Liu, C., J. J. Pouliot, et al. (2002). "Repair of topoisomerase I covalent complexes in the absence of the tyrosyl-DNA phosphodiesterase Tdp1." Proc Natl Acad Sci U S A **99**(23): 14970-5.
- Lobachev, K., E. Vitriol, et al. (2004). "Chromosome fragmentation after induction of a double-strand break is an active process prevented by the RMX repair complex." Curr Biol **14**(23): 2107-12.
- Lobrich, M., S. Ikpeme, et al. (1994). "Measurement of DNA double-strand breaks in mammalian cells by pulsed-field gel electrophoresis: a new approach using rarely cutting restriction enzymes." Radiat Res **138**(2): 186-92.
- Longo, J. A., B. Nevaldine, et al. (1997). "An assay for quantifying DNA double-strand break repair that is suitable for small numbers of unlabeled cells." Radiat Res **147**(1): 35-40.
- Longtine, M. S., A. McKenzie, 3rd, et al. (1998). "Additional modules for versatile and economical PCR-based gene deletion and modification in *Saccharomyces cerevisiae*." Yeast **14**(10): 953-61.
- Ma, J. L., E. M. Kim, et al. (2003). "Yeast Mre11 and Rad1 proteins define a Ku-independent mechanism to repair double-strand breaks lacking overlapping end sequences." Mol Cell Biol **23**(23): 8820-8.
- Mages, G. J., H. M. Feldmann, et al. (1996). "Involvement of the *Saccharomyces cerevisiae* HDF1 gene in DNA double-strand break repair and recombination." J Biol Chem **271**(14): 7910-5.
- Malkova, A., E. L. Ivanov, et al. (1996). "Double-strand break repair in the absence of RAD51 in yeast: a possible role for break-induced DNA replication." Proc Natl Acad Sci U S A **93**(14): 7131-6.
- Malkova, A., M. L. Naylor, et al. (2005). "RAD51-dependent break-induced replication differs in kinetics and checkpoint responses from RAD51-mediated gene conversion." Mol Cell Biol **25**(3): 933-44.
- Martini, E. M., S. Keeney, et al. (2002). "A role for histone H2B during repair of UV-induced DNA damage in *Saccharomyces cerevisiae*." Genetics **160**(4): 1375-87.

- Masson, J. Y. and D. Ramotar (1997). "Normal processing of AP sites in *Apn1*-deficient *Saccharomyces cerevisiae* is restored by *Escherichia coli* genes expressing either exonuclease III or endonuclease III." *Mol Microbiol* **24**(4): 711-21.
- McMillan, T. J., S. Tobi, et al. (2001). "The use of DNA double-strand break quantification in radiotherapy." *Int J Radiat Oncol Biol Phys* **49**(2): 373-7.
- Meadows, K. L., B. Song, et al. (2003). "Characterization of AP lyase activities of *Saccharomyces cerevisiae* Ntg1p and Ntg2p: implications for biological function." *Nucleic Acids Res* **31**(19): 5560-7.
- Mewes, H. W., K. Albermann, et al. (1997). "Overview of the yeast genome." *Nature* **387**(6632 Suppl): 7-65.
- Milne, G. T., S. Jin, et al. (1996). "Mutations in two Ku homologs define a DNA end-joining repair pathway in *Saccharomyces cerevisiae*." *Mol Cell Biol* **16**(8): 4189-98.
- Milne, G. T. and D. T. Weaver (1993). "Dominant negative alleles of RAD52 reveal a DNA repair/recombination complex including Rad51 and Rad52." *Genes Dev* **7**(9): 1755-65.
- Minesinger, B. K. and S. Jinks-Robertson (2005). "Roles of RAD6 epistasis group members in spontaneous polzeta-dependent translesion synthesis in *Saccharomyces cerevisiae*." *Genetics* **169**(4): 1939-55.
- Miyazaki, T., D. A. Bressan, et al. (2004). "In vivo assembly and disassembly of Rad51 and Rad52 complexes during double-strand break repair." *Embo J* **23**(4): 939-49.
- Moore, C. W., J. McKoy, et al. (2000). "DNA damage-inducible and RAD52-independent repair of DNA double-strand breaks in *Saccharomyces cerevisiae*." *Genetics* **154**(3): 1085-99.
- Moore, J. K. and J. E. Haber (1996). "Cell cycle and genetic requirements of two pathways of nonhomologous end-joining repair of double-strand breaks in *Saccharomyces cerevisiae*." *Mol Cell Biol* **16**(5): 2164-73.
- Morrison, C. and S. Takeda (2000). "Genetic analysis of homologous DNA recombination in vertebrate somatic cells." *Int J Biochem Cell Biol* **32**(8): 817-31.
- Mortensen, U. H., C. Bendixen, et al. (1996). "DNA strand annealing is promoted by the yeast Rad52 protein." *Proc Natl Acad Sci U S A* **93**(20): 10729-34.
- Mortensen, U. H., N. Erdeniz, et al. (2002). "A molecular genetic dissection of the evolutionarily conserved N terminus of yeast Rad52." *Genetics* **161**(2): 549-62.
- Nelson, J. R., C. W. Lawrence, et al. (1996). "Deoxycytidyl transferase activity of yeast REV1 protein." *Nature* **382**(6593): 729-31.
- Nelson, J. R., C. W. Lawrence, et al. (1996). "Thymine-thymine dimer bypass by yeast DNA polymerase zeta." *Science* **272**(5268): 1646-9.
- New, J. H., T. Sugiyama, et al. (1998). "Rad52 protein stimulates DNA strand exchange by Rad51 and replication protein A." *Nature* **391**(6665): 407-10.

- Nugent, C. I., G. Bosco, et al. (1998). "Telomere maintenance is dependent on activities required for end repair of double-strand breaks." Curr Biol **8**(11): 657-60.
- O'Brien, T. J., J. L. Fornsaglio, et al. (2002). "Effects of hexavalent chromium on the survival and cell cycle distribution of DNA repair-deficient *S. cerevisiae*." DNA Repair (Amst) **1**(8): 617-27.
- Olive, P. L. (1998). "The role of DNA single- and double-strand breaks in cell killing by ionizing radiation." Radiat Res **150**(5 Suppl): S42-51.
- Orr-Weaver, T. L. and J. W. Szostak (1983). "Yeast recombination: the association between double-strand gap repair and crossing-over." Proc Natl Acad Sci U S A **80**(14): 4417-21.
- Otterlei, M., B. Kavli, et al. (2000). "Repair of chromosomal abasic sites in vivo involves at least three different repair pathways." Embo J **19**(20): 5542-51.
- Ozawa, T., J. Wang, et al. (1999). "Radiation-induced DNA double-strand breaks and rejoining in malignant glioma cells." Int J Radiat Biol **75**(5): 563-70.
- Palmer, S., E. Schildkraut, et al. (2003). "Gene conversion tracts in *Saccharomyces cerevisiae* can be extremely short and highly directional." Nucleic Acids Res **31**(4): 1164-73.
- Paques, F. and J. E. Haber (1999). "Multiple pathways of recombination induced by double-strand breaks in *Saccharomyces cerevisiae*." Microbiol Mol Biol Rev **63**(2): 349-404.
- Pastink, A., J. C. Eeken, et al. (2001). "Genomic integrity and the repair of double-strand DNA breaks." Mutat Res **480-481**: 37-50.
- Pastwa, E. and J. Blasiak (2003). "Non-homologous DNA end joining." Acta Biochim Pol **50**(4): 891-908.
- Paull, T. T. and M. Gellert (2000). "A mechanistic basis for Mre11-directed DNA joining at microhomologies." Proc Natl Acad Sci U S A **97**(12): 6409-14.
- Pfander, B., G. L. Moldovan, et al. (2005). "SUMO-modified PCNA recruits Srs2 to prevent recombination during S phase." Nature **436**(7049): 428-33.
- Pohlit, W. and I. R. Heyder (1977). "Growth of cells on solid culture medium. II. Cell physiological data of stationary yeast cells and the initiation of cell cycle in nutrient free buffer solution." Radiat Environ Biophys **14**(3): 213-30.
- Polotnianka, R. M., J. Li, et al. (1998). "The yeast Ku heterodimer is essential for protection of the telomere against nucleolytic and recombinational activities." Curr Biol **8**(14): 831-4.
- Popoff, S. C., A. I. Spira, et al. (1990). "Yeast structural gene (APN1) for the major apurinic endonuclease: homology to *Escherichia coli* endonuclease IV." Proc Natl Acad Sci U S A **87**(11): 4193-7.
- Porter, S. E., P. W. Greenwell, et al. (1996). "The DNA-binding protein Hdf1p (a putative Ku homologue) is required for maintaining normal telomere length in *Saccharomyces cerevisiae*." Nucleic Acids Res **24**(4): 582-5.

- Potter, T. and W. Kohnlein (2001). "Pulsed-field gel electrophoresis of chromosomal DNA of *Saccharomyces pastorianus* after exposure to x-rays (30-50 keV) and neutrons (14 MeV)." Radiat Environ Biophys **40**(1): 39-45.
- Povirk, L. F. (1996). "DNA damage and mutagenesis by radiomimetic DNA-cleaving agents: bleomycin, neocarzinostatin and other enediynes." Mutat Res **355**(1-2): 71-89.
- Prado, F., F. Cortes-Ledesma, et al. (2003). "Mitotic recombination in *Saccharomyces cerevisiae*." Curr Genet **42**(4): 185-98.
- Prakash, S. and L. Prakash (2002). "Translesion DNA synthesis in eukaryotes: a one- or two-polymerase affair." Genes Dev **16**(15): 1872-83.
- Putnam, C. D., V. Pennaneach, et al. (2005). "*Saccharomyces cerevisiae* as a model system to define the chromosomal instability phenotype." Mol Cell Biol **25**(16): 7226-38.
- Ramotar, D., S. C. Popoff, et al. (1991). "Cellular role of yeast Apn1 apurinic endonuclease/3'-diesterase: repair of oxidative and alkylation DNA damage and control of spontaneous mutation." Mol Cell Biol **11**(9): 4537-44.
- Rose M., N. P., Thomas J.H., Botstein D., Fink G.R.; (1987). "A *Saccharomyces cerevisiae* genomic plasmid bank based on a centromere-containing shuttle vector." Gene **60**:237-243.
- Sancar A., L.-B. L. A., Ünsal-Kacmaz K., Linn S. (2004). "Molecular Mechanisms of Mammalian DNA Repair and the DNA Damage Checkpoints." Annual Review Biochemie **73**:39-85.
- Scharer, O. D. and J. Jiricny (2001). "Recent progress in the biology, chemistry and structural biology of DNA glycosylases." Bioessays **23**(3): 270-81.
- Schüller, M. (1995). "Molekulare Analyse von Mutationen in *rev2* Mutanten und dem isogenen Wildtyp-Stamm der Hefe *Saccharomyces cerevisiae*." Diplomarbeit der Fakultät für Biologie der LMU München.
- Senturker, S., P. Auffret van der Kemp, et al. (1998). "Substrate specificities of the *ntg1* and *ntg2* proteins of *Saccharomyces cerevisiae* for oxidized DNA bases are not identical." Nucleic Acids Res **26**(23): 5270-6.
- Shinohara, A. and T. Ogawa (1998). "Stimulation by Rad52 of yeast Rad51-mediated recombination." Nature **391**(6665): 404-7.
- Shinohara, A., M. Shinohara, et al. (1998). "Rad52 forms ring structures and co-operates with RPA in single-strand DNA annealing." Genes Cells **3**(3): 145-56.
- Siede, W., A. A. Friedl, et al. (1996). "The *Saccharomyces cerevisiae* Ku autoantigen homologue affects radiosensitivity only in the absence of homologous recombination." Genetics **142**(1): 91-102.
- Simon, J. A., P. Szankasi, et al. (2000). "Differential toxicities of anticancer agents among DNA repair and checkpoint mutants of *Saccharomyces cerevisiae*." Cancer Res **60**(2): 328-33.

- Smirnova, M. and H. L. Klein (2003). "Role of the error-free damage bypass postreplication repair pathway in the maintenance of genomic stability." Mutat Res **532**(1-2): 117-35.
- Smith, S., J. Y. Hwang, et al. (2004). "Mutator genes for suppression of gross chromosomal rearrangements identified by a genome-wide screening in *Saccharomyces cerevisiae*." Proc Natl Acad Sci U S A **101**(24): 9039-44.
- Song, B. and P. Sung (2000). "Functional interactions among yeast Rad51 recombinase, Rad52 mediator, and replication protein A in DNA strand exchange." J Biol Chem **275**(21): 15895-904.
- Sonoda, E., H. Hohegger, et al. (2006). "Differential usage of non-homologous end-joining and homologous recombination in double strand break repair." DNA Repair (Amst).
- Sonoda, E., T. Okada, et al. (2003). "Multiple roles of Rev3, the catalytic subunit of polzeta in maintaining genome stability in vertebrates." Embo J **22**(12): 3188-97.
- Stasiak, A. Z., E. Larquet, et al. (2000). "The human Rad52 protein exists as a heptameric ring." Curr Biol **10**(6): 337-40.
- Stenerlow, B., K. H. Karlsson, et al. (2003). "Measurement of prompt DNA double-strand breaks in mammalian cells without including heat-labile sites: results for cells deficient in nonhomologous end joining." Radiat Res **159**(4): 502-10.
- Sugawara, N., T. Goldfarb, et al. (2004). "Heteroduplex rejection during single-strand annealing requires Sgs1 helicase and mismatch repair proteins Msh2 and Msh6 but not Pms1." Proc Natl Acad Sci U S A **101**(25): 9315-20.
- Sugawara, N. and J. E. Haber (1992). "Characterization of double-strand break-induced recombination: homology requirements and single-stranded DNA formation." Mol Cell Biol **12**(2): 563-75.
- Sugawara, N., G. Ira, et al. (2000). "DNA length dependence of the single-strand annealing pathway and the role of *Saccharomyces cerevisiae* RAD59 in double-strand break repair." Mol Cell Biol **20**(14): 5300-9.
- Sugawara, N., X. Wang, et al. (2003). "In vivo roles of Rad52, Rad54, and Rad55 proteins in Rad51-mediated recombination." Mol Cell **12**(1): 209-19.
- Sung, P. (1997). "Function of yeast Rad52 protein as a mediator between replication protein A and the Rad51 recombinase." J Biol Chem **272**(45): 28194-7.
- Swanson, R. L., N. J. Morey, et al. (1999). "Overlapping specificities of base excision repair, nucleotide excision repair, recombination, and translesion synthesis pathways for DNA base damage in *Saccharomyces cerevisiae*." Mol Cell Biol **19**(4): 2929-35.
- Symington, L. S. (2002). "Role of RAD52 epistasis group genes in homologous recombination and double-strand break repair." Microbiol Mol Biol Rev **66**(4): 630-70, table of contents.
- Szostak, J. W., T. L. Orr-Weaver, et al. (1983). "The double-strand-break repair model for recombination." Cell **33**(1): 25-35.

- Takata, M., M. S. Sasaki, et al. (1998). "Homologous recombination and non-homologous end-joining pathways of DNA double-strand break repair have overlapping roles in the maintenance of chromosomal integrity in vertebrate cells." *Embo J* **17**(18): 5497-508.
- Teng, S. C., J. Chang, et al. (2000). "Telomerase-independent lengthening of yeast telomeres occurs by an abrupt Rad50p-dependent, Rif-inhibited recombinational process." *Mol Cell* **6**(4): 947-52.
- Thompson, L. H. and D. Schild (2001). "Homologous recombinational repair of DNA ensures mammalian chromosome stability." *Mutat Res* **477**(1-2): 131-53.
- Tsukamoto, M., K. Yamashita, et al. (2003). "The N-terminal DNA-binding domain of Rad52 promotes RAD51-independent recombination in *Saccharomyces cerevisiae*." *Genetics* **165**(4): 1703-15.
- Ulrich, H. D. (2001). "The srs2 suppressor of UV sensitivity acts specifically on the RAD5- and MMS2-dependent branch of the RAD6 pathway." *Nucleic Acids Res* **29**(17): 3487-94.
- Ulrich, H. D. (2003). "Protein-protein interactions within an E2-RING finger complex. Implications for ubiquitin-dependent DNA damage repair." *J Biol Chem* **278**(9): 7051-8.
- Ulrich, H. D. (2005). "The RAD6 pathway: control of DNA damage bypass and mutagenesis by ubiquitin and SUMO." *Chembiochem* **6**(10): 1735-43.
- Valencia, M., M. Bentele, et al. (2001). "NEJ1 controls non-homologous end joining in *Saccharomyces cerevisiae*." *Nature* **414**(6864): 666-9.
- van den Bosch, M., P. H. Lohman, et al. (2002). "DNA double-strand break repair by homologous recombination." *Biol Chem* **383**(6): 873-92.
- Van Dyck, E., A. Z. Stasiak, et al. (1999). "Binding of double-strand breaks in DNA by human Rad52 protein." *Nature* **398**(6729): 728-31.
- Vance, J. R. and T. E. Wilson (2001). "Repair of DNA strand breaks by the overlapping functions of lesion-specific and non-lesion-specific DNA 3' phosphatases." *Mol Cell Biol* **21**(21): 7191-8.
- Vongsamphanh, R., P. K. Fortier, et al. (2001). "Pir1p mediates translocation of the yeast Apn1p endonuclease into the mitochondria to maintain genomic stability." *Mol Cell Biol* **21**(5): 1647-55.
- Wach, A. (1996). "PCR-synthesis of marker cassettes with long flanking homology regions for gene disruptions in *S. cerevisiae*." *Yeast* **12**(3): 259-65.
- Wach, A., A. Brachat, et al. (1994). "New heterologous modules for classical or PCR-based gene disruptions in *Saccharomyces cerevisiae*." *Yeast* **10**(13): 1793-808.
- Wallace, S. S. (1998). "Enzymatic processing of radiation-induced free radical damage in DNA." *Radiat Res* **150**(5 Suppl): S60-79.

- Wang, H., A. R. Perrault, et al. (2003). "Biochemical evidence for Ku-independent backup pathways of NHEJ." Nucleic Acids Res **31**(18): 5377-88.
- Wang, X. and J. E. Haber (2004). "Role of saccharomyces single-stranded DNA-binding protein RPA in the strand invasion step of double-strand break repair." PLoS Biol **2**(1): E21.
- Whitaker, S. J., Y. C. Ung, et al. (1995). "DNA double-strand break induction and rejoining as determinants of human tumour cell radiosensitivity. A pulsed-field gel electrophoresis study." Int J Radiat Biol **67**(1): 7-18.
- White, C. I. and J. E. Haber (1990). "Intermediates of recombination during mating type switching in *Saccharomyces cerevisiae*." Embo J **9**(3): 663-73.
- Wilson, T. E. (2002). "A genomics-based screen for yeast mutants with an altered recombination/end-joining repair ratio." Genetics **162**(2): 677-88.
- Wilson, T. E. and M. R. Lieber (1999). "Efficient processing of DNA ends during yeast nonhomologous end joining. Evidence for a DNA polymerase beta (Pol4)-dependent pathway." J Biol Chem **274**(33): 23599-609.
- Wolner, B. and C. L. Peterson (2005). "ATP-dependent and ATP-independent roles for the Rad54 chromatin remodeling enzyme during recombinational repair of a DNA double strand break." J Biol Chem **280**(11): 10855-60.
- Wolner, B., S. van Komen, et al. (2003). "Recruitment of the recombinational repair machinery to a DNA double-strand break in yeast." Mol Cell **12**(1): 221-32.
- Xiao, W., B. L. Chow, et al. (2000). "The *Saccharomyces cerevisiae* RAD6 group is composed of an error-prone and two error-free postreplication repair pathways." Genetics **155**(4): 1633-41.
- Xiao, W., B. L. Chow, et al. (1999). "Genetic interactions between error-prone and error-free postreplication repair pathways in *Saccharomyces cerevisiae*." Mutat Res **435**(1): 1-11.
- You, H. J., R. L. Swanson, et al. (1999). "*Saccharomyces cerevisiae* Ntg1p and Ntg2p: broad specificity N-glycosylases for the repair of oxidative DNA damage in the nucleus and mitochondria." Biochemistry **38**(35): 11298-306.
- Yu, J., K. Marshall, et al. (2004). "Microhomology-dependent end joining and repair of transposon-induced DNA hairpins by host factors in *Saccharomyces cerevisiae*." Mol Cell Biol **24**(3): 1351-64.
- Yu, X. and A. Gabriel (2003). "Ku-dependent and Ku-independent end-joining pathways lead to chromosomal rearrangements during double-strand break repair in *Saccharomyces cerevisiae*." Genetics **163**(3): 843-56.

7.3. Talks and poster presentations

Talks

- Gomez-Paramio, I. (2003) Analysis of the interplay between *RAD5*, *HDF1* and *RAD52* yeast genes concerning gamma radiation and DSB repair. 1. Treffen des wissenschaftlichen Nachwuchses der Studiengruppe "Biochemische Pharmakologie und Toxikologie", Ulm (Germany)
- Gomez-Paramio, I. (2005) Role of Rad5 protein for ⁶⁰Co-gamma-induced DNA damage. Workshop „Responses to DNA Damages“, Neuherberg (Germany)

Poster presentations

- Gomez-Paramio, I., Mörtl, S., Ahne, F., Eckardt Schupp, F.(2002) DNA-double strand breakrepair in yeast: Análisis of the interplay between *RAD5*, *HDF1* and *RAD5*. DNA Repair 2002, 7. Tagung des DNA-Reparatur-Netzwerks. Karlsruhe (Germany)
- Gomez-Paramio, I., Mörtl, S., Ahne, F., Eckardt-Schupp, F.(2003) Role of the Rad5 protein for the balance of homologous recombination and non-homologous end joining in yeast. Annual Meeting of the German Genetics Society, Kassel (Germany).
- Gomez-Paramio, I., Mörtl, S., Ahne, F., Eckardt-Schupp, F.(2004) Balance between homologous recombination and non-homologous end joining is influenced by the Rad5 protein. 4th DNA Repair Workshop, Bratislava (Slovakia).
- Gomez-Paramio, Braselmann, H., I, Mörtl, S., Eckardt Schupp, F. (2005) Geltool: a new PFGE evaluation method for the quantification of chromosomal breaks in haploid yeast strains. Programm orientierte Förderung (POF), Neuherberg, Germany

7.4. Curriculum Vitae

Personal Information

Name	Idoia Gómez Paramio
Date of Birth	2.3.1976
Place of Birth	Valladolid, Spain
Nationality	Spanish

Academic studies

May 02- present	PhD at the Ludwig Maximilianeum University (LMU) of Munich in cooperation with the GSF-Forschungszentrum <u>Topic:</u> "Analysis of the role of Rad5 for the regulation of repair of DSB, small deletions and oxidative damage" <u>Supervision:</u> Prof. Dr. Friederike Eckardt-Schupp.
Nov. 01- May. 02	Course for master degree at the LMU, Munich <u>Topic:</u> "Analysis of the <i>rad5</i> , <i>rad52</i> , and <i>hdf1</i> yeast mutants concerning DNA repair and radiation sensitivity" <u>Supervision:</u> Prof. Dr. Friederike Eckardt-Schupp.
Oct. 99- Sep. 01	Degree in Biochemistry at the University of Salamanca. Study of Biochemistry at LMU with an exchange grant.
Oct. 00- Sep. 01	
Oct. 94- Feb. 00	Degree in Biology at the University of Salamanca. Study of Biology at Ruprecht Karl University, Heidelberg, Germany with an ERASMUS exchange grant.
Oct. 97- Jul. 98	

Education

1990 - 1994	High School at the Instituto Santa Teresa de Jesús, Valladolid, Spain
1981 - 1990	Primary School at the Colegio Leon Felipe, Valladolid, Spain